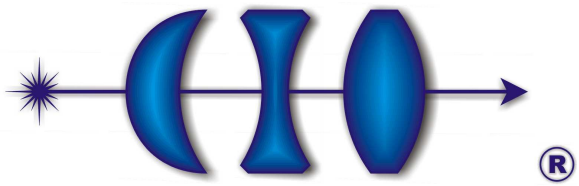

CENTRO DE INVESTIGACIONES
EN OPTICA, A.C.

OPTICAL INJECTION OF SPIN POPULATION AND SPIN CURRENT IN SEMICONDUCTOR SURFACES

By

Tonatiuh Rangel Gordillo

SUBMITTED IN PARTIAL FULFILLMENT OF THE
REQUIREMENTS FOR THE DEGREE OF
MASTERS IN SCIENCES (OPTICS)
AT
CENTRO DE INVESTIGACIONES EN OPTICA, A.C.
DEPARTMENT OF PHOTONICS
LEÓN GUANAJUATO, MÉXICO
DECEMBER 2006

Supervisor: Dr. Bernardo Mendoza Santoyo

Internal examiners:

Dr. Norberto Arzate Plata

External examiners:

Dr. Guillermo Pablo Ortiz

(Centro Universitario de los lagos Universidad de Guadalajara)

Table of Contents

List of Figures

Abstract

We present an *ab initio* study of the GaAs(11) surface. In particular, the spin injection current, the electrical injection current and the degree of spin polarization are calculated for one-photon excitations. First, we present a formal derivation of the formulas used to obtain such responses; we explicitly obtain the expressions for both the total and the layered contributions. In the second chapter, we give an introduction of the method used to calculate the wave function for a crystalline surface along with all its approximations. In the third chapter, we make a convergence study to ensure that our calculations will be correct within our approximations. Finally, in chapter 4, we present our results and its possible applications.

Acknowledgements

I thank *Dr. Bernardo Mendoza Santoyo* for his unvaluable guidance and friendship which made possible the elaboration of this thesis.

I thank *Dr. Norberto Arzate Plata* for his teaching and his patience.

In a special way, I thank *my mother*, *my father*, *my grand mother* and *my brother* for giving me all the necessary tools to achieve a masters degree.

I gratefully acknowledge financial support from the Mexico's National Council of Science and Technology *CONACYT*.

Chapter 1

Introduction

In the last decade the field of spintronics or spin electronics was positioned as an important scientific activity. Statistical studies made during the years 1996 and 2001 by Stephan von Molnár show that the number of research papers that were published on this subject had increased continously [1]. Year by year papers on spin injection, detection and manipulation had increased. Moreover, the areas involving semiconductors has also received special attention because of the fact that much of the actual electronics is based on semiconductors.

In electronics we use the electron charge as a basic property to work with. However, it is well known that electrons also posses a *spin* angular momentum. It is an intrinsic property whose value does not depend on the electron mass or angular velocity. Moreover, the spin is connected to a magnetic moment which makes it act as a magnet. So that, in a magnetic field, the spin can have two directions, loosely speaking, they are known as *up* and *down*. This property provides an extra degree of freedom leading to an electronics field known as spintronics. Spin electronics exploits the spin properties as well as the charge properties offering more opportunities to new electronic devices.

One of these devices is the so-called giant-magneto-resistive (GMR) structure, which is a device that is used as a read head and a memory-storage cell. It consists of alternating multi-layers composed of magnetic and non-magnetic metals and alloys, and, its performance depends on the relative orientation of the magnetizations in the layers. The device resistance changes from small (parallel magnetizations) to large (antiparallel magnetizations) values. This change in resistance is an important effect known as *magneto-resistance* which is used to sense

changes in magnetic fields. This resulted in the first spintronics device: the GMR structure launched by IBM in 1997.

Some recording devices, such as hard disks already employ the GMR effect. Data is recorded and stored in magnetized iron or chromium oxides. In order to read it, a read head detects resistance changes in the disk that is rotating underneath it. GMR technology enables increases in storage capacity of hard disks. As an example, a popular spintronics device is the Apple iPOD 60GB which has a GMR read head inside.

Recent innovations in GMR technology have introduced magnetic tunnel junction devices where the tunneling current is related to spin orientations of the electrons at the electrodes. These devices have two magnetic layers separated by an insulating metal-oxide layer. Electrons at both sides are able to tunnel only when their spin polarizations are aligned in the same direction. The resistance is 1000 times higher than in the standard GMR devices.

In the future it is expected that the merger of electronics, photonics and magnetics will provide novel spin-devices such as spin resonant tunneling devices, optical switches and spin-transistors. However, the development of these devices depends on the knowledge we can acquire in managing the spin of the electron. Thus, the investigation on spintronics areas is crucial for the improvement of the electronic industry.

Current investigations in the field of spin electronics are under two different approaches. The first one has the aim of perfecting the GMR-based technology by introducing new materials or by engineering better designs on the existing devices. The second effort is in the field of generation and utilization of spin currents. This can lead to new devices which can be easily incorporated to existing integrated circuitry.

In the aim of producing and controlling spin currents, recent discoveries have given attention to semiconductors as both sources and carriers of spin information. One of them by Kikkawa *et al.* [2] demonstrated that the spin relaxation time can be extended to 100 ns in bulk n-GaAs with a negative doping density of $10^6 \mathrm{cm}^{-3}$, and they have shown that spin can be transported over macroscopic scales of 100 micrometers without loss of coherence. Also, Malajovich *et al.* [3] have shown that spin coherence can even be transported across semiconductor junctions with different band gaps, such as GaAs/ZnSe hetero-junctions.

The use of semiconductors in quantum computers has potential benefits. It will

be easy to incorporate them to the actual devices because of the fact that the electronic technology is based on semiconductors such as silicon and gallium arsenide. What is more, semiconductors allow various characteristics to be controlled by external fields such as light and electro-magnetic fields. Moreover, semiconductors can be controlled by quantum confinement at nanoscales.

Knowing the potential that have semiconductors in spintronics, we decided to study optical properties of GaAs[110]. We studied a surface because it is formed of a small number of layers minimizing the size of the quantum integrated circuits. Among the optical properties that the surface presents we focused on the injection of electrical and spin currents due to linear absorption of light.

Our study is purely theoretical, however, *ab initio* calculations have been used for years giving correct results in most cases. Moreover, understanding the physical processes that are involved on matter is important in developing a new scientific area. Spintronics will become a mature science only when the physical processes inherit to the control and injection of spin currents are completely understood.

All in all, we have introduced spintronics as a new relevant scientific area which is concerned with the understanding and control of spin currents for its potential application in spin-electronic devices. As it has been explained, we will study a semiconductor surface because semiconductors have attracted special attention after it has been demonstrated that they can be used to store and transport spin currents. Moreover, a major understanding and control of the spin in nanomaterials will lead to the development of new devices which will revolutionize the electronic industry.

Chapter 2

Ab initio calculations

In modern chemistry, computer modeling has been widely used in order to obtain the physical properties of molecular systems. These simulations have a lot of advantages over traditional experiments. They save money and time, and, it is easier to control the parameters in a simulation than in a real situation. Therefore, they are a powerful tool in the field of material sciences.

First, we can calculate all the optical properties of a material with just one computer. Second, we need different apparatus for each of the different properties we want to find in traditional experiments. Moreover, in theoretical calculations we can easily change one parameter and find its response. In contrast, in real experiments it is difficult to isolate one variable and measure its particular contribution.

However, theoretical calculations will not replace traditional techniques. On the contrary, they complement each other. We need theory to understand the intrinsic physical processes of the materials and we need experiments to validate the theory. *Ab initio* calculations have been used for years. They have succeeded over the time giving us the opportunity to use them as a predictive tool.

In the following sections it will become obvious that we need to solve the Schrödinger equation for a system of many bodies. However, this equation can only by solved analytically for an Hydrogen atom. For all other cases we must use approximations. The approximation methods can be categorized as either *ab initio* or *semiempirical*. The main difference is that *ab initio* calculations use only the position and the atomic number of the atoms while we employ some data extracted from experiments to make *semiempirical* calculations.

Ab initio means from the beginning. In sciences it is also known as *first principles*. A calculation is said to be *ab initio* when we do not use experimental input in the calculations. We just limit ourselves to values of fundamental physical constants such as atomic numbers and dielectric constants among others.

In this chapter we will explain how *ab initio* techniques can be employed to obtain optical properties of a semiconductor surface. To start our calculations we will use the coordinates of the atoms in the crystal lattice, and, we will calculate all the energies among ions and electrons on the system. Then we will solve the many-body Schrodinger equation for this system in order to obtain the wave function that describes it. At the end we will use this wave function to calculate the optical properties of the system.

2.1 Total energy calculations

In 1924 de Broglie proposed the idea that particles behave as waves. He made it possible by joining the ideas of Einstein and Planck. To illustrate, if you join Planck's expression for the quantization of the energy $E = h\nu$ to the Einstein's relativity formula $E = mc^2$ you can easily obtain that $\lambda = h/p$. This formula states that electromagnetic radiation has a particle nature (momentum) and wave characteristics (wavelength).*

It was Schrödinger who associated the classical equation for waves to the de Broglie's particle waves. With this aim he developed his so called *Schrödinger equation* $\hat{\mathcal{H}}\psi = E\psi$. Max Born gave the wave-function ψ a wider meaning. He named it a probability wave because the square of the wave function $|\psi(x)|^2$ give us the probability of finding the particle at position x. Moreover, later works have proved that from the wave function we can obtain other physical properties, *i.e.*, observables as the position and the momentum can be easily obtained from the wave function and there are many other properties that can be derived from them. Thus, it is extremely important to obtain the wave function ψ in order to get other physical characteristics of the system.

One of the main quantities we are trying to find is the total energy of the system E_{tot} because of the fact it is related with the wave function by an eigenvalue equation, the *Schrödinger equation*. As it is expected, the energy of a system E

*Here h is the Planck's constant, ν is the light frequency, λ is the light wavelength, c is the speed of light and p is the particle's momentum.

can be obtained from ψ by the following general expression:

$$E_{tot} = \frac{\langle\psi|\hat{\mathcal{H}}|\psi\rangle}{\langle\psi|\psi\rangle}. \tag{2.1}$$

Thus, we will start by defining the Hamiltonian $\hat{\mathcal{H}}$ for a system of electrons and nuclei:

$$\begin{aligned}\hat{\mathcal{H}} &= -\frac{\hbar^2}{2m_e}\sum_i \nabla_i^2 - \sum_{i,I}\frac{Z_I e^2}{|\mathbf{r}_i - \mathbf{R}_I|} + \frac{1}{2}\sum_{i\neq j}\frac{e^2}{|\mathbf{r}_i - \mathbf{r}_j|} \\ &\quad -\sum_I \frac{\hbar^2}{2M_I}\nabla_I^2 + \frac{1}{2}\sum_{I\neq J}\frac{Z_I Z_J e^2}{|\mathbf{R}_I - \mathbf{R}_J|},\end{aligned} \tag{2.2}$$

where $\{\mathbf{R}_I\}$ are the positions of the ions and $\{\mathbf{r}_i\}$ denote the electrons. The electron mass is m_e, the atomic charge is denoted by Z and the atomic mass by M.

The problem of solving this equation is formidable. The first approximation that we are going to use is the Oppenheimer approximation. This treats the nuclei as being static because of the differences of masses between electrons and nuclei. Then, the problem is reduced to a system of electrons moving along a frozen nuclei. If the ions are at rest the Hamiltonian can be rewritten as:

$$\hat{\mathcal{H}} = -\frac{\hbar^2}{2m_e}\sum_i \nabla_i^2 - \sum_{i,I}\frac{Z_I e^2}{|\mathbf{r}_i - \mathbf{R}_I|} + \frac{1}{2}\sum_{i\neq j}\frac{e^2}{|\mathbf{r}_i - \mathbf{r}_j|} + \frac{1}{2}\sum_{I\neq J}\frac{Z_I Z_J e^2}{|\mathbf{R}_I - \mathbf{R}_J|}, \tag{2.3}$$

If we define the total external potential V_{ec} experienced by an electron due to the presence of ions located at positions $\{\mathbf{R}_I\}$ as,

$$V_{ec}(\mathbf{r}) = -\sum_I \frac{Z_I e^2}{|\mathbf{R}_I - \mathbf{r}|}, \tag{2.4}$$

the Hamiltonian can be rewritten as:[†]

$$\hat{\mathcal{H}} = -\frac{\hbar^2}{2m_e}\sum_i \nabla_i^2 + \sum_i V_{ec}(\mathbf{r}_i) + \frac{1}{2}\sum_{i\neq j}\frac{e^2}{|\mathbf{r}_i - \mathbf{r}_j|}. \tag{2.5}$$

Further simplications will be made to the problem. As it is explained by M. C. Payne [5] we will use *density functional theory* to model the electron-electron interactions and *pseudopotential theory* to model the electron-ion interactions.

[†]The last term of equation (2.3) was neglected because it is simply a constant, usually called the Madelung energy. At the end, this constant will be calculated by using the Ewalds method [4].

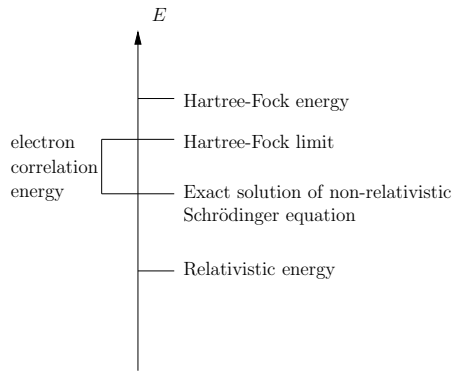

Figure 2.1 : We show the electron correlation energy, which is equal to the Hartree-Fock limit minus the energy obtained by solving the unrelativistic Schrödinger equation under the Oppenheimer approximation.

2.2 Electron-electron interactions

The third term of equation (2.3) describes a relation between electrons on the system. We know by Coulomb's law that electrons repulse each other by a force which is inversely proportional to the square of the distance between them. In a real life system it is extremely difficult to know the exact positions of all electrons at a given time, therefore, we will made further approximations to simplify this term.

2.2.1 Hartree-Fock method

Because of the fact that electrons are fermions, the wave function must be antisymmetric under exchange of any two electrons. That is, each electron has a unique set of quantum numbers. The antisymmetry of the wavefunctions produce separation among electrons having the same spin orientation. Moreover, these separations cause a reduction of the Coulombic energy of the system. The reduction of the energy due to the antisymmetry of the wave functions is known as the *exchange energy*.

The *exchange correlation* is the only correlation considered in the Hartree-Fock method (HFM). However, there are other correlations to consider. The Coulomb correlation describes the correlation between spatial electrons of opposite spin. Their repulsion causes a separation that reduces the energy of the system. Moreover, there is also a correlation related to the overall symmetry of the system.

In quantum chemistry we can solve the Schrödinger's equation using the HFM. In this method the wave function is approximated by a Slater determinant. However, single determinants cannot always describe exact wave functions. In this case

this approximation does not take into account the Coulomb correlation. Therefore, the total energy calculation will be slightly different from the exact solution of the Schrödinger equation given by (2.3). The difference between both solutions is known as the *correlation energy.*[‡]

Fig. 2.1 shows the differences among energies calculated by different methods. The lowest energy is the energy calculated by relativistic equations, and, the use of non-relativistic equations leads to a higher energy value. Moreover, when introducing the Hartree-Fock approximation the energy obtained is slightly higher than the exact solution of the Schrödinger equation. The difference between the lowest energy that we can obtain by using the Hartree-Fock approximation (Hartree-Fock limit) and the energy obtained by the non-relativistic Schrödinger equation is called *electron correlation energy.*

It is extremely difficult to calculate the correlation energy of a complex system. Many approximations have been used such as Monte Carlo simulations [8]. On the other hand, there are other methods that describe the effects of the electron-electron interaction, such as the Density Functional Theory.

2.2.2 Density Functional Theory

The main idea of the Density Functional Theory (DFT) is that any property of a system conformed of many bodies can be expressed as a functional of the ground state density $\rho_o(\mathbf{r})$. That is, the electronic density is set as the basic quantity in the many-body wavefunction. The electronic wave function is dependent on $3N$ variables, three spatial variables for any of the N electrons. On the other hand, the electronic density is only a function of three variables. Therefore, we will have a simpler quantity to work with.

The Kohn-Sham (KS) method is a common implementation of the DFT. It allows to convert the many-body problem of interacting electrons moving in a static external potential into a problem of non-interacting electrons in an effective potential. So that the system of electrons can be thought as a classical liquid of density $\rho_o(\mathbf{r})$. The effective potential includes the electron-electron interactions along with the external potential.

[‡]It was Per-Olov Löwdin who made numerous studies on the Hartree-Fock approximation and coined the term *correlation energy* [6], [7].

2.2.3 Kohn-Sham energy functional

Hohenberg and Kohn showed [9] that the ground-state energy of an interacting inhomogeneous electron gas in a static potential $V(\mathbf{r})$ can be written as:

$$E_{tot} = \int V(\mathbf{r})\rho(\mathbf{r})\mathrm{d}\mathbf{r} + \frac{1}{2}\int\int \frac{\hat{\rho}(\mathbf{r})\rho(\mathbf{r}')}{|\mathbf{r}-\mathbf{r}'|}\mathrm{d}\mathbf{r}\mathrm{d}\mathbf{r}' + G[\rho] \tag{2.6}$$

where $\rho(\mathbf{r})$ is the density and $G[\rho]$ is a universal functional of the density.

Kohn and Sham [10] proposed an approximation for $G[\rho]$ that contains the major part of the effects of exchange and correlation. This is,

$$G[\rho] \equiv T_s[\rho] + E_{xc}[\rho], \tag{2.7}$$

where $T_s[\rho]$ is the kinetic energy functional and $E_{xc}[\rho]$ is the exchange-correlation energy functional. If $\rho(\mathbf{r})$ is slowly variant then we can show that [10]:

$$E_{xc}[\rho] = \int \rho(\mathbf{r})\epsilon_{xc}\left(\rho(\mathbf{r})\right)\mathrm{d}\mathbf{r}, \tag{2.8}$$

where $\epsilon_{xc}(\rho)$ is the exchange and correlation energy per electron of a uniform electron gas of density ρ.[§]

Using Eq. (2.8) Kohn and Sham [10] proposed a set of equations that must be solved self-consistently,

$$\int \delta\rho(\mathbf{r})\left\{V_H(\mathbf{r}) + V(\mathbf{r}) + \frac{\delta T_s[\rho]}{\delta\rho(\mathbf{r})} + V_{xc}(\rho(\mathbf{r}))\right\}\mathrm{d}\mathbf{r} = 0; \tag{2.9}$$

$$V_H(\mathbf{r}) = \int \frac{\rho(\mathbf{r}')}{|\mathbf{r}-\mathbf{r}'|}\mathrm{d}\mathbf{r}' \tag{2.10}$$

$$V_{xc}(\rho) = \mathrm{d}(\rho\epsilon_{xc}(\rho))/\mathrm{d}\rho \tag{2.11}$$

where V_{xc} is the exchange and correlation contribution to the chemical potential of a uniform gas of density ρ, and, V_H is the Hartree potential.[¶]

[§]This expression is only valid for slow varying densities because it does not takes into account inhomogeneities in the electron density. This is the so-called *Local Density Approximation (LDA)* because we are assuming that the exchange-correlation energy functional is purely local, *i.e.*, the electron exchange and correlation energy at any point of the space is a function of the electron density at that point in space only.

[¶]The Hartree energy, E_H, is the self-interaction energy of the density $\rho(\mathbf{r})$ treated as a classical charge density. It is explicity given by: $E_H = \frac{1}{2}\int \rho(\mathbf{r})V_H\mathrm{d}\mathbf{r} = \frac{1}{2}\int\int \frac{\rho(\mathbf{r})\rho(\mathbf{r}')}{|\mathbf{r}-\mathbf{r}'|}\mathrm{d}\mathbf{r}\mathrm{d}\mathbf{r}'$.

Equations (2.9), (2.10) and (2.11) describe a system of noninteracting electrons moving in a potential $V_H(\mathbf{r}) + V(\mathbf{r}) + V_{xc}(\rho(\mathbf{r}))$. Knowing this potential can find the density $\rho(\mathbf{r})$ by solving the Schrödinger equation

$$\left\{-\frac{1}{2}\nabla^2 + [V_H(\mathbf{r}) + V(\mathbf{r}) + V_{xc}(\rho(\mathbf{r}))]\right\}\psi_i(\mathbf{r}) = \epsilon_i\psi_i(\mathbf{r}), \tag{2.12}$$

and by using the Born's relation

$$\rho(\mathbf{r}) = \sum_{i=1}^{N} |\psi_i(\mathbf{r})|^2, \tag{2.13}$$

where N is the number of electrons.

The set of Eqs. (2.9)-(2.13) must be solved self-consistently. That is, we first give an initial $\rho(\mathbf{r})$, then we obtain the potentials V, V_H and V_{xc} from Eqs. (2.10) and (2.11). At last we find a new $\rho(\mathbf{r})$ by using Eq. (2.12). We repeat the procedure until the initial ρ and the new ρ are the same considering a given error tolerance.

It is important to note that only the minimum value of the KS energy functional has physical meaning. At this minimum the electronic density $\rho(\mathbf{r})$ becomes the ground state density $\rho_o(\mathbf{r})$ of the system, *i.e.*, all the other densities $\rho(\mathbf{r})$ do not have physical meaning.

2.2.4 Bloch's theorem

We just showed that it is possible to solve the Schrödinger's equation for a system of many atoms. However, the problem remains extremely difficult because we have to solve this equation for each one of the electrons conforming the system. There are two main problems: the number of electrons in the system is infinite, and, because of the fact that each electronic function extends over the entire solid, the basis set needed to expand each wave function is also infinite. These problems will be solved by applying the Bloch's theorem.

The Bloch's theorem states that the wavefunctions ψ for a periodic solid can be made of two parts; a plane wave times a function with the periodicity of the solid [11]:

$$\psi_n(\mathbf{r}) = e^{i\mathbf{k}\cdot\mathbf{r}}u_n(\mathbf{r}) \tag{2.14}$$

If we use reciprocal lattice vectors to expand the periodic part, we find out that each wave function can be written as a sum of plane waves [5],

$$\psi_n(\mathbf{r}) = \sum_{\mathbf{G}} c_{n,\mathbf{k}+\mathbf{G}} e^{i(\mathbf{k}+\mathbf{G})\cdot\mathbf{r}}, \tag{2.15}$$

where $\mathbf{G}$ denotes reciprocal lattice vectors and $\mathbf{k}$ is for reciprocal vectors.

Then it follows that by using the Bloch theorem we will only calculate the response functions at a unit cell, the *irreducible Brillouin zone*. This unit cell will fill all the lattice space without leaving gaps by repetition of crystal translation operations.

The Bloch's theorem modifies the initial problem in the following way. We no longer need to compute an infinite number of wave functions but a finite number of wave functions at an infinite number of $\mathbf{k}$-points $\mathbf{k}$. According to the boundary conditions of a particular solid, we find out that the electronic states are discretized. Thus, we have a finite number of allowed states at an infinite number of $\mathbf{k}$-points $\mathbf{k}$. Each $\mathbf{k}$ contributes to the electronic potential, so that, we need to calculate an infinite number of $\mathbf{k}$-point contributions in order to compute the total potential. However, it has been proved that the contributions of $\mathbf{k}$-points which are very close together are almost identical. Thus, we can represent a region of $\mathbf{k}$-points by only one $\mathbf{k}$-point. To illustrate, we will only consider some $\mathbf{k}$-point samples at each zone of the crystal in order to calculate the total energy of the crystal.

2.2.5 Cutoff energy

Up to now, we have considered a finite number of wave functions in a finite number of $\mathbf{k}$-points. Moreover, Bloch's theorem states that we can expand each wave function in a set of plane waves. Theorically, we need an infinite number of plane waves to expand a single wave function. Thus, we will introduce another concept in order to overcome this problem; the cutoff energy.

The coefficients $c_{i,\mathbf{k}+\mathbf{G}}$ used to expand a wave function with small kinetic energy are more important than those with large kinetic energy [5]. Therefore, we will only consider the plane waves with coefficients having a kinetic energy no longer than a *cutoff energy*. That is, we will truncate our calculations when we reach the *cutoff energy*. The bigger the cutoff energy is, the more accurate the result will be. However, it will take more time to compute. Thus, it is important

to choose the minimum cutoff energy at which the results converge in order to save computing resources and time.

We have overcome the problem of electron-electron interactions, but, how are we going to solve the electron-ion interactions?

2.3 Electron-ion interactions

2.3.1 Pseudopotential formalism

The core electrons, are nearly unresponsive to many of the physical phenomena that we can observe in a material. In fact, the column structure of the periodic table of the elements is based on the passivity of the core states and the reactivity of the valence states. Thus, it is natural to eliminate the need to include atomic core states, which is achieved by replacing the strong core potential by a weaker one, a pseudopotential.

As it was explained Bloch's theorem states that wave functions can be expanded in a set of plane waves, however, a very large number of plane waves are needed in order to follow the rapid oscillations of the electrons in the core region. That is, a large *cutoff energy* will be needed, leading to a vast amount of computing time. On the other hand, when we replace the Coulombic core potential by a weaker one we no longer need a high *cutoff energy* to expand the wave functions in the core regions.

All in all, the pseudopotential theory (PST) overcomes two problems; it simplifies the complicated effects caused by the motion of the core electrons of an atom and its nucleus and guarantees that the valence wavefunction be orthogonal to all the core states.

The pseudo-potentials are generally repulsive at the origin, and, the resulting wave functions usually have the correct shape outside the core region, however, they differ from the real wave functions in its magnitude [12]. Having this in mind, we will normalize the first ones to ensure that both wave functions be identical outside the core region as you can see in Fig. 2.2.

At large distances the pseudopotential is identical to the Coulombic potential of the form $Z/\mathbf{r}$, where Z if the atomic number. When finding its Fourier transformation we can find that it diverges as $Z/\mathbf{G}^2$ when $\mathbf{G}$ tends to zero. It is not alarming because the Coulomb contributions to the total energy from the three

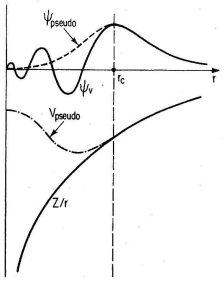

Figure 2.2 : Sketch of all-electron (solid lines) and pseudo (dashed lines) potentials along with their respective wave functions. The wave functions oscillate rapidly in the core region because of the strong Coulombic attraction. Outside the core region the two potentials are identical. Source [5].

interactions (ion-ion, electron-ion and electro-electron) cancel each other [5]. Because of the fact that the system is charge-neutral, there is no Coulomb potential at $\mathbf{G} = 0$. Thus, there cannot be a contribution to the total energy from the $\mathbf{G} = 0$ component of the Coulomb potential.

2.4 Ion-ion interactions

The last term of equation (2.2) describes the interactions between all ions in the array. It is the Coulombic energy due to atoms positioned at $\mathbf{R}_2$ and the array of ions positioned at $\mathbf{r}_J = \mathbf{r}_1 + \mathbf{l}$. As you may note this is an infinite sum. In order to solve this problem we use the Ewald's method which will convert this infinite sum in convergent summations. It is based in the following identity, [5]

$$\begin{aligned} \sum_\ell \frac{1}{|\mathbf{R}_1 + \ell - \mathbf{R}_2|} &= \frac{2}{\sqrt{\pi}} \sum_\ell \int_\eta^\infty exp\left[-|\mathbf{R}_1 + \ell - \mathbf{R}_2|^2 \rho^2\right] \mathrm{d}\rho \\ &+ \frac{2\pi}{\Omega} \sum_{\mathbf{G}} \int_0^\eta exp\left[-\frac{|\mathbf{G}|^2}{4\rho^2}\right] e^{i(\mathbf{R}_1 - \mathbf{R}_2)\cdot\mathbf{G}} \frac{1}{\rho^3} \mathrm{d}\rho, \\ &\eta > 0, \end{aligned} \tag{2.16}$$

where ℓ denotes lattice vectors, $\mathbf{G}$ is for reciprocal lattice vectors and Ω is the volume of the unit cell. It is important to note that if one chooses a correct value for η the two summations on the right will converge very rapidly.

As it was mentioned in the previous section the contributions to the total energy at $\mathbf{G} = 0$ will cancel. Therefore we have to omit the terms at $\mathbf{G} = 0$ at real space and reciprocal space.

2.5 Computation

As it was explained before, the main idea is to be able to find the total energy of the system E_{tot}. Theoretically, this can be done by solving the general equation (2.1) with the Hamiltonian (2.2). However, the problem of solving the Schrödinger equation by using the Hamiltonian (2.2) is extremely difficult. Therefore, we introduced a series of approximations in this chapter; the DFT, the PST, the Bloch's theorem and the Ewald methods. At last we explained that the terms for $\mathbf{G} = 0$ had to be ignored for the Ewald series to converge. All in all, we have arrived to an alternative form for the total energy E_{tot}:

$$E_{tot} = E_{kin} + E_{ec} + E_H + E_{xc}[\rho] + E_{cc} \tag{2.17}$$

where E_{kin} is the kinetic energy, E_{ec} is the energy corresponding to the interactions between ions and electrons, E_H is the Hartree energy, $E_{xc}[\rho]$ is the exchange-correlation energy, and, E_{cc} is the term that describes the ion-ion interactions. These terms (per cell) are given explicitly by: [13, 14]

$$E_{kin} = \frac{1}{N_c}\sum_{i,\mathbf{G}} n_i |\psi_i(\mathbf{k}_i + \mathbf{G})|^2 \frac{\hbar^2 |\mathbf{k}_i + \mathbf{G}|^2}{2m}, \tag{2.18a}$$

$$E_{ec} = \frac{1}{N_c}\sum_{i} n_i \int \mathrm{d}\mathbf{r}\, \psi_i^*(\mathbf{r}) V_{ec}(\mathbf{r}) \psi_i(\mathbf{r}), \tag{2.18b}$$

$$E_H = \frac{\Omega}{2}\sum_{\mathbf{G}\neq 0} |\rho(\mathbf{G})|^2 \frac{4\pi e^2}{|\mathbf{G}|^2}, \tag{2.18c}$$

$$E_{xc} = \frac{\Omega}{2}\sum_{\mathbf{G}} \rho^*(\mathbf{G}) \epsilon_{xc}(\mathbf{G}), \tag{2.18d}$$

$$\begin{aligned} E_{cc} \;=\; & \frac{1}{2}\sum_{s,s'} Z_s Z_{s'} e^2 \left\{ \frac{4\pi}{\Omega}\sum_{\mathbf{G}\neq 0}\left[\frac{1}{|\mathbf{G}|^2}\cos[\mathbf{G}\cdot(\mathbf{R}_s - \mathbf{R}'_s)] exp\left[-\frac{|\mathbf{G}|^2}{4\eta^2}\right]\right]\right. \\ & \left. -\frac{\pi}{\eta^2\Omega} + \sum_{l'}\left[\frac{erfc(\eta \mathbf{x})}{\mathbf{x}}\right]_{x=|\mathbf{l}+\mathbf{R}_s-\mathbf{R}'_s|} - \frac{2\eta}{\sqrt{\pi}}\delta_{ss'}\right\}. \end{aligned} \tag{2.18e}$$

The symbols n_i, N_c, Ω are, respectively, the occupation number, the total number of cells in the system and the cell volume. Z_s and $\mathbf{R}_s$ are the atomic

number and the position vector for the sth atom in the basis. $\rho(\mathbf{G})$ stands for the Fourier transform of the pseudo valence charge density. $V_{ec}(\mathbf{r})$ is the potential due to the interaction among ions and electrons in the system. $\epsilon_{xc}(\mathbf{G})$ is the exchange correlation energy per electron in Fourier's space. The prime in the $\mathbf{l}$ summation is used to indicate that the $\mathbf{l} = 0$ term when $\mathbf{R}_s = \mathbf{R}'_s$ will be excluded to make the Edwald summations converge.

As you can notice, this expression for the total energy depends on the electronic density $\rho(\mathbf{r})$. Therefore, we need first to compute $\rho(\mathbf{r})$ in order to find E_{tot}. The procedure to get $\rho(\mathbf{r})$ is based on the following theorem: [15]

Theorem 1 (Hohenberg-Kohn) *For any system of interacting particles in an external effective potential $V^{eff}(\mathbf{r})$, the potential $V^{eff}(\mathbf{r})$ is determined uniquely, except for a constant, by the ground state particle density $\rho_o(\mathbf{r})$.*

That is, given a density $\rho_o(\mathbf{r})$ we can find the effective potential $V^{eff}(\mathbf{r}) = V_{ec}(\mathbf{r}) + V_H(\mathbf{r}) + V_{xc}(\rho(\mathbf{r}))$. It follows from equation (2.12) that we can obtain the density $\rho_o(\mathbf{r})$ from the potential $V^{eff}(\mathbf{r})$. Thus, we will repeat this procedure until the difference between two subsequent values of the calculated densities $\rho_o(\mathbf{r})$ are less than a given error tolerance. At this time we can say that the result has converged, and we are ready to calculate the total energy by using Eq. (2.17).

As it is shown in Fig. 2.3 the complete process is as follows:

1. Given the atomic coordinates we will construct an ionic potential V_{ec}. This is achieved by using the pseudopotential method.[‖]
2. We will choose a *cutoff energy* for the plane-wave basis set $e^{i(\mathbf{k}+\mathbf{G})\cdot\mathbf{r}}$ given by Eq. (2.15).
3. We will give a trial density $\rho(\mathbf{r})$.
4. The exchange-correlation potential $V_{xc}(\rho(\mathbf{r}))$ and the Hartree potential $V_H(\mathbf{r})$ will be calculated using Eqs. (2.9), (2.10) and (2.11) for the given density $\rho(\mathbf{r})$.
5. We will find a new density $\rho(\mathbf{r})$ solving the eigenvalue equation (2.12).
6. We will repeat the last two steps until the results converge.

[‖] When constructing the pseudo-potentials, there are several details that we have to deal with, however, we will not go into these details here.

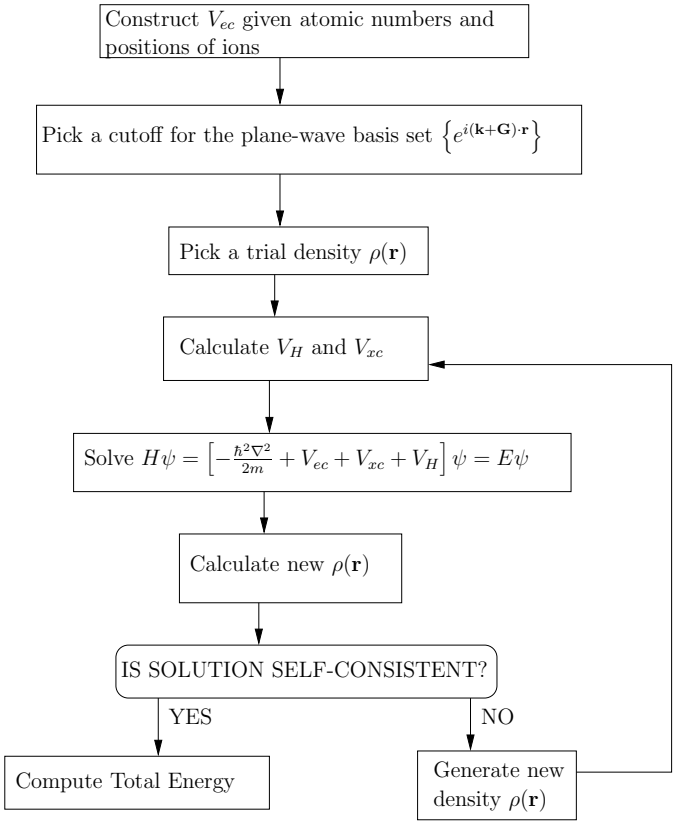

Figure 2.3 : We show the computational procedure to calculate the total energy of a solid. Source: [5]

7. Having the density $\rho(\mathbf{r})$ we will calculate the total energy E_{tot} by using expression (2.17).

Chapter 3

Injection process

In order to develop spintronics devices, the methods of injection, conduction and manipulation of charge carriers into semiconductor materials have to be improved. Since two decades ago the so-called magneto-electric effect has been used to successfully inject spin currents into semiconductors. It was first proved by Johnson and Silsbee [16] in an experiment in which they could transport non-equilibrium magnetization across the interface made of a ferromagnetic metal and a paramagnetic metal. The main idea of this approach was the use of a ferromagnetic metal to inject spin into a semiconductor due to the differences of voltage and magnetization potential at the interface.

After it was proved that a ferromagnetic metal could be used to inject a preferable spin polarization, applications were developed based on this principle. Among the first works in this field, there is a current modulator proposed by Supriyo Datta and B. Das [17]. This device uses magnetized contacts to launch and detect spin polarizations. Moreover it uses a narrow-gap semiconductor as an analog of an electro-optic material to control phase shifts between $+z$ polarized and $-z$ polarized electrons via a gate voltage. In these devices magnetized contacts have been used to inject spin polarizations. We can question ourselves; is there another way of launch spin polarizations?

Light, which is an electromagnetic (EM) field, can cause this effect. As it is shown in Fig. 3.1, Ali Najmaie *et al.* [18] proved that monochromatic fields at ω and 2ω can be used to inject and control spin and electrical currents in quantum wells. The main difference between both approaches is that the former uses a magnetized contact to produce a preferable spin polarization while the latter uses

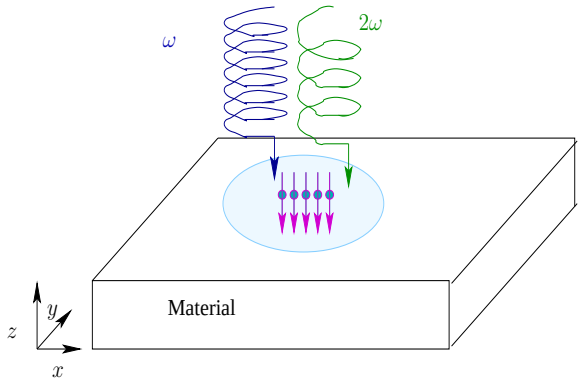

Figure 3.1 : Scheme showing that circularly polarized optical fields of frequencies ω and 2ω produce an average spin population pointing to the $-z$ direction in a given material.

light in order to do so.

In this Chapter we show the equations that predict the changes in spin when a semiconductor is exposed to light, *i.e.*, an incident EM field will produce a non equilibrium spin polarization producing majority of either spin-up electrons or spin-down electrons in the material surface. In order to do so, we are going to use a semiclassical approximation to show how an observable changes due to a radiation field.

3.1 Hamiltonian of a system immersed in a radiation field

The Hamiltonian is an operator corresponding to the total energy that a system has. That is, according to the Schrödinger's equation when applying the Hamiltonian to a particular state we obtain the energy of the state. Moreover, obtaining the total energy is extremely important because it is useful to get some other quantities such as the dielectric function. *.

*Some of the results which we are going to show in this thesis are based on total energy calculations. That is, we need to get the energy in order to know other quantities. To know more about this topic you can refer to J. E. Sipe [19].

The Hamiltonian must involve all the potential and kinetic energies of the system. For example, for an electron inside a Hydrogen atom, it just has the kinetic energy term of the electron and a potential energy term due to the interaction of the electron and the nuclei. Our case is a little more complex for we have a radiating field that induces a magnetic moment on the electrons due to their intrinsic spin. Therefore, we need to find the expressions that can model our system when it is radiated by fileds with frequencies of ω and 2ω. We use these frequencies because the system will evolve by small perturbations, and for our purposes a second order approximation in the perturbation is sufficient, see Appendix C.

Our study becomes more complex because we will model a structure of atoms instead of just an isolated atom, as it was in the Hydrogen case. It is important to note that a particular electron will feel a potential due to a periodic array of nucleus and all the electrons around those nucleus. For the moment we will define the potential $\mathcal{V}$ as the sum of all the potential energy in the system. Then in the future we will consider all the potential terms involved in our structure.

In this section we will get the Hamiltonian of a system radiated by light. In other words, we will find the physical expressions that model the energy of a crystal immersed in a monochromatic field of 2ω and ω.

The first step is to describe the radiation field. We could quantize it, but, for our purposes a classical approach is sufficient. The vector potential describing the field is given by

$$\mathbf{A}(t) = \mathbf{A}(\omega)e^{-i(\omega+i\epsilon)t} + \mathbf{A}(-\omega)e^{i(\omega-i\epsilon)t} + \mathbf{A}(2\omega)e^{-i(2\omega+i\epsilon)t} + \mathbf{A}(-2\omega)e^{i(2\omega-i\epsilon)t} \tag{3.1}$$

where ϵ is a positive number that tends to zero and defines the *adiabatic turning on* . So that, when the time t tends to minus infinity the vector potential $\mathbf{A}(t)$ is zero ($\mathbf{A}(-\infty) = 0$).

The vector potential does not have a physical meaning but it is related to a physical observable. Using the Coulomb gauge the Maxwell's equations can be written in the following form [20]:

$$\Phi = 0, \tag{3.2a}$$

$$\nabla \cdot \mathbf{A} = 0, \tag{3.2b}$$

$$\mathbf{B} = \nabla \times \mathbf{A}, \tag{3.2c}$$

$$\mathbf{E} = -\frac{1}{c}\frac{\partial \mathbf{A}}{\partial t}. \tag{3.2d}$$

Substituting Eqs. (3.1) into (3.2d) we can find out that the electric field $\mathbf{E}(\omega)$ is related to the vector potential $\mathbf{A}(\omega)$ as follows:

$$\mathbf{E}(\omega) = (i\omega/c)\mathbf{A}(\omega). \tag{3.3}$$

We have described the external electric field. Then, it is time to find the Hamiltonian operator. The time-independent Hamiltonian in its general form is defined by

$$\hat{\mathcal{H}} = \frac{\hat{\mathbf{p}}^2}{2m} + \mathcal{V}, \tag{3.4}$$

where $\mathcal{V}$ is an arbitrary potential and the first term is the kinetic energy. In our case $\mathcal{V}$ is the time-independent potential due to the ions interaction inside the crystal lattice.

When an electron is inside of an electromagnetic field, the moment $\hat{\mathbf{p}}$ of the Hamiltonian has to be substituted by a generalized moment $\hat{\mathbf{p}}(t)$. That is, an electromagnetic field induces a moment $\hat{\mathbf{p}}(t)$ [21] given by:

$$\hat{\mathbf{p}}(t) = \hat{\mathbf{p}} - \frac{e}{c}\mathbf{A}(t). \tag{3.5}$$

Combining Eqs.(3.4) and (3.5) we find that

$$\hat{\mathcal{H}} = \frac{\hat{\mathbf{p}}^2}{2m} + \mathcal{V} - \frac{e}{2mc}\hat{\mathbf{p}}\cdot\mathbf{A}(t) - \frac{e}{2mc}\mathbf{A}(t)\cdot\hat{\mathbf{p}} + \frac{e}{c}\mathbf{A}^2(t). \tag{3.6}$$

We can separate the ground state Hamiltonian $\hat{\mathcal{H}}_o$ from the interaction terms as follows

$$\hat{\mathcal{H}} = \hat{\mathcal{H}}_o - \frac{e}{2mc}\hat{\mathbf{p}}\cdot\mathbf{A}(t) - \frac{e}{2mc}\mathbf{A}(t)\cdot\hat{\mathbf{p}} + \frac{e}{2mc}\mathbf{A}^2(t), \tag{3.7a}$$

$$\hat{\mathcal{H}}_o = \frac{\hat{\mathbf{p}}^2}{2m} + \mathcal{V} \tag{3.7b}$$

It is convenient to simplify Eq. (3.7a). To do so we can neglect the last term of the equation because in the case of a weak field the term $\mathbf{A}^2(t)$ is small compared with the term linear in $\mathbf{A}(t)$. That is, with ordinary light sources, the intensity is sufficiently low that the effect of the $\mathbf{A}^2(t)$ can be neglected compared to that of the $\mathbf{A}(t)$ [22]. After applying this approximation, the following expression defines the interaction Hamiltonian:

$$\hat{\mathcal{H}} = \hat{\mathcal{H}}_o - \frac{e}{2mc}\hat{\mathbf{p}}\cdot\mathbf{A}(t) - \frac{e}{2mc}\mathbf{A}(t)\cdot\hat{\mathbf{p}} \tag{3.8a}$$

Using the properties of the differential operator $\hat{\mathbf{p}}$:

$$\begin{aligned}\hat{\mathcal{H}} &= \hat{\mathcal{H}}_o - \frac{e}{2mc}\left[\mathbf{A}(t)\cdot\hat{\mathbf{p}} + (\hat{\mathbf{p}}\cdot\mathbf{A}(t))\right] - \frac{e}{2mc}\mathbf{A}(t)\cdot\hat{\mathbf{p}} \\ &= \hat{\mathcal{H}}_o - \frac{e}{mc}\mathbf{A}(t)\cdot\hat{\mathbf{p}} - \frac{e}{2mc}\hat{\mathbf{p}}\cdot\mathbf{A}(t)\end{aligned}$$

The last term is zero using the fact that $\nabla\cdot\mathbf{A}=0$ according to Eq. (3.2b). Then it follows that

$$\hat{\mathcal{H}} = \hat{\mathcal{H}}_o + \hat{\mathcal{H}}_i\,, \tag{3.8b}$$

where

$$\hat{\mathcal{H}}_i = -\frac{e}{mc}\mathbf{A}(t)\cdot\hat{\mathbf{p}} \tag{3.8c}$$

In the last equation we have find a Hamiltonian with two terms. The first one $\hat{\mathcal{H}}_o$ is the ground state Hamiltonian which represents the system at its initial state. The second one is the interaction Hamiltonian $\hat{\mathcal{H}}_i$ which defines the perturbations that the system will suffer, *i.e.*, the system experiments a transition from its initial state to an excited state due to the Hamiltonian $\hat{\mathcal{H}}_i$.

3.2 Second quantization

The second quantization (SQ) approach usually referred to as the *occupation number representation* give us the opportunity to use vector states. The first state is the ground state $|0\rangle$ which represents the system at its lower energy state where there are no excited electrons, and, there are other states representing systems with one or more excited electrons. In order to make it clearer to understand we will define the ground state as the following ket,

$$|0\rangle = |1_{v_1}, 1_{v_2}, 1_{v_3}, ..., 1_{v_{nmax}}, 0_{c_1}, 0_{c_2}, 0_{c_3}, ..., 0_{c_{nmax}}\rangle, \tag{3.9}$$

where the subindex c indicates a conduction band and a valence band is indicated by v. A filled band is represented by 1 and we set a 0 for an empty band. In such a way that 1_{v_1} indicates that the first valence band, v_1, is occupied by one electron. In the same form, there is a state representing each one of the scenarios that might exists, for example, the ket representing a system in which a transition has occurred between the third valence state and the first conduction state is:

$$|1_{v_1}, 1_{v_2}, 0_{v_3}, ..., 1_{v_{nmax}}, 1_{c_1}, 0_{c_2}, 0_{c_3}, ..., 0_{c_{nmax}}\rangle \tag{3.10}$$

In our case it will be much easier because we will define just two possible states $|0\rangle$ for the ground state system, and $|c, v, \mathbf{k}\rangle$ to indicate that a transition occurred. Therefore, this quantization approach will make easier our calculations. As shown in the Appendix A, when using SQ we can represent the ground-state Hamiltonian as [†] (A.20)

$$\hat{\mathcal{H}}_o = \sum_{c,\mathbf{k}} \hbar\omega_{c,\mathbf{k}} \hat{a}^\dagger_{c,\mathbf{k}} \hat{a}_{c,\mathbf{k}} - \sum_{v,\mathbf{k}} \hbar\omega_{v,\mathbf{k}} \hat{b}^\dagger_{v,\mathbf{k}} \hat{b}_{v,\mathbf{k}} \tag{3.11}$$

The operators $\hat{a}^\dagger$ and $\hat{a}$ are known as the creation-annihilation operators because they create or annhilate electrons respectively when applied to a certain ket. The same holds for $\hat{b}$ and $\hat{b}^\dagger$, but, instead of acting on electrons they annihilate or create holes in valence bands. For a more detailed explanation about SQ and the creation-annihilator operators read the Appendix A.

Moreover, any observable $\hat{\mathcal{O}}$ can be represented by: (see A.21)

$$\begin{aligned}\hat{\mathcal{O}} = &\sum_{c,c',\mathbf{k}} \mathcal{O}_{cc'}(\mathbf{k}) \hat{a}^\dagger_{c,\mathbf{k}} \hat{a}_{c',\mathbf{k}} + \sum_{c,v,\mathbf{k}} \mathcal{O}_{cv}(\mathbf{k}) \hat{a}^\dagger_{c\mathbf{k}} \hat{b}^\dagger_{v,\mathbf{k}} \\ &+ \sum_{v,c,\mathbf{k}} \mathcal{O}_{vc}(\mathbf{k}) \hat{b}_{v,\mathbf{k}} \hat{a}_{c,\mathbf{k}} - \sum_{v,v',\mathbf{k}} \mathcal{O}_{vv'}(\mathbf{k}) \hat{b}^\dagger_{v',\mathbf{k}} \hat{b}_{v,\mathbf{k}}\end{aligned} \tag{3.12}$$

By using this equation it can be easily shown that the interaction Hamiltonian in its SQ form has the following form [‡]:

$$\hat{\mathcal{H}}_i = -\frac{e}{mc}\mathbf{A}(t) \cdot \left\{ \begin{array}{l} \sum_{c,c',\mathbf{k}} \mathbf{p}_{cc'}(\mathbf{k}) \hat{a}^\dagger_{c,\mathbf{k}} \hat{a}_{c',\mathbf{k}} e^{i(\omega_{cc'})t} \\ + \sum_{c,v,\mathbf{k}} \mathbf{p}_{cv}(\mathbf{k}) \hat{a}^\dagger_{c,\mathbf{k}} \hat{b}^\dagger_{v,\mathbf{k}} e^{i(\omega_{cv})t} \\ + \sum_{c,v,\mathbf{k}} \mathbf{p}_{vc}(\mathbf{k}) \hat{b}_{v,\mathbf{k}} \hat{a}_{c,\mathbf{k}} e^{i(\omega_{vc})t} \\ - \sum_{v,v',\mathbf{k}} \mathbf{p}_{vv'}(\mathbf{k}) \hat{b}^\dagger_{v',\mathbf{k}} \hat{b}_{v,\mathbf{k}} e^{i(\omega_{vv'})t} \end{array} \right\}, \tag{3.13}$$

where $\omega_{ab} = \omega_a - \omega_b$.

[†] The subindex $\mathbf{k}$, usually refered to as the plane wave vector (or Bloch wave vector), represents a vector in reciprocal space. It is repeated an infinite number of times over a periodic lattice, but, it is unique up to a reciprocal lattice. Thus, we only need to consider the wave vector inside the first Brillouin zone. It is proportional to the particle crystal momentum, that is, if it is multiplied by the reduced Planck's constant we get the particle crystal momentum.

For more details on reciprocal lattices see [11]. We use n to refer to an arbitrary band while c and v are for conduction and valence bands respectively.

[‡] A formal deduction of this equation can be found in Appendix B. See Eq. (B.17)

In conclusion, SQ is a scheme that permit us to reduce our problem to a set of equations in which the creation-annihilation operators are used. The algebra associated with this operators is simple. Therefore, we are going to use the operators in their SQ form in order to simplify our future calculations.

3.3 Probability of transitions

Let us consider that we want to measure a particular property of a material using optics; first we need to project light to the material, lets say a laser light with frequency ω. As the ray of light touches the surface of the material, some effects will be observed on the material. At this point, we have to measure these responses and we will be able to find the optical properties of the material.

Let us see the microscopic point of view of this imaginary experiment. We know by Planck's quantization of light that it is composed of small particles of energy $\hbar\omega$. When these particles are launched into a semiconductor surface they will transfer their energy and momentum to the electrons in the material. When doing so, the electrons that were located in a valence band v will be raised to a higher energy band called a conduction band c provided that $E_{cv} = \hbar\omega$. This is called a *transition*. These transitions will cause the material to change to an excited state and to experiment changes that we can measure.

Therefore, it is extremely important to find the probability of these transitions in order to know how the material will be affected after it is radiated. Moreover, by doing this we will be able to find other properties of the material, *e. g.*, transitions that are responsible of the response that the material can have.

We start by defining the ket $|0\rangle$ to represent the system in its ground state, and, the ket $|c, v, \mathbf{k}\rangle$ to represent the system in an excited state. $|c, v, \mathbf{k}\rangle$ indicates that an electron has experimented a transition from v to c in a particular $\mathbf{k}$-point. We need to know the $\mathbf{k}$-point where it happens because $\mathbf{k}$-points are crystal locations in reciprocal space.

In our ideal model the system will be made up of two states: it can be either in $|c, v, \mathbf{k}\rangle$ or in $|0\rangle$. These two states form a complete base because they are the only possible states and because they are mutually orthogonal. In other words, if the system is known to be at state $|0\rangle$ at time t it cannot be at $|c, v, \mathbf{k}\rangle$ at the same time and vice versa. Having these ideas in mind, we can divide the system

$|\psi\rangle$ into two possible states $|0\rangle$ and $|c, v, \mathbf{k}\rangle$ as follows:

$$|\psi\rangle = \mathcal{C}_o(t)|0\rangle + \mathcal{C}_{c,v,\mathbf{k}}(t)|c, v, \mathbf{k}\rangle. \tag{3.14}$$

The probability of being at state $|\psi(t)\rangle$ is represented by $|\psi(t)|^2$ where $|\psi(t)|^2 = \langle\psi(t)|\psi(t)\rangle$. With this definition and using Eq. (3.14) we find that:

$$|\psi(t)|^2 = |\mathcal{C}_o(t)|^2 + |\mathcal{C}_{c,v,\mathbf{k}}(t)|^2. \tag{3.15}$$

This equation is helpful because we can see that $|\mathcal{C}_o|^2$ is the probability of being at state $|0\rangle$ while $|\mathcal{C}_{c,v,\mathbf{k}}|^2$ is that of being at state $|c, v, \mathbf{k}\rangle$. Summing both we find the probability of being at any state $|\psi(t)|^2 = 1$.

Having two arbitrary states $|a\rangle$ and $b\rangle$ we will define $\langle a|b\rangle$ as the probability of passing from the state $|b\rangle$ to the state $|a\rangle$. This cannot be proven for it is one of the quantum mechanics postulates [23]. By using this definition we find out that the probability of experimenting a transition to an excited state is:

$$\langle c, v, \mathbf{k}|\psi(t)\rangle = \mathcal{C}_{c,v,\mathbf{k}}(t). \tag{3.16}$$

Now we are going to give another form to this probability coefficient $\mathcal{C}_{c,v,\mathbf{k}}(t)$. In perturbations theory the ground state $|0\rangle$ evolves by small perturbations, that can be represented by a unitary operator $\hat{U}$, in order to get the system at its final state $\psi(t)$, from Appendix C:

$$|\psi(t)\rangle = \hat{U}(t)|0\rangle. \tag{3.17}$$

then by using Eqs. (C.14) and (3.16) we can obtain[§]:

$$\mathcal{C}_{c,v,\mathbf{k}}(t) \quad = \quad \langle c, v, \mathbf{k}|e^{-i\frac{\hat{\mathcal{H}}_o t}{\hbar}}\hat{U}_{int}(t)|0\rangle, \tag{3.18a}$$

$$\hat{U}_{int}(t) = 1 + \frac{1}{i\hbar}\int_{-\infty}^{t} \hat{\mathcal{H}}_{iI}(t')\ \mathrm{d}t' + \frac{1}{(i\hbar)^2}\int_{-\infty}^{t} \mathrm{d}t' \int_{-\infty}^{t'} \mathrm{d}t''\ \hat{\mathcal{H}}_{iI}(t')\hat{\mathcal{H}}_{iI}(t'') + ..., \tag{3.18b}$$

where,

$$\hat{\mathcal{H}}_{iI}(t) = \hat{U}_o^{\dagger}(t)\hat{\mathcal{H}}_i(t)\hat{U}_o(t) \tag{3.18c}$$

[§]A complete deduction of these equations can be found in the Appendix C.

When the ground state Hamiltonian $\hat{\mathcal{H}}_o$ acts on the ground state $|0\rangle$ it give us the minimum energy of the system E_o, where it follows that $e^{-i\frac{\hat{\mathcal{H}}_o t}{\hbar}}|0\rangle = e^{\frac{-iE_o t}{\hbar}}|0\rangle$. Then we can observe that the first term of Eq. (3.18a) is zero because all the states of the system were defined to be orthogonal, leading to the following relation: $\langle c, v, \mathbf{k}|0\rangle = 0$.

Dividing the terms in Eq. (3.18a) by order of perturbation, we can find n-order approximations. We define $\mathcal{C}^{(1)}_{c,v,\mathbf{k}}(t)$ as the first order approximation in order to say that the system was affected by $\hat{\mathcal{H}}_{iI}$ just once, and the second order approximation as $\mathcal{C}^{(2)}_{c,v,\mathbf{k}}(t)$:

$$\mathcal{C}^{(1)}_{c,v,\mathbf{k}}(t) = \frac{1}{i\hbar}\langle c, v, \mathbf{k}|e^{-i\frac{\hat{\mathcal{H}}_o t}{\hbar}} \int_{-\infty}^{t} \mathrm{d}t' \hat{\mathcal{H}}_i(t')|0\rangle, \tag{3.19a}$$

$$\mathcal{C}^{(2)}_{c,v,\mathbf{k}}(t) = \frac{1}{(i\hbar)^2}\langle c, v, \mathbf{k}|e^{-i\frac{\hat{\mathcal{H}}_o t}{\hbar}} \int_{-\infty}^{t} \mathrm{d}t' \int_{-\infty}^{t'} \mathrm{d}t'' \ \hat{\mathcal{H}}_i(t')\hat{\mathcal{H}}_i(t'')|0\rangle. \tag{3.19b}$$

In conclusion, we have found the explicit equations that give us the probability of experimenting a transition from a lower energy band to a higher energy band, up to second order, since it is enough for our purposes.¶

3.4 Carrier and spin population

We will decompose the time evolution of an operator $\mathrm{d}\langle\hat{\mathcal{O}}\rangle/\mathrm{d}t$ due to excitations caused by one photon of 2ω, two photons of ω and the interaction between both excitations. That is,

$$\frac{\mathrm{d}\langle\hat{\mathcal{O}}\rangle}{\mathrm{d}t} = \frac{\mathrm{d}\langle\hat{\mathcal{O}}\rangle_1}{\mathrm{d}t} + \frac{\mathrm{d}\langle\hat{\mathcal{O}}\rangle_2}{\mathrm{d}t} + \frac{\mathrm{d}\langle\hat{\mathcal{O}}\rangle_I}{\mathrm{d}t}, \tag{3.20}$$

where the subindex 1 refers to transitions caused by one photon, the subindex 2 to transitions caused by two photons and I to the interaction between both of them.

¶Numerous studies that use a perturbative approach have shown that experimental results can be reproduced by taking into account up to a second order in the perturbation. See [24,25].

Now, using the second quantized form of a state $|\psi(t)\rangle$ (Eq. (3.14)) we find out that,

$$\frac{\mathrm{d}\langle\hat{\mathcal{O}}\rangle}{\mathrm{d}t} = \frac{\mathrm{d}\langle\psi'|\hat{\mathcal{O}}|\psi\rangle}{\mathrm{d}t} = \frac{\mathrm{d}}{\mathrm{d}t}\sum_{c,v,\mathbf{k}}\sum_{c',v',\mathbf{k}'}\mathcal{C}^*_{c',v',\mathbf{k}'}\mathcal{C}_{c,v,\mathbf{k}}\langle c',v',\mathbf{k}'|\hat{\mathcal{O}}|c,v,\mathbf{k}\rangle, \tag{3.21}$$

where $\mathcal{C}_{c,v,\mathbf{k}}$ is the probability of an electron undergoing a transition defined by Eqs. (3.19).

The operators for carrier density $\hat{n}$ and spin density $\hat{S}^a$ are defined as

$$\hat{n} = \frac{1}{V}\sum_{\mathbf{k}}\hat{n}(\mathbf{k}), \tag{3.22}$$

$$\hat{S}^a = \frac{1}{V}\sum_{\mathbf{k}}\hat{S}^a(\mathbf{k}), \tag{3.23}$$

where ,

$$\hat{n}(\mathbf{k}) = \sum_{c}\hat{a}^\dagger_{c,\mathbf{k}}\hat{a}_{c,\mathbf{k}}, \tag{3.24}$$

$$\hat{S}^a(\mathbf{k}) = \sum_{c,c'}S^a_{c'c}(\mathbf{k})\hat{a}^\dagger_{c',\mathbf{k}}\hat{a}_{c,\mathbf{k}}, \tag{3.25}$$

and, the superscript a denotes a cartesian component and V refers to the volume of the unit cell. Here the spin density operator $\hat{S}^a$ is constructed by the Pauli matrices:

$$\hat{S}^a = \frac{\hbar}{2}\sigma^a \tag{3.26a}$$

$$\sigma^x = \frac{1}{2}\begin{pmatrix} 0 & 1 \\ 1 & 0 \end{pmatrix}\ ,\ \sigma^y = \frac{1}{2}\begin{pmatrix} 0 & -i \\ i & 0 \end{pmatrix}\ ,\ \sigma^z = \frac{1}{2}\begin{pmatrix} 1 & 0 \\ 0 & -1 \end{pmatrix} \tag{3.26b}$$

From Eq. (3.20) it follows that

$$\frac{\mathrm{d}\langle\hat{n}\rangle}{\mathrm{d}t} = \frac{\mathrm{d}\langle\hat{n}\rangle_1}{\mathrm{d}t} + \frac{\mathrm{d}\langle\hat{n}\rangle_2}{\mathrm{d}t} + \frac{\mathrm{d}\langle\hat{n}\rangle_I}{\mathrm{d}t} \tag{3.27a}$$

$$\frac{\mathrm{d}\langle\hat{S}^a\rangle}{\mathrm{d}t} = \frac{\mathrm{d}\langle\hat{S}^a\rangle_1}{\mathrm{d}t} + \frac{\mathrm{d}\langle\hat{S}^a\rangle_2}{\mathrm{d}t} + \frac{\mathrm{d}\langle\hat{S}^a\rangle_I}{\mathrm{d}t} \tag{3.27b}$$

Starting with the one photon (2ω) contributions, it will be shown in the Appendix D that [‖]

$$\frac{\mathrm{d}\langle\hat{n}\rangle_1}{\mathrm{d}t} = \xi_1^{bc}(2\omega)E^{b*}(2\omega)E^{c}(2\omega), \tag{3.28a}$$

$$\frac{\mathrm{d}\langle\hat{S}^a\rangle_1}{\mathrm{d}t} = \zeta_1^{abc}(2\omega)E^{b*}(2\omega)E^{c}(2\omega), \tag{3.28b}$$

where,

$$\xi_1^{bc}(2\omega) = \frac{1}{V}\sum_{\mathbf{k}} \xi_1^{bc}(2\omega;\mathbf{k}), \tag{3.28c}$$

$$\zeta_1^{abc}(2\omega) = \frac{1}{V}\sum_{\mathbf{k}} \zeta_1^{abc}(2\omega;\mathbf{k}), \tag{3.28d}$$

and,

$$\xi_1^{bc}(2\omega;\mathbf{k}) = \frac{2\pi e^2}{\hbar^2}\sum_{c,v}\frac{\mathbf{v}_{cv}^{b*}(\mathbf{k})\mathbf{v}_{cv}^{c}(\mathbf{k})}{(2\omega)^2}\delta(2\omega-\omega_{cv}(\mathbf{k})) \tag{3.28e}$$

$$\zeta_1^{abc}(2\omega;\mathbf{k}) = \frac{2\pi e^2}{\hbar^2}\sum_{c,v}\frac{S_{c'c}^{a}(\mathbf{k})\mathbf{v}_{c'v}^{b*}(\mathbf{k})\mathbf{v}_{cv}^{c}(\mathbf{k})}{(2\omega)^2}\delta(2\omega-\omega_{cv}(\mathbf{k})) \tag{3.28f}$$

where the super-indices indicate cartesian components, and repeated indices are summed. Here $\mathbf{v}_{ab}$ are velocity matrix elements which are calculated as it is explained in Appendix E.

In order to construct the two photon contributions we use the Eq. (3.20) and we substitute Eq. (3.19) into (3.21) to get:

$$\frac{\mathrm{d}\langle\hat{n}\rangle_2}{\mathrm{d}t} = \xi_2^{bcdf}(\omega)E^{b*}(\omega)E^{c*}(\omega)E^{d}(\omega)E^{f}(\omega), \tag{3.29a}$$

$$\frac{\mathrm{d}\langle\hat{S}^a\rangle_2}{\mathrm{d}t} = \zeta_2^{abcdf}(\omega)E^{b*}(\omega)E^{c*}(\omega)E^{d}(\omega)E^{f}(\omega), \tag{3.29b}$$

where,

$$\xi_2^{bcdf}(\omega) = \frac{1}{V}\sum_{\mathbf{k}} \xi_2^{bcdf}(\omega;\mathbf{k}),$$

$$\zeta_2^{abcdf}(\omega) = \frac{1}{V}\sum_{\mathbf{k}} \zeta_2^{abcdf}(\omega;\mathbf{k}), \tag{3.29c}$$

[‖] All of the following expressions will be demonstrated in the Appendix D. They were originally proposed by Ali Najmaie *et al.* see [18].

and,

$$\xi_2^{bcdf}(\omega;\mathbf{k}) = \frac{2\pi e^4}{\hbar^4}\sum_{c,v,n,m}\frac{\mathbf{v}_{cm}^{b*}(\mathbf{k})\mathbf{v}_{mv}^{c*}(\mathbf{k})\mathbf{v}_{cn}^{d}(\mathbf{k})\mathbf{v}_{nv}^{f}(\mathbf{k})}{\omega^4\left[\omega_{cv}(\mathbf{k})/2+\omega_{vn}(\mathbf{k})\right]\left[\omega_{c'v}(\mathbf{k})/2+\omega_{vm}(\mathbf{k})\right]} \times\delta(2\omega-\omega_{cv}(\mathbf{k})), \tag{3.29d}$$

$$\zeta_2^{abcdf}(\omega;\mathbf{k}) = \frac{2\pi e^4}{\hbar^4}\sum_{c,c',v,n,m}\frac{S_{c'c}^{a}(\mathbf{k})\mathbf{v}_{c'm}^{b*}(\mathbf{k})\mathbf{v}_{mv}^{c*}(\mathbf{k})\mathbf{v}_{cn}^{d}(\mathbf{k})\mathbf{v}_{nv}^{f}(\mathbf{k})}{\omega^4\left[\omega_{cv}(\mathbf{k})/2+\omega_{vn}(\mathbf{k})\right]\left[\omega_{c'v}(\mathbf{k})/2+\omega_{vm}(\mathbf{k})\right]} \times\delta(2\omega-\omega_{cv}(\mathbf{k})). \tag{3.29e}$$

The interaction terms,

$$\frac{\mathrm{d}\langle\hat{n}\rangle_I}{\mathrm{d}t} = \xi_I^{bcd}(\omega)E^{b*}(\omega)E^{c*}(\omega)E^{d}(2\omega)+c.c., \tag{3.30a}$$

$$\frac{\mathrm{d}\langle\hat{S}^a\rangle_I}{\mathrm{d}t} = \zeta_I^{abcd}(\omega)E^{b*}(\omega)E^{c*}(\omega)E^{d}(2\omega)+c.c., \tag{3.30b}$$

where *c.c.* stands for *complex conjugate* and the pseudo-tensors ζ_I^{bcd} and ξ_I^{abcd} are determined by

$$\xi_I^{bcd}(\omega) = \frac{1}{V}\sum_{\mathbf{k}}\xi_I^{bcd}(\omega;\mathbf{k}),$$
$$\zeta_I^{abcd}(\omega) = \frac{1}{V}\sum_{\mathbf{k}}\zeta_I^{abcd}(\omega;\mathbf{k}), \tag{3.30c}$$

where,

$$\xi_I^{bcd}(\omega;\mathbf{k}) = -i\frac{\pi e^3}{\hbar^3}\sum_{c,v,n}\frac{\mathbf{v}_{cn}^{b*}(\mathbf{k})\mathbf{v}_{nv}^{c*}(\mathbf{k})\mathbf{v}_{cv}^{d}(\mathbf{k})}{\omega^3\left[\omega_{cv}(\mathbf{k})/2+\omega_{vn}(\mathbf{k})\right]} \times\delta(2\omega-\omega_{cv}(\mathbf{k})), \tag{3.30d}$$

$$\zeta_I^{abcd}(\omega;\mathbf{k}) = -i\frac{\pi e^3}{\hbar^3}\sum_{c,c',v,n}\frac{S_{c'c}^{a}(\mathbf{k})\mathbf{v}_{cn}^{b*}(\mathbf{k})\mathbf{v}_{nv}^{c*}(\mathbf{k})\mathbf{v}_{c'v}^{d}(\mathbf{k})}{\omega^3\left[\omega_{cv}(\mathbf{k})/2+\omega_{vn}(\mathbf{k})\right]} \times\delta(2\omega-\omega_{cv}(\mathbf{k})). \tag{3.30e}$$

You may notice that all these results have a Dirac's delta $\delta(2\omega-\omega_{cv}(\mathbf{k}))$. This is expected because a transition is only allowed when the frequency of the

incident photon is equal to the energy size of the band gap. In our case, it has to be equal to 2ω because we are focusing on the second harmonic. Moreover, it can be seen explicitly from Eq. (D.26) that our results are coherent with the Fermi's Golden Rule [23]. That is, in order to have a transition we need to have a coupling between the initial and final band and the frequency of the incident photon has to be equal to the difference of energies between both bands. Finally, we have arrived to coherent expressions that show the spin and carrier population responses due to an incident field of frequencies ω and 2ω.

3.5 Electrical and spin currents

Using a similar approach we can calculate the electrical and spin currents injected in a material. We employ the electrical current density $\hat{\mathbf{J}}^a$ and spin current density

$$\hat{K}^{ab} = \hat{\mathbf{v}}^b \hat{S}^a \tag{3.31}$$

operators, defined as:

$$\begin{aligned} \hat{\mathbf{J}}^a &= \frac{1}{V}\sum_{\mathbf{k}} \hat{\mathbf{J}}^a(\mathbf{k}), \\ \hat{K}^{ab} &= \frac{1}{V}\sum_{\mathbf{k}} \hat{K}^{ab}(\mathbf{k}), \end{aligned} \tag{3.32}$$

where

$$\begin{aligned} \hat{\mathbf{J}}^a(\mathbf{k}) &= e\sum_{c,c'} \mathbf{v}^a_{c,c'}(\mathbf{k})\hat{a}^\dagger_{c',\mathbf{k}}\hat{a}_{c,\mathbf{k}}, \\ \hat{K}^{ab}(\mathbf{k}) &= \sum_{c,c'} \hat{K}^{ab}_{c,c'}(\mathbf{k})\hat{a}^\dagger_{c',\mathbf{k}}\hat{a}_{c,\mathbf{k}}. \end{aligned} \tag{3.33}$$

Here the operator $\hat{\mathbf{v}}$ is the velocity operator.

Following the same steps we took to obtain Eq. (3.27), we get

$$\frac{\mathrm{d}\langle\hat{\mathbf{J}}^a\rangle}{\mathrm{d}t} = \frac{\mathrm{d}\langle\hat{\mathbf{J}}^a\rangle_1}{\mathrm{d}t} + \frac{\mathrm{d}\langle\hat{\mathbf{J}}^a\rangle_2}{\mathrm{d}t} + \frac{\mathrm{d}\langle\hat{\mathbf{J}}^a\rangle_I}{\mathrm{d}t} \tag{3.34a}$$

$$\frac{\mathrm{d}\langle\hat{K}^{ab}\rangle}{\mathrm{d}t} = \frac{\mathrm{d}\langle\hat{K}^{ab}\rangle_1}{\mathrm{d}t} + \frac{\mathrm{d}\langle\hat{K}^{ab}\rangle_2}{\mathrm{d}t} + \frac{\mathrm{d}\langle\hat{K}^{ab}\rangle_I}{\mathrm{d}t} \tag{3.34b}$$

In this case the terms for one-photon excitations are:

$$\frac{\mathrm{d}\langle\hat{\mathbf{J}}^a\rangle_1}{\mathrm{d}t} = \eta_1^{acd}(2\omega)E^{c*}(2\omega)E^d(2\omega), \tag{3.35a}$$

$$\frac{\mathrm{d}\langle\hat{K}^{ab}\rangle_1}{\mathrm{d}t} = \mu_1^{abcd}(2\omega)E^{c*}(2\omega)E^d(2\omega), \tag{3.35b}$$

where,

$$\eta_1^{acd}(2\omega) = \frac{1}{V}\sum_{\mathbf{k}}\eta_1^{acd}(2\omega;\mathbf{k}), \tag{3.35c}$$

$$\mu_1^{abcd}(2\omega) = \frac{1}{V}\sum_{\mathbf{k}}\mu_1^{abcd}(2\omega;\mathbf{k}), \tag{3.35d}$$

and,

$$\eta_1^{acd}(2\omega;\mathbf{k}) = \frac{2\pi e^3}{\hbar^2}\sum_{c,v}\frac{\mathbf{v}^a_{c'c}(\mathbf{k})\mathbf{v}^{c*}_{c'v}(\mathbf{k})\mathbf{v}^d_{cv}(\mathbf{k})}{(2\omega)^2}\delta(2\omega-\omega_{cv}(\mathbf{k})), \tag{3.35e}$$

$$\mu_1^{abcd}(2\omega;\mathbf{k}) = \frac{2\pi e^2}{\hbar^2}\sum_{c,v}\frac{K^{ab}_{c'c}(\mathbf{k})\mathbf{v}^{c*}_{c'v}(\mathbf{k})\mathbf{v}^d_{cv}(\mathbf{k})}{(2\omega)^2}\delta(2\omega-\omega_{cv}(\mathbf{k})). \tag{3.35f}$$

The two-photon terms are:

$$\frac{\mathrm{d}\langle\hat{\mathbf{J}}^a\rangle_2}{\mathrm{d}t} = \eta_2^{acdfg}(\omega)E^{c*}(\omega)E^{d*}(\omega)E^f(\omega)E^g(\omega), \tag{3.36a}$$

$$\frac{\mathrm{d}\langle\hat{K}^{ab}\rangle_2}{\mathrm{d}t} = \mu_2^{acdfg}(\omega)E^{c*}(\omega)E^{d*}(\omega)E^f(\omega)E^g(\omega), \tag{3.36b}$$

where,

$$\eta_2^{acdfg}(\omega) = \frac{1}{V}\sum_{\mathbf{k}}\eta_2^{acdfg}(\omega;\mathbf{k}),$$

$$\mu_2^{abcdfg}(\omega) = \frac{1}{V}\sum_{\mathbf{k}}\mu_2^{abcdfg}(\omega;\mathbf{k}), \tag{3.36c}$$

and,

$$\eta_2^{acdfg}(\omega) = \frac{2\pi e^5}{\hbar^4}\sum_{c,c',v,n,m}\frac{\mathbf{v}^a_{c'c}(\mathbf{k})\mathbf{v}^{c*}_{c'm}(\mathbf{k})\mathbf{v}^{d*}_{mv}(\mathbf{k})\mathbf{v}^f_{cn}(\mathbf{k})\mathbf{v}^g_{nv}(\mathbf{k})}{\omega^4\left[\omega_{cv}(\mathbf{k})/2+\omega_{vn}(\mathbf{k})\right]\left[\omega_{c'v}(\mathbf{k})/2+\omega_{vm}(\mathbf{k})\right]} \times\delta(2\omega-\omega_{cv}(\mathbf{k})), \tag{3.36d}$$

$$\mu_2^{abcdfg}(\omega) = \frac{2\pi e^4}{\hbar^4}\sum_{c,c',v,n,m}\frac{K^{ab}_{c'c}(\mathbf{k})\mathbf{v}^{c*}_{c'm}(\mathbf{k})\mathbf{v}^{d*}_{mv}(\mathbf{k})\mathbf{v}^f_{cn}(\mathbf{k})\mathbf{v}^g_{nv}(\mathbf{k})}{\omega^4\left[\omega_{cv}(\mathbf{k})/2+\omega_{vn}(\mathbf{k})\right]\left[\omega_{c'v}(\mathbf{k})/2+\omega_{vm}(\mathbf{k})\right]} \times\delta(2\omega-\omega_{cv}(\mathbf{k})). \tag{3.36e}$$

The interaction terms are:

$$\frac{\mathrm{d}\langle\hat{\mathbf{J}}^a\rangle_I}{\mathrm{d}t} = \eta_I^{acdf}(\omega)E^{c*}(\omega)E^{d*}(\omega)E^f(2\omega)+c.c., \tag{3.37a}$$

$$\frac{\mathrm{d}\langle\hat{K}^{ab}\rangle_I}{\mathrm{d}t} = \mu_I^{abcdf}(\omega)E^{c*}(\omega)E^{d*}(\omega)E^f(2\omega)+c.c., \tag{3.37b}$$

where,

$$\eta_I^{acdf}(\omega) = \frac{1}{V}\sum_{\mathbf{k}}\xi_I^{acdf}(\omega;\mathbf{k}),$$
$$\mu_I^{abcdf}(\omega) = \frac{1}{V}\sum_{\mathbf{k}}\zeta_I^{abcdf}(\omega;\mathbf{k}), \tag{3.37c}$$

and,

$$\eta_I^{acdf}(\omega) = -i\frac{\pi e^4}{\hbar^3}\sum_{c,c',v,n}\frac{\mathbf{v}^a_{c,c'}(\mathbf{k})\mathbf{v}^{c*}_{c'n}\mathbf{v}^{d*}_{nv}(\mathbf{k})\mathbf{v}^f_{cv}(\mathbf{k})}{\omega^3\left[\omega_{cv}(\mathbf{k})/2+\omega_{vn}(\mathbf{k})\right]}\delta(2\omega-\omega_{cv}(\mathbf{k})), \tag{3.37d}$$

$$\mu_I^{abcdf}(\omega) = -i\frac{\pi e^3}{\hbar^3}\sum_{c,c',v,n}\frac{K^{ab}_{c,c'}(\mathbf{k})\mathbf{v}^{c*}_{c'n}(\mathbf{k})\mathbf{v}^{d*}_{nv}(\mathbf{k})\mathbf{v}^f_{cv}(\mathbf{k})}{\omega^3\left[\omega_{cv}(\mathbf{k})/2+\omega_{vn}(\mathbf{k})\right]}\delta(2\omega-\omega_{cv}(\mathbf{k})). \tag{3.37e}$$

All in all, we have obtained the general expressions that we will use to calculate the carriers and spin current injection into a GaAs[110] surface. As you may notice, we need to find the velocity matrix elements, $\mathbf{v}_{ab}$, as well as, the spin matrix elements, S_{bc}. To do so we must find the system wave function by using several approximations explained in Chapter 2.

Chapter 4

Injection process in GaAs(110)

In this chapter our goal is to determine the correct value of the variables to be used in our future calculations. First, we need to ensure that our results will converge. Second, we have to make sure that our calculations will not consume a huge amount of resources. For example, if we choose a large set of **k**-points the wave function can get extremely big, so that we cannot manage it. Thus, it is important to choose the correct values of the variables in order to make calculations feasible.

It is interesting to study the GaAs(110) surface because it contains equal number of Ga and As atoms; other surface planes in this crystal contain only one of the two species of atoms present in the crystal. Bulk and surface views of GaAs are shown in Figure 4.1.

As it was explained in Chapter 2, we use the Bloch's theorem to solve the Schrödinger equation for a periodic system. However, a surface is not periodic. The question that arises is: how are we going to solve the Schrödinger equation if our slab is not periodic?

The answer is simple, we will repeat the slab an infinite number of times and treat it as an infinite slab. The only restriction we have is that slabs must not interact among them. To overcome this problem we introduce a vacuum between each consecutive slabs. The vacuum size will be chosen according to a convergence study that will be shown in later in this chapter.

Once we choose the vacuum size we have to set a value for other variables, such as the cutoff-energy and the size of the **k**-point set among others. This is not trivial, for instance, if we choose a small cutoff-energy the results may be

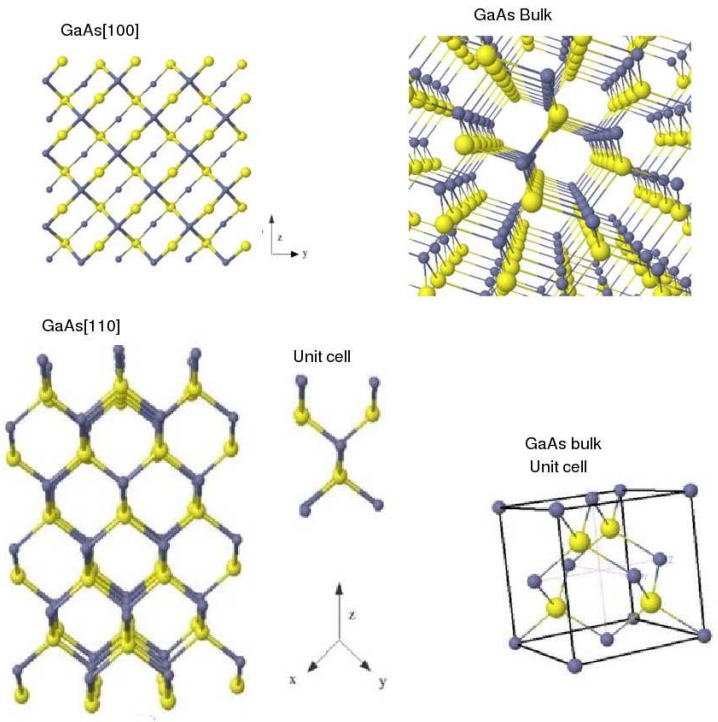

Figure 4.1 : Graphic representation of the GaAs crystal. The Gallium and Arsenide atoms are represented with blue and yellow balls spheres respectively. At the **top left corner** we find the GaAs(100) surface. At the **top right corner** we show a representation of the infinite bulk structure. At the **bottom left corner** the GaAs(110) surface along with its unit cell are shown. At the **bottom right corner** we show the unit cell of the GaAs bulk.

wrong, and, as we increase this value the calculations start to converge while the computation time increases. Thus, a convergence study must be done to ensure that our calculations will be correct and that they will not consume many resources.

4.1 Non-periodic slab

Bloch's theorem cannot be employed when we have a non-periodic system, i.e., it cannot be employed neither in the perpendicular direction of a crystal surface not in a slab which has a defect [5]. However, we can construct a super-cell from a non-periodic slab and repeat it an infinite number of times changing the problem to one of a periodic super-cell.

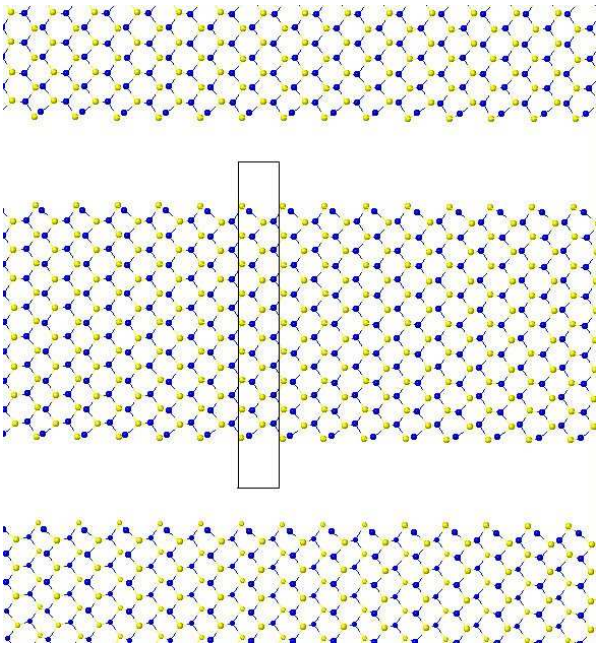

Figure 4.2 : GaAs(110) super-cell. The super-cell is composed of the atoms and vacuum delimited by the rectangle shown in the picture. This cell is repeated an infinite number of times to conform an infinite slab. The Gallium atoms are represented by blue spheres while the arsenic atoms are represented by yellow spheres.

The super-cell is made of non-periodic slabs and vacuum spaces among them. They are arranged periodically so that we can employ the Bloch's theorem. The vacuum among slabs is chosen sufficiently big so that the surfaces do not interact between two different slabs.

For the GaAs(110) surface we constructed a super-cell made of slabs with a fixed number of layers and a vacuum among all slabs. The vacuum size and the number of layers in the slab will be fixed to a certain value. But, it will be discussed later on this chapter. Fig. 4.2 shows a representation of the GaAs(110) super-cell we used in our calculations.

4.2 Relaxation

There is a notable difference between the atoms at the bulk and the atoms at the surface of a semiconductor. Each atom in the material is exposed to a potential due to all the other ions. Moreover, the atoms at the surface are surrounded by less ions than those at the bulk. Thus, the potential that an ion in the surface feels is different from the potential at which a bulk ion is exposed.

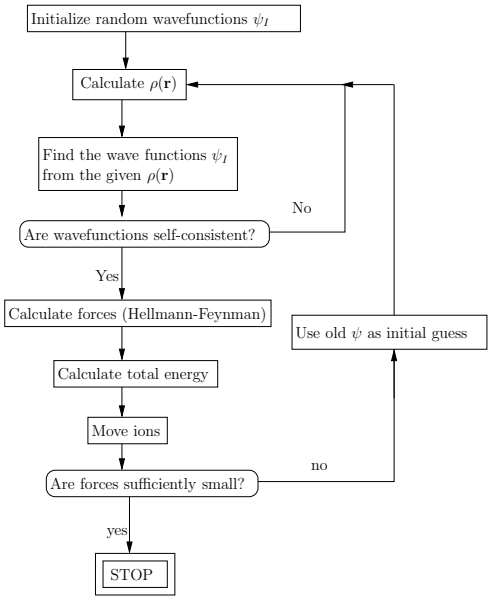

Figure 4.3 : Diagram showing the relaxation process used in *ab initio* simulations. Source [26]

This potential difference makes the ions at the surface move from their ideal positions to a minimum energy position. We usually refer to this process as the *ionic relaxation*. In other words, the transition of an atom or molecule from a higher energy level to a lower one is known as *relaxation*.

We can model the ionic relaxation by using full dynamical simulation in which we will find the path that the ions follow to get to their minimum energy position. On the other hand, we can simplify the process by following a different path if we arrive to the same final position. This can be done because of the fact that only the final stage is important and the path we follow is irrelevant for our pourposes.

The relaxation process can be achieved by following the next steps: First, we find the wave function of the system for a given ionic coordinates. Then we calculate forces among ions using the Hellmann-Feynman theorem, which will be explained later. We proceed to move the ions and recalculate forces until we find the minimum-energy position [5]. The whole process is shown in Fig. 4.3.*

The relaxation procedure for the GaAs[100] surface is shown in Fig. 4.4. The

*There are many variables to consider when moving the ions in order to find the minium energy state. But, we will not discuss this point in this work. For instance, we can use the Hellmann-Feynman forces to find the position of a local energy minimum. To know more on this topic please refer to Payne *et al.* [5].

atoms at their initial positions suffer a series of displacements to get to their minimum energy position. The initial positions are shown at the top while their final positions are shown at the bottom. As you may notice the atoms closer to the vacuum suffered bigger displacements. This is due to the fact that the atoms close to the vacuum are surface atoms while the other ones are bulk atoms.

4.2.1 Hellmann-Feynman theorem

The Hellmann-Feynman theorem will be used to calculate the forces acting on the ions. It uses the wave functions calculated on a previous step, so that, we have to find the total energies before proceeding to this point. What is more, it is near to its classical counterpart, that is, the forces are calculated in a similar way as it is done in classical mechanics.

Theorem 2 (Hellmann-Feynman) *Once the spatial distribution of the electron clouds has been determined by solving the Schrödinger equation, the intermolecular forces may be calculated on the basis of straightforward classical electrostatics.*

Classically, the force $\mathbf{F}$ acting on a particle at $\mathbf{R}$ is given by the derivative of the potential energy:

$$\mathbf{F} = -\nabla_{\mathbf{R}} V(\mathbf{R}) \tag{4.1}$$

In quantum mechanics we might expect to have an equivalent expression for the force $\mathbf{F}$.

$$\mathbf{F} = -\nabla_{\mathbf{r}} \langle E \rangle, \tag{4.2a}$$

where

$$\langle E \rangle = \langle \psi | \hat{\mathcal{H}} | \psi \rangle \tag{4.2b}$$

In fact, the Hellmann-Feynman theorem [27] states that once the wave functions ψ have been calculated we can find the force $\mathbf{F}_I$ acting at a particular particle on the system, by

$$\mathbf{F}_I = \frac{\partial E}{\partial \mathbf{R}_I} = \langle \psi | \frac{\partial \hat{\mathcal{H}}}{\partial \mathbf{R}_I} | \psi \rangle. \tag{4.3}$$

The Hellmann-Feynman theorem can be easily demonstrated as follows: Expanding the derivative over the position $\mathbf{R}_I$,

$$\frac{\partial E}{\partial \mathbf{R}_I} = \langle \frac{\partial \psi}{\partial \mathbf{R}_I} | \hat{\mathcal{H}} | \psi \rangle + \langle \psi | \frac{\partial \hat{\mathcal{H}}}{\partial \mathbf{R}_I} | \psi \rangle + \langle \psi | \hat{\mathcal{H}} | \frac{\partial \psi}{\partial \mathbf{R}_I} \rangle \tag{4.4}$$

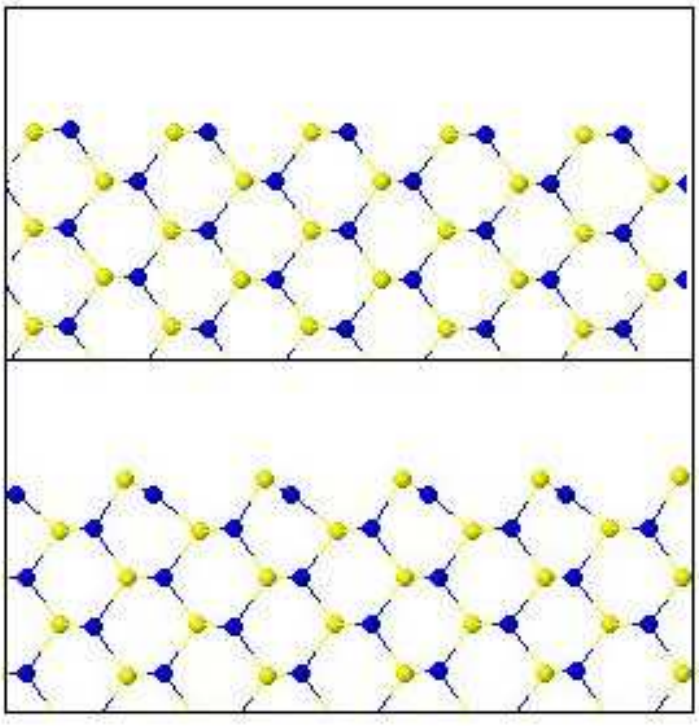

Figure 4.4 : Relaxation of the GaAs(110) surface. The atoms at their ideal positions (top) were moved to their minimum energy positions (bottom). The yellow and blue spheres represent arsenic and gallium atoms respectively.

If E is an eigenvalue of $\hat{\mathcal{H}}$ the first and last term sum to zero, i.e.,

$$\frac{\partial E}{\partial \mathbf{R}_I} = \langle\psi|\frac{\partial \hat{\mathcal{H}}}{\partial \mathbf{R}_I}|\psi\rangle + E\frac{\partial}{\partial \mathbf{R}_I}\langle\psi|\psi\rangle = \langle\psi|\frac{\partial \hat{\mathcal{H}}}{\partial \mathbf{R}_I}|\psi\rangle \tag{4.5}$$

Then, it follows that we can introduce errors via the wave functions, in case they are wrong.

4.2.2 Relaxation of GaAs(110) surface

The GaAs(110) surface was relaxed by using the *abinit* software. [†] It was achieved by using the Broyden-Fletcher-Goldfarb-Shanno minimization (BFGS), modified to take into account the total energy as well as the gradients [28].

[†]Abinit is a project of the Université Catholique de Louvaine. For more information visit `http://www.abinit.org/`

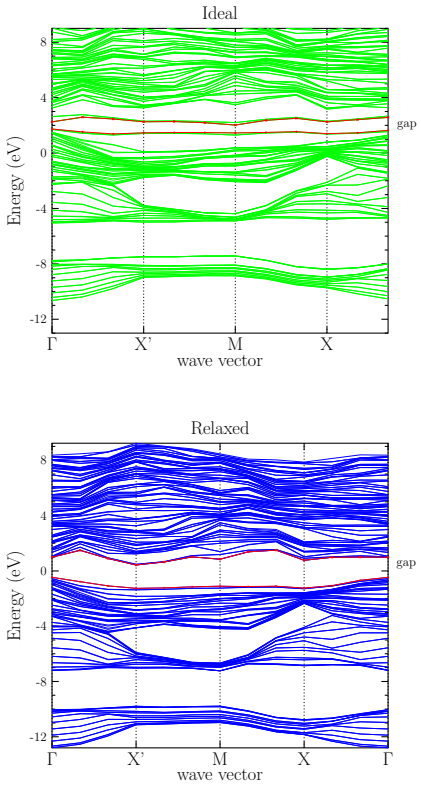

Figure 4.5 : Bandstructure of the GaAs(110) surface. **Up:** We used ideal coordinates when constructing the slab. **Down:** The same case is presented, but, we used relaxed coordinates. The difference between both graphics is notorious at the band gap, i.e., when using ideal coordinates the band gap almost disappears.

The band structure for the GaAs(110) surface was calculated for both the relaxed coordinates and the ideal coordinates. The shape of the bands were similar, however, the ideal-coordinates case gave us a band structure without energy gap. Illustrations can be seen in Fig. 4.5.

4.3 Convergence parameters

Now we will make a brief study to choose the correct parameters for our final calculations. The procedure is easy, we choose a parameter and vary it while leaving everything else constant. That is, we calculate the same property several times to see how it changes with respect to a given variable. Moreover, according to our results we choose the minimum value of a given variable at which the results converge.

We will see that at low values of a certain parameter the response calculated

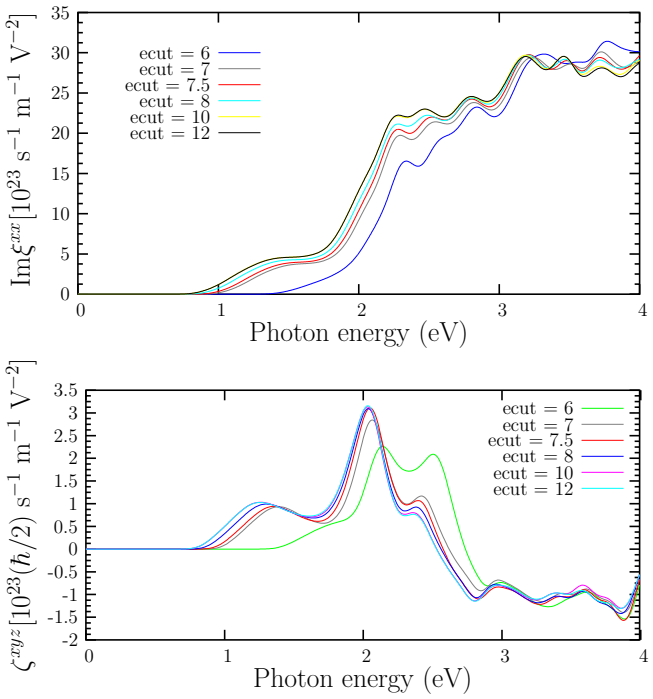

Figure 4.6 : Spin population pseudo-tensor ζ^{xyz} and the carrier population pseudo-tensor ξ^{xx} in a GaAs(110) surface. The cutoff energy was varied from 6 Ha to 12 Ha to verify the convergence of this variable. The number of layers was fixed to be eleven, the vacuum size was set to nine layers, we used 28 **k**-points and the tolerance on the difference of total energy was 1×10^{-6} Ha.

will not have a correct form, but, as we increase its value the results start to converge. We can keep on increasing it, but, we will find out that the response will remain the same while the time it takes to compute it will get larger. Therefore, it is important to determine the minimum values at which calculations converge.

All wave functions in subsequent calculations were found by using the *abinit* software, and, we used Hartwigsen-Goedecker-Hutter pseudopotentials

All responses were calculated from Eqs. (3.28) and (3.35) introduced on chapter 3. We used Eqs. (3.28) to calculate the carrier and spin population due to one photon excitations, and, we used Eqs. (3.35) to find the carrier and spin injection currents due to one photon excitations.

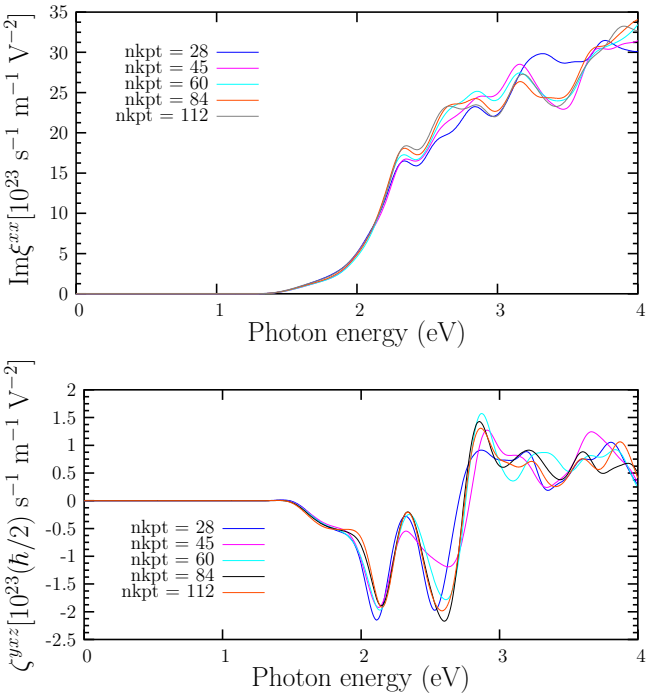

Figure 4.7 : Spin population pseudo-tensor ζ^{yxz} and the carrier population pseudo-tensor ξ^{xx} in a GaAs(110) surface. The size of the **k**-point set was varied from 28 **k**-points to 112 **k**-points. The number of layers was fixed to be eleven, the *ecut* value was 6 Ha, the vacuum size was set to nine layers, we used 28 **k**-points and the tolerance on the difference of total energy was 1×10^{-6} Ha.

4.3.1 Cutoff energy (*ecut*)

We calculated the carrier and spin population pseudo-tensors for the GaAs(110) surface. We used a **k**-point set of 28 **k**-points over the first Brillouin zone.[‡]

We made a series of calculations with cutoff energies ranging from 4 Ha to 12 Ha as it is shown in Fig. 4.6. As you can verify, in this study we found that the responses start to converge at a cutoff energy of 7.5 Ha.

4.3.2 k-point set size

This time we started with 28 **k**-points distributed homogeneously into the first Brilloin zone, and, we found out that when increasing the number of **k**-points

[‡]In the following calculations the number of layers was fixed to be eleven, the *ecut* value was 6 Ha, the vacuum size was set to nine layers, we used 28 **k**-points and the tolerance on the difference of total energy was 1×10^{-6} Ha. This values will remain constant unless it is indicated.

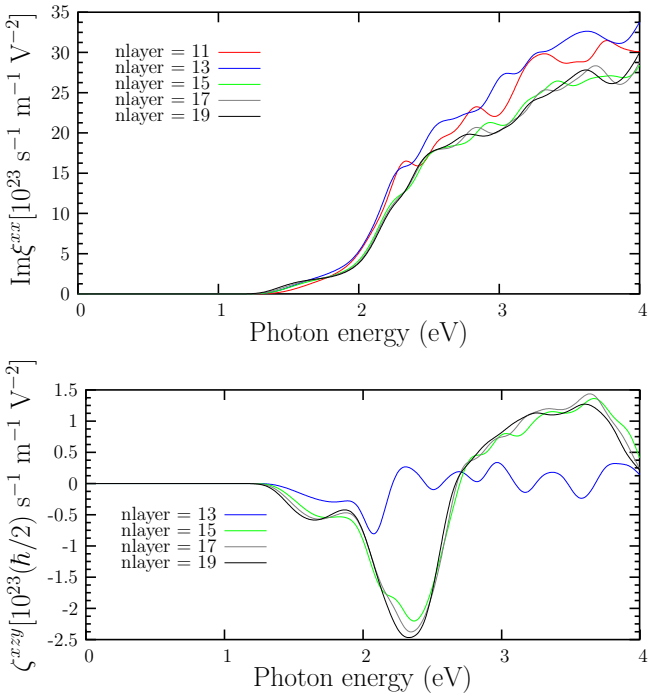

Figure 4.8 : Spin population pseudo-tensor ζ^{xzy} and the carrier population pseudo-tensor ξ^{xx} in a GaAs(110) surface. The number of atomic layers at the slab was changed from 13 to 19 layers. The *ecut* value was 6 Ha, the vacuum size was set to nine layers, we used 28 **k**-points and the tolerance on the difference of total energy was 1×10^{-6} Ha.

(*nkpt*) the responses start to converge for **k**-point sets larger than 60 **k**-points.

As you can see in Fig. 4.7, the calculations start to fluctuate for energies larger than 3.5 eV. So that, we will have errors for energies larger than this value. However, the results converge for energies smaller than 3.5 eV.

4.3.3 Number of layers (*nlayer*)

In this case the slab size was varied. We started with a slab made of 11 atomic layers and we increased its size by 2 atomic layers until we reached a slab size of 19 atomic layers. During all these calculations the vacuum size was chosen to be equal to the slab size, for example, a slab of 11 atomic layers would have a vacuum size equal to 11 atomic layers. This was made in order to keep the slabs isolated. At the end, we found out that our results start to converge at slab sizes larger than 15 atomic layers. See Fig. 4.8.

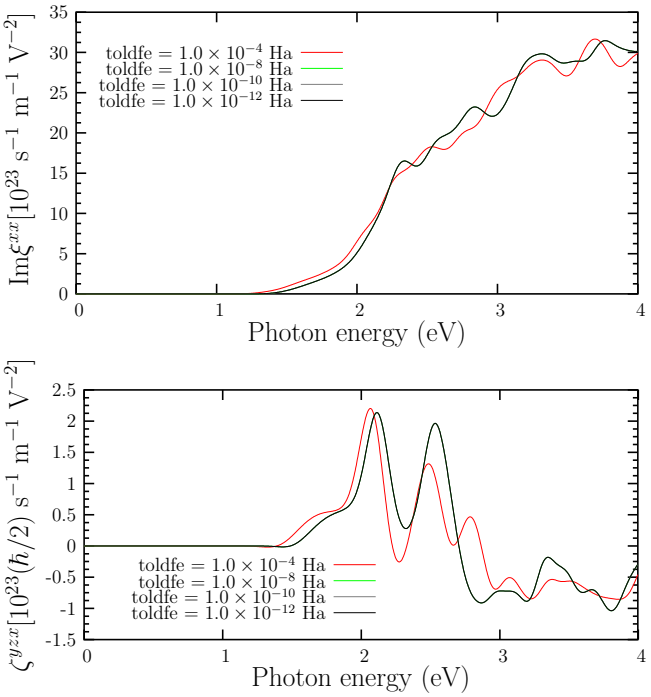

Figure 4.9 : Spin population pseudo-tensor ζ^{yzx} and the carrier population pseudo-tensor ξ^{xx} in a GaAs(110) surface. The number of atomic layers was fixed to be eleven, the *ecut* value was 6 Ha, the **k**-point set size was set to 28 **k**-points and the vacuum size was set to nine layers. All graphics for toldfe $\leq 1 \times 10^{-8}$ coincide.

4.3.4 Tolerance on the difference of total energy (*toldfe*)

The *toldfe* sets a tolerance for differences of total energy that, reached twice successively, will cause one self-consistent field cycle to stop. Thus, if this value is set to be too small, the calculations will take more time to be computed but they will be more accurate. We chose different values for the *toldfe* as it is shown in Fig. 4.9. As you may notice, all graphics coincide for a *toldfe* minor to 1×10^{-8} Ha.

4.3.5 Vacuum size

It is important to choose the vacuum size correctly because at small vacuum sizes collateral effects start to appear. In Fig. 4.10 we can see the electronic density of two slabs; one of which has a vacuum bigger than the other one. The slab with smaller vacuum shows a major density in the vacuum region for the conduction bands, and, this density is due to the tunneling effect. It is present because of the interaction between two subsequent slabs, moreover, it can modify the total

energy of the slab leading to errors in our calculations.[§]

Knowing this, we proceeded to make a final convergence study. This time the slab was composed of 17 atomic layers, and, the vacuum size was varied from 3 to 12 atomic layers.

As you can see in Fig. 4.11 the vacuum size in the case of the GaAs(110) surface can be chosen to be as small as 5 atomic layers without affecting the final response.

All in all, we have found the minimum values that we can assign to variables such as the *ecut* = 7.5 Ha, the *toldfe*= 1×10^{-8} Ha, the *nkpt* = 60 , a slab of 17 atomic layers and a vacuum size of 7 atomic layers. to ensure the responses converge. In other words, we have found the variables we need to make our calculations feasible and congruent.

[§]Tunneling is a quantum mechanical (QM) phenomena that does not have counterpart in classical theory. In QM an electron behaves as a probabilistic wave. That is, a wave function represents the probability of that electron to be in a certain position at a time t. In our example, if the vacuum between two slabs is infinite, an electron that is in one slab will not have a probability to be at the other slab. But, as the vacuum decreases the probabilities to be at the other side increases. There will be a point when electrons will start to move from one slab to another, and, this is called *quantum tunneling*.

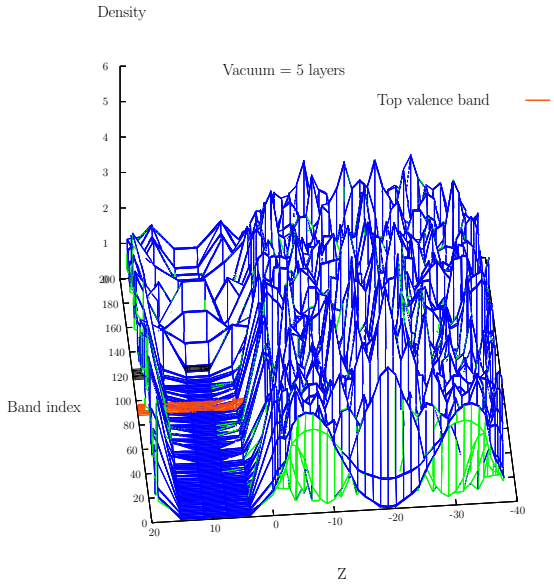

Figure 4.10 : Graphic that shows electronic density of the GaAs(110) surface at one **k**-point. The yellow line shows the location of the last valence bands. The black line is just a reference to make clearer the differences between both graphics. The slab size was equal to 11 atomic layers. **Up:** The vacuum size was equal to five layers. **Down:** The vacuum size was equal to seven layers.

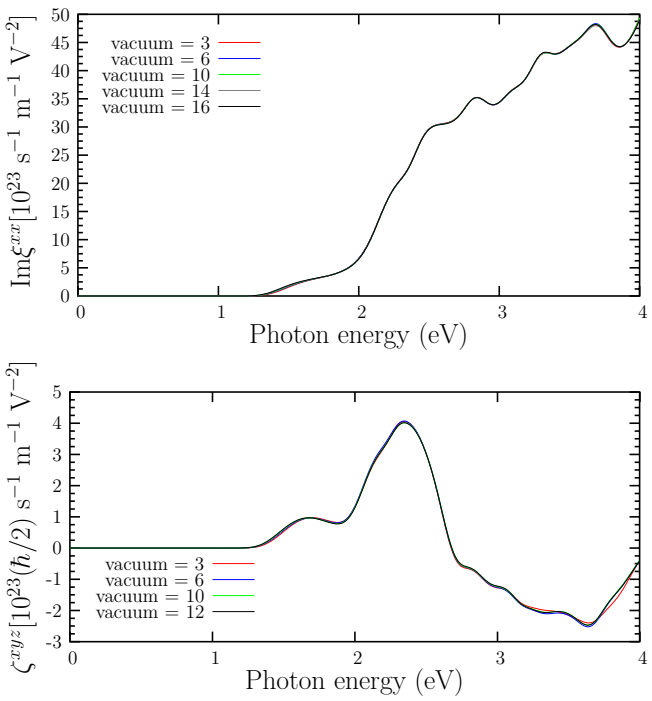

Figure 4.11 : Spin population pseudo-tensor ζ^{xyz} and the carrier population pseudo-tensor ξ^{xx} in a GaAs(110) surface. The number of atomic layers was fixed to be eleven, the *ecut* value was 6 Ha, the **k**-point set size was set to 28 **k**-points and the tolerance on the difference of total energy was 1×10^{-6} Ha. All graphics were normalized to the same volume.

Chapter 5

Layered calculations

As it is explained in the Appendix E the velocity and spin matrix elements we need were obtained from the wave function ψ of the system. Moreover, ψ can be easily obtained by solving the Schrödinger equation for an Hydrogen atom, which is composed of just one electron around a nuclei. However, our problem is a complex system of a semi-infinite number of atoms arranged periodically to form a crystal surface. Since the problem is too complex to be solved analytically we used several approximations explained in Chapter (2). After using these approximations our problem was changed to one of solving the Schrödinger equation of a super-cell composed of a number N of layers ℓ in a slab and a vacuum which is repeated an infinite number of times.

5.1 Calligraphic momentum matrix elements

All tensors (Eqs. (3.28e) and (3.35e)) calculated in Chapter 3 for one-photon excitations are similar to the microscopic current density $\hat{\mathbf{j}}$, given by

$$\hat{\mathbf{j}}(\mathbf{r},t) = \Omega \int \frac{\mathrm{d}^3k}{8\pi^3} \sum_{mn} \mathcal{C}_{mn}(\mathbf{k},t)\mathbf{j}_{nm}(\mathbf{k};\mathbf{r}), \tag{5.1}$$

where Ω is the unit cell volume and $\mathbf{j}_{nm}(\mathbf{k};\mathbf{r})\delta(\mathbf{k}-\mathbf{k}')$ is the matrix element of the microscopic current operator $\mathbf{j}$, [29]

$$\hat{\mathbf{j}} = \frac{e}{2}\left[\hat{\mathbf{v}}|\mathbf{r}\rangle\langle\mathbf{r}| + |\mathbf{r}\rangle\langle\mathbf{r}|\hat{\mathbf{v}}\right] \tag{5.2}$$

Here $\mathcal{C}_{mn}$ is defined as [29]:

$$\mathcal{C}_{mn}(\mathbf{k},t) = \frac{-ie}{\hbar}\int \mathrm{d}\omega \frac{f_{nm}\mathbf{v}^b_{mn}}{\omega_{mn}(\mathbf{k})[\omega_{mn}(\mathbf{k})-\omega]} E^b(\omega)e^{i\omega t}, \tag{5.3}$$

where the sub-indices m and n are for bands, the super-incides a and b indicate cartesian components, $\hbar$ is the Planck's constant, e is the elemental charge and $\mathbf{v}_{mn}$ are the velocity matrix elements. With this example we will show how to find the layered matrix elements used to calculate the layered responses.

We start by finding the velocity matrix elements by using the motion equation $\hat{\mathbf{v}} = (1/i\hbar)[\mathbf{r}, \hat{\mathcal{H}}]$,

$$\mathbf{v}_{mn}(\mathbf{k})\delta(\mathbf{k}-\mathbf{k}') \equiv \int \mathrm{d}^3\mathbf{r}\langle m\mathbf{k}|\mathbf{r}\rangle\langle|\hat{\mathbf{v}}|n\mathbf{k}'\rangle. \tag{5.4}$$

Since we are using the DFT with the LDA the Hamiltonian is just local and we can neglect the nonlocal pseudopotential in $[\mathbf{r}, \hat{\mathcal{H}}]$ to get [29]:

$$\langle\mathbf{r}|\hat{\mathbf{v}}|n\mathbf{k}\rangle \approx \frac{1}{m}\hat{\mathbf{p}}\psi_{n,\mathbf{k}}(\mathbf{r}) \tag{5.5}$$

where $\hat{\mathbf{p}} = -i\hbar\nabla$ and $\psi_{n,\mathbf{k}}(\mathbf{r}) = \langle\mathbf{r}|n\mathbf{k}\rangle$.

Up to now, we have shown how to find several responses of a material due to an incident light field. However, we may want to isolate just one of the two surfaces on a slab. To calculate the response of just one surface Reining *et al.* [30] Mendoza *et al.* [31] and Mejía *et al.* [32] proposed that we should replace the momentum operator $\hat{\mathbf{p}}$ by $\hat{\mathcal{P}}$,

$$\hat{\mathbf{p}} \to \hat{\mathcal{P}} \equiv \frac{1}{2}\left[\hat{\mathbf{p}}S(\mathbf{z}) + S(\mathbf{z})\hat{\mathbf{p}}\right], \tag{5.6}$$

in a slab susceptibility calculation, where $S(\mathbf{z})$ is known as the *cut function*, which is usually zero over one half of the slab and unity over the other half. Moreover, Mendoza *et al.* [29] extended this idea limiting the calculated current response to a particular layer of the slab. This is done by replacing the cut function $S(\mathbf{z})$ by a top-hat cut function $S_\ell(\mathbf{z})$ that selects a given layer, [29]

$$S_\ell(\mathbf{z}) = \Theta\left(\mathbf{z}-\mathbf{z}_\ell+\Delta^b_\ell\right)\Theta\left(\mathbf{z}_\ell-\mathbf{z}+\Delta^f_\ell\right), \tag{5.7}$$

where Θ is the Heaviside function. Δ^{flb}_ℓ is the distance that the ℓth layer extends towards the front (f) or the back (b) from its $\mathbf{z}_\ell$ position. Furthermore, $\Delta^f_\ell + \Delta^b_\ell$ is the thickness of layer ℓ.

Having these ideas in mind we find that the contribution to the current density from the ℓth layer of the slab. Integrating the microscopic electric current $\mathbf{j}(t)$ over the entire cell and dividing by the unit cell volume gives the macroscopic contribution. But, if we want to know the contribution of just one region of the unit cell to the total response we can integrate over the desired region:

$$\frac{1}{\Omega}\int \mathrm{d}^3\mathbf{r}\, S_\ell(\mathbf{z})\mathbf{j}(\mathbf{r},t) \equiv \mathbf{j}^{(\ell)}(t) = \int \frac{\mathrm{d}^3k}{8\pi^3}\sum_{m,n}\mathcal{C}_{mn}(\mathbf{k},t)\int \mathrm{d}^3\mathbf{r}\, S_\ell(\mathbf{z})\mathbf{j}_{nm}(\mathbf{k};\mathbf{r}) \quad (5.8)$$

where $\mathbf{j}^{(\ell)}(t)$ is the microscopic current in the ℓth layer. Then, using Eq. (5.1) we obtain that the velocity matrix element for a given layer $\mathcal{V}^{(\ell)}_{mn}(\mathbf{k})$ are given by:

$$\begin{aligned}\int \mathrm{d}^3\mathbf{r}\, S_\ell(\mathbf{z})\mathbf{j}_{nm}(\mathbf{k};\mathbf{r}) &= \int \mathrm{d}^3\mathbf{r}\, S_\ell(\mathbf{z})\frac{e}{2}\left[\langle n\mathbf{k}|\hat{\mathbf{v}}|\mathbf{r}\rangle\langle\mathbf{r}|m\mathbf{k}\rangle + \langle n\mathbf{k}|\mathbf{r}\rangle\langle\mathbf{r}|\hat{\mathbf{v}}|m\mathbf{k}\rangle\right] \\ &\equiv e\mathcal{V}^{(\ell)}_{nm}(\mathbf{k}). \end{aligned} \quad (5.9)$$

The layered matrix elements of the velocity operator $\mathcal{V}^{(\ell)}$ should not be replaced on all matrix elements $\mathbf{p}_{mn}$ found in Eq. (5.1), but only on the matrix elements directly associated with the generated current. That is, only in the velocity matrix elements found in Eq. (5.2) has to be replaced by $\mathcal{V}^{(\ell)}$. Using Eqs. (5.9) and (5.5), we obtain [29]:

$$\mathcal{V}_{nm}(\mathbf{k}) = \frac{1}{m}\int \mathrm{d}^3\psi^*_{n\mathbf{k}}(\mathbf{r})\mathcal{P}\psi_{m\mathbf{k}}(\mathbf{r}) \equiv \frac{1}{m}\mathcal{P}_{nm}(\mathbf{k}). \quad (5.10)$$

5.1.1 Matrix elements for plane waves

As it was explained before when computing optical responses using *ab initio* methods we use plane waves to expand the wave function ψ in the following form:

$$\psi_{n\mathbf{k}}(\mathbf{r}) = \sum_{\mathbf{G}} C_{n\mathbf{k}}(\mathbf{G})\exp[i(\mathbf{k}+\mathbf{G})\cdot\mathbf{r}], \quad (5.11)$$

were $C_{n\mathbf{k}}$ are plane waves coefficients. Finally by using Eqs. (5.1.1) and (5.1) we find an expression similar to that of the *non layered* momentum matrix elements shown in Eq. (E.3) (source [29]):

$$\mathcal{V}^{(\ell)}_{mn}(\mathbf{k}) = \frac{\hbar}{2}\sum_{\mathbf{G},\mathbf{G}'} C^*_{m\mathbf{G}'}(\mathbf{k})C_{n\mathbf{G}}(\mathbf{k})[2\mathbf{k}+\mathbf{G}+\mathbf{G}']\delta_{\mathbf{G}_\parallel,\mathbf{G}'_\parallel} f_\ell\left(G_\perp - G'_\perp\right) \quad (5.12)$$

where the reciprocal lattice vectors $\mathbf{G}$ are decomposed into components parallel to the surface $\mathbf{G}_{\parallel}$, and perpendicular to the surface $\mathbf{G}_{\perp}\hat{\mathbf{z}}$, so that $\mathbf{G} = \mathbf{G}_{\parallel} + \mathbf{G}_{\perp}\hat{\mathbf{z}}$, and

$$f_\ell(g) = \frac{1}{L}\int_{z_\ell-\Delta_\ell^b}^{z_\ell+\Delta_\ell^f} e^{igz}\mathrm{d}z. \tag{5.13}$$

5.2 Calligraphic spin matrix elements

Using a similar idea we will find the calligraphic spin matrix elements $\mathcal{S}_{mn}$. The microscopic spin current *mick* is given by

$$\mathbf{K}(\mathbf{r},t) = \Omega\int\frac{\mathrm{d}^3k}{8\pi^3}\sum_{mn}\mathcal{C}_{mn}(\mathbf{k},t)\mathbf{K}_{nm}(\mathbf{k};\mathbf{r}), \tag{5.14}$$

where $\mathbf{K}_{nm}(\mathbf{k};\mathbf{r})\delta(\mathbf{k}-\mathbf{k}')$ is the matrix element of the microscopic current operator $\mathbf{K}$,

$$\mathbf{K} = \frac{1}{2}\left[\hat{\mathbf{v}}S|\mathbf{r}\rangle\langle\mathbf{r}| + |\mathbf{r}\rangle\langle\mathbf{r}|\hat{\mathbf{v}}S\right] \tag{5.15}$$

Here the coefficient $\mathcal{C}_{mn}$ is given by Eq. (5.3).

The contribution to the spin current density from the ℓth layer of the slab is given by

$$\frac{1}{\Omega}\int\mathrm{d}^3\mathbf{r}\,S_\ell(\mathbf{z})\mathbf{j}(\mathbf{r},t) \equiv \mathbf{K}^{(\ell)}(t) = \int\frac{\mathrm{d}^3k}{8\pi^3}\sum_{m,n}\mathcal{C}_{mn}(\mathbf{k},t)\int\mathrm{d}^3\mathbf{r}\,S_\ell(\mathbf{z})\mathbf{K}_{nm}(\mathbf{k};\mathbf{r}) \tag{5.16}$$

Then, using Eq. (5.14) we obtain that the velocity matrix element for a given layer $\mathcal{V}_{mn}^{(\ell)}(\mathbf{k})$ are given by:

$$\begin{aligned}\int\mathrm{d}^3\mathbf{r}\,S_\ell(\mathbf{z})\mathbf{K}_{nm}(\mathbf{k};\mathbf{r}) &= \int\mathrm{d}^3\mathbf{r}\,S_\ell(\mathbf{z})\frac{1}{2}\left[\langle n\mathbf{k}|\hat{\mathbf{v}}S|\mathbf{r}\rangle\langle\mathbf{r}|m\mathbf{k}\rangle + \langle n\mathbf{k}|\mathbf{r}\rangle\langle\mathbf{r}|\hat{\mathbf{v}}S|m\mathbf{k}\rangle\right]\\ &\equiv \mathcal{K}_{nm}^{(\ell)}(\mathbf{k}).\end{aligned} \tag{5.17}$$

Likewise, setting $\hat{\mathbf{v}} = 0$ we find the expression for the calligraphic spin matrix elements:

$$\begin{aligned}\int\mathrm{d}^3\mathbf{r}\,\mathcal{S}_\ell(\mathbf{z})\hat{S}_{nm}^a(\mathbf{k};\mathbf{r}) &= \int\mathrm{d}^3\mathbf{r}\,S_\ell(\mathbf{z})\frac{1}{2}\left[\langle n\mathbf{k}|S|\mathbf{r}\rangle\langle\mathbf{r}|m\mathbf{k}\rangle + \langle n\mathbf{k}|\mathbf{r}\rangle\langle\mathbf{r}|S|m\mathbf{k}\rangle\right]\\ &\equiv \mathcal{S}_{nm}^{(\ell)}(\mathbf{k}).\end{aligned} \tag{5.18}$$

5.2.1 Matrix elements for plane waves

The spin matrix elements are given by the Pauli matrices:

$$\hat{S}^a = \frac{\hbar}{2}\sigma^a \tag{5.19a}$$

$$\sigma^x = \begin{pmatrix} 0 & 1 \\ 1 & 0 \end{pmatrix} \ , \ \sigma^y = \begin{pmatrix} 0 & -i \\ i & 0 \end{pmatrix} \ , \ \sigma^z = \begin{pmatrix} 1 & 0 \\ 0 & -1 \end{pmatrix} \tag{5.19b}$$

When using plane waves (Eq. (5.1.1)) we have to follow the steps to find the spin matrix elements indicated in Appendix. E to find:

$$\begin{aligned}
\mathcal{S}^{(\ell)x}_{mn} &= \frac{\hbar}{2}\sum_{\mathbf{G}}\left(C^{-}_{m\mathbf{k}}(\mathbf{G})^{*}C^{+}_{n\mathbf{k}}(\mathbf{G}) + C^{+}_{m\mathbf{k}}(\mathbf{G})^{*}C^{-}_{n\mathbf{k}}(\mathbf{G})\right)\delta_{\mathbf{G}_{\parallel},\mathbf{G}'_{\parallel}} f_\ell\left(G_\perp - G'_\perp\right) \\
\mathcal{S}^{(\ell)y}_{mn} &= \frac{i\hbar}{2}\sum_{\mathbf{G}}\left(C^{-}_{m\mathbf{k}}(\mathbf{G})^{*}C^{+}_{n\mathbf{k}}(\mathbf{G}) - C^{+}_{m\mathbf{k}}(\mathbf{G})^{*}C^{-}_{n\mathbf{k}}(\mathbf{G})\right)\delta_{\mathbf{G}_{\parallel},\mathbf{G}'_{\parallel}} f_\ell\left(G_\perp - G'_\perp\right) \\
\mathcal{S}^{(\ell)z}_{mn} &= \frac{\hbar}{2}\sum_{\mathbf{G}}\left(C^{+}_{m\mathbf{k}}(\mathbf{G})^{*}C^{+}_{n\mathbf{k}}(\mathbf{G}) - C^{-}_{m\mathbf{k}}(\mathbf{G})^{*}C^{-}_{n\mathbf{k}}(\mathbf{G})\right)\delta_{\mathbf{G}_{\parallel},\mathbf{G}'_{\parallel}} f_\ell\left(G_\perp - G'_\perp\right)
\end{aligned} \tag{5.20}$$

5.3 Carrier population (layered response)

The calligraphic momentum matrix elements $\mathcal{V}^{(\ell)}$are used to calculated the layered responses which use tensors of a form similar to that in Eq. (5.1). However, the expression for the carriers population xi^{ab} found in Eq. (3.28e) does not have that form. Thus, we will introduce a formalism to find the layered contributions for the carriers population.

We define $\hat{\rho}(\mathbf{r};\mathbf{k})$ as a charge density operator, such that,

$$\hat{\rho}(\mathbf{r};\mathbf{k}) = \sum_{n,m,\mathbf{k}} \hat{a}^{\dagger}_{n,\mathbf{k}}\hat{a}_{m,\mathbf{k}}\rho_{nm}(\mathbf{r};\mathbf{k}), \tag{5.21}$$

where

$$\rho_{nm}(\mathbf{r};\mathbf{k}) = e\psi^{*}_{n,\mathbf{k}}(\mathbf{r})\psi_{m,\mathbf{k}}(\mathbf{r}). \tag{5.22}$$

Using a SQ approach we can rewrite the operator $\hat{\rho}(\mathbf{r};\mathbf{k})$; by using Eq. (A.21) and directly substituting $\hat{\rho}(\mathbf{r};\mathbf{k})$ we get,

$$\begin{aligned}\hat{\rho}(\mathbf{r};\mathbf{k}) = &\sum_{c,c'\mathbf{k}} \rho_{cc}(\mathbf{r};\mathbf{k})\hat{a}^{\dagger}_{c,\mathbf{k}}\hat{a}_{c',\mathbf{k}} + \sum_{c,v\mathbf{k}} \rho_{cv}(\mathbf{r};\mathbf{k})\hat{a}^{\dagger}_{c,\mathbf{k}}\hat{b}^{\dagger}_{v,\mathbf{k}} \\ &+ \sum_{v,c\mathbf{k}} \rho_{vc}(\mathbf{r};\mathbf{k})\hat{b}_{v,\mathbf{k}}\hat{a}_{c,\mathbf{k}} - \sum_{v,v'\mathbf{k}} \rho_{vv'}(\mathbf{r};\mathbf{k})\hat{b}^{\dagger}_{v',\mathbf{k}}\hat{b}_{v,\mathbf{k}}\end{aligned} \tag{5.23}$$

From Eq. (3.21) we find that,

$$\frac{\mathrm{d}\langle\hat{\rho}(\mathbf{r};\mathbf{k})\rangle}{\mathrm{d}t} = \frac{\mathrm{d}\langle\psi'|\hat{\rho}(\mathbf{r};\mathbf{k})|\psi\rangle}{\mathrm{d}t} = \frac{\mathrm{d}}{\mathrm{d}t}\sum_{c,v,\mathbf{k}}\sum_{c',v',\mathbf{k}'} \mathcal{C}^{*}_{c',v',\mathbf{k}'}\mathcal{C}_{c,v,\mathbf{k}}\langle c',v',\mathbf{k}'|\hat{\rho}(\mathbf{r};\mathbf{k})|c,v,\mathbf{k}\rangle. \tag{5.24}$$

The coefficient $\mathcal{C}_{c,v,\mathbf{k}}$ give us the probability of a transition to happen, and, it obeys the Fermi's Golden Rule, Eq. (D.26):

$$\begin{aligned}\lim_{\epsilon\to 0}\frac{\mathrm{d}}{\mathrm{d}t}|\mathcal{C}_{c,v,\mathbf{k}}(t)|^2 &= |\mathcal{K}_{c,v}(t;\mathbf{k})|^2 \lim_{\epsilon\to 0}\frac{e^{2\epsilon t}}{(2\omega-\omega_{cv}(\mathbf{k}))^2+\epsilon^2} \\ &= 2\pi|\mathcal{K}_{c,v}(t;\mathbf{k})|^2\delta(2\omega-\omega_{cv}(\mathbf{k}))\end{aligned} \tag{5.25}$$

where $\mathcal{K}_{c,v}(t;\mathbf{k})$ has two terms; one for one-photon transitions and one for two-photons transitions:

$$\mathcal{K}_{c,v}(t;\mathbf{k}) = \frac{ie}{\hbar\omega_{cv}(\mathbf{k})}\mathbf{E}(2\omega)\cdot\mathbf{v}_{cv}(\mathbf{k}) - \left(\frac{2e}{\hbar\omega_{cv}(\mathbf{k})}\right)^2\sum_{n}\frac{\mathbf{v}_{cn}(\mathbf{k})\cdot\mathbf{E}(\omega)\mathbf{v}_{nv}(\mathbf{k})\cdot\mathbf{E}(\omega)}{\overline{\omega}-\omega_n(\mathbf{k})} \tag{5.26}$$

By directly substituting Eq. (5.23) into Eq. (5.24), and performing the intermediate algebraic steps, we obtain that the carrier population due to one and two-photon excitations is given by,

$$\frac{\mathrm{d}\langle\hat{\rho}(\mathbf{r};\mathbf{k})\rangle}{\mathrm{d}t} = \frac{2\pi}{\mathcal{A}}\sum_{c,v,\mathbf{k}}|\mathcal{K}_{c,v}(t)|^2\left[\rho_{cc}(\mathbf{r};\mathbf{k})-\rho_{vv}(\mathbf{r};\mathbf{k})\right]\delta(\omega_{cv}(\mathbf{k})-2\omega) \tag{5.27}$$

In the above expression, the one-photon excitations term is

$$\frac{\mathrm{d}\langle\hat{\rho}(\mathbf{r};\mathbf{k})\rangle_1}{\mathrm{d}t} = \xi_1^{ab}(\mathbf{r},2\omega;\mathbf{k})E^a(-2\omega)E^b(2\omega), \tag{5.28}$$

where,

$$\xi_1^{ab}(\mathbf{r}, 2\omega; \mathbf{k}) = \frac{2\pi e^2}{\mathcal{A}\hbar^2} \sum_{c,v,\mathbf{k}} \frac{\mathbf{v}_{cv}^b(\mathbf{k})\mathbf{v}_{vc}^a(\mathbf{k})}{\omega_{cv}^2(\mathbf{k})} \left[\rho_{cc}(\mathbf{r}; \mathbf{k}) - \rho_{vv}(\mathbf{r}; \mathbf{k})\right] \delta(\omega_{cv}(\mathbf{k}) - 2\omega). \tag{5.29}$$

Now, with the help of the last expression and the top hat cut function $S_\ell(\mathbf{z})$ we will construct the layer-by-layer contributions. First, we use the function $S_\ell(\mathbf{z})$, which selects a given layer in the following way:

$$\begin{aligned} \xi_1^{(\ell)ab}(\mathbf{r}, 2\omega; \mathbf{k}) &= \int \mathrm{d}^3\mathbf{r}\, S_\ell(\mathbf{z}) \xi_1^{ab}(\mathbf{r}, 2\omega; \mathbf{k}) \\ &= \frac{2\pi e^2}{\mathcal{A}\hbar^2} \sum_{c,v,\mathbf{k}} \frac{\mathbf{v}_{cv}^{b(\ell)}(\mathbf{k})\mathbf{v}_{vc}^{a(\ell)}(\mathbf{k})}{\omega_{cv}^2(\mathbf{k})} \\ &\quad \times \left(\int \mathrm{d}^3\mathbf{r}\ S_\ell(\mathbf{z}) \left[\rho_{cc}(\mathbf{r}; \mathbf{k}) - \rho_{vv}(\mathbf{r}; \mathbf{k})\right] \right) \delta(\omega_{cv}(\mathbf{k}) - 2\omega) \end{aligned} \tag{5.30}$$

Then, by combining Eqs. (5.21) and (5.30) it follows that the carrier population for one-photon excitations is given by:

$$\frac{\mathrm{d}\langle \hat{\rho}(\mathbf{r}; \mathbf{k})\rangle_1^{(\ell)}}{\mathrm{d}t} = \xi_1^{ab(\ell)}(\mathbf{r}, 2\omega; \mathbf{k}) E^a(-2\omega) E^b(2\omega), \tag{5.31}$$

where,

$$\xi_1^{ab(\ell)}(2\omega; \mathbf{k}) = \frac{2\pi e^2}{\mathcal{A}\hbar^2} \sum_{c,v,\mathbf{k}} \frac{\mathbf{v}_{cv}^b(\mathbf{k})\mathbf{v}_{vc}^a(\mathbf{k})}{\omega_{cv}^2(\mathbf{k})} \left[\rho_{cc}^{(\ell)}(\mathbf{k}) - \rho_{vv}^{(\ell)}(\mathbf{k})\right] \delta(\omega_{cv}(\mathbf{k}) - 2\omega). \tag{5.32}$$

Here $\rho^{(\ell)_{nn}(\mathbf{k})}$, which represents the number of carriers in a given layer ℓ and k-point $\mathbf{k}$, is defined as:

$$\rho_{nn}^{(\ell)}(\mathbf{k}) = \int S_\ell(\mathbf{z}) \psi_{n,\mathbf{k}}^*(\mathbf{r}) \psi_{n,\mathbf{k}}(\mathbf{r}) \mathrm{d}^3\mathbf{r}. \tag{5.33}$$

Using these results, we can find the carrier population $\mathrm{d}\langle \hat{\rho}(\mathbf{r}; \mathbf{k})\rangle_1/\mathrm{d}t$ for a particular layer ℓ and one photon excitations.

Chapter 6

Results

Up to this point, we have all the elements needed to find the carriers and spin population, as well as, the electronic and spin injection currents in a GaAs(110) surface. Along Chapter 3 we found the mathematical expressions for such responses. In Chapter 4 we made several studies to ensure that our final results converge.

According to the convergence study performed in Chapter 4, we chose an *energy cutoff* equal to 7.5 Ha, a set of 60 **k**-points was distributed on the first Brillouin zone. The super-cell was formed by 17 atomic layers and a vacuum having a length of 7 atomic layers. The *tolerance on the difference of total energy* was set to be 1×10^{-8} Ha.

We divided our GaAs(110) surface into seventeen layers as it is shown in Fig. 6.1. We made this division in such a way that at the end all layers contained two atoms per layer.

6.1 Degree of Spin polarization

We derive the mathematical expression to obtain the degree of spin polarization for one photon excitations DSP into the GaAs(110) surface. From equations (3.28) we define:

$$\mathrm{DSP}^a = \frac{1}{\hbar/2} \frac{\mathrm{d}\langle \hat{S}^a \rangle / \mathrm{d}t}{\mathrm{d}\langle \hat{n} \rangle / \mathrm{d}t} \tag{6.1}$$

as the degree of spin polarization, DSP^a, along the cartesian direction a. It can be seen as the percentage of spin polarized electrons among a population of n

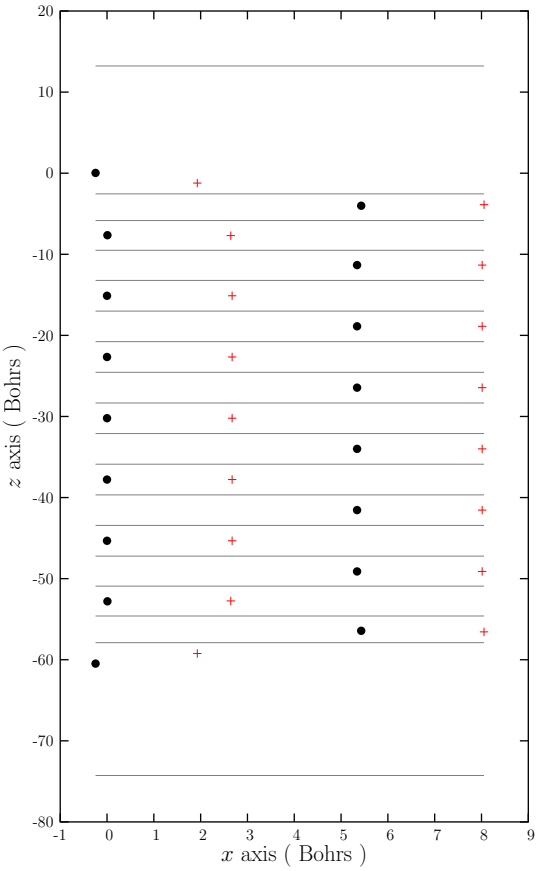

Figure 6.1 : A lateral view of the GaAs(110) surface along the z and x axis is shown. We divided it into 17 layers denoted by gray lines. Each layer contains two atoms. The arsenide atoms are drawn as black points while the gallium atoms are represented by red crosses.

electrons injected into the surface.

In a real experiment we would radiate the GaAs(110) surface along the $\hat{\mathbf{z}}$ direction by a circularly polarized field parallel to the surface of the following form:

$$\mathbf{E}(\omega) = E(\omega)e^{i\phi_\omega}\frac{\hat{\mathbf{x}} + \alpha_\omega i\hat{\mathbf{y}}}{\sqrt{2}} \tag{6.2}$$

where $e^{i\phi_\omega}$ is the phase and α_ω can be either 1 or -1 for left or right circular polarizations, respectively.

Then from Eqs. (3.28) and (6.2) it follows that,

$$\frac{\mathrm{d}\langle\hat{n}\rangle}{\mathrm{d}t} = \xi^{xx}\mathbf{E}^{x*}(\omega)\mathbf{E}^{x}(\omega) + \xi^{yy}\mathbf{E}^{y*}(\omega)\mathbf{E}^{y}(\omega)$$

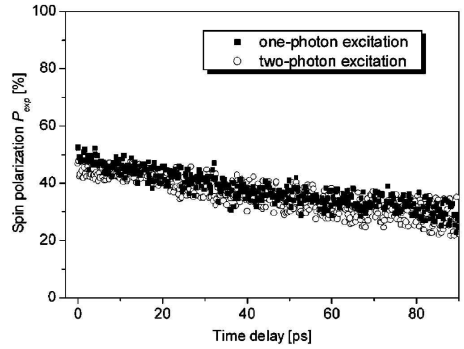

Figure 6.2 : Experimental dynamics of DSP in GaAs bulk obtained by Bhat *et al.* [24]. The dynamics after excitation by circularly polarized pump pulses with the excess energy of 90 meV were measured using probe pulses with circular polarization for one- and two-photon excitations.

$$= \frac{E^2(\omega)}{2}\left(\xi^{xx} + \xi^{yy}\right), \tag{6.3}$$

and that,

$$\begin{aligned}\frac{\mathrm{d}\langle \hat{S}^z\rangle}{\mathrm{d}t} &= \zeta^{zxy}\mathbf{E}^{x*}(\omega)\mathbf{E}^{y}(\omega) + \zeta^{zyx}\mathbf{E}^{y*}(\omega)\mathbf{E}^{x}(\omega) \\ &= -i\alpha_\omega \frac{E^2(\omega)}{2}\left(\zeta^{zyx} - \zeta^{zxy}\right). \end{aligned} \tag{6.4}$$

Because of symmetry reasons, the tensor component $\zeta^{abc} = \zeta^{acb}$. Moreover, for the GaAs(110) surface $\zeta^{abb} = \zeta^{bab} = \zeta^{bba} = 0$, and, $\xi^{ab} = \delta_{ab}\xi^a$. Using these relations and knowing that $\zeta^{abc}(\omega)$ is purely imaginary, we can obtain that the DSP^z is equal to:

$$\mathrm{DSP}^z = \frac{\alpha_\omega}{\hbar/2}\frac{2\zeta^{zxy}}{\xi^{xx} + \xi^{yy}} \tag{6.5}$$

We have obtained a expression to calculate the degree of spin polarization along the z direction (DSP^z) into a semiconductor surface radiated by an electro-magnetic field circularly polarized.

Now we have all the elements to calculate the spin and carriers populations by one photon excitations given by Eqs. (3.28d) and (3.28c) respectively. Moreover, using these results and Eq. (6.5) we proceeded to calculate the responses.

The carrier population pseudo-tensor ξ^{xx} shown in Fig. 6.4 is found to be similar to ξ^{yy} shown in Fig. 6.5. They start at an energy close to 0.6 eV and they have their maxima at an energy close to 4.2 eV.

As you can see in Fig. 6.6 ζ^{zxy} starts at energies close to 0.6 eV and has its maxima at an energy of 2.17 eV. After reaching its maxima, it can reach values

below zero meaning that the spin population is on the other preferential direction. That is, the intrinsic spin property has two possible polarizations $+\hbar/2$ and $-\hbar/2$ also known as spin-up and spin-down polarizations. A positive ζ^{abc} has a spin polarization opposite to a negative one.

The DSP^z shown in Fig. 6.7 starts abruptly at an energy close to 0.6 eV which is the energy at which the surface starts to absorb (see Fig. 6.4) and has a second maxima at 2.1 eV which is the maxima of the spin injection pseudo-tensor ζ^{zxy} shown in Fig. (6.6). It reaches a DSP polarization of 70% at $\omega = 0.6$ eV and one of 20% at $\omega = 2.1$ eV. It has a minimum at 1.7 eV which is also a minimum for the spin injection pseudo-tensor ζ^{yxz}. As you may notice, after reaching its second maxima it approaches to zero just as ζ^{zxy} in Fig. 6.6.

The layered responses have a similar behavior. In Figs. 6.4, 6.5 and 6.6 we show the contributions of the 17 layers conforming the slab. We put on purpose the first 6 layers on the first graphic because they conform the top surface. At the second graphic we always show the bulk layer responses and at the third graphic we show the contributions of the last 6 layers which conform the back surface. We also chose the same colors for the layers at the back and top surface so that you can verify that, in effect, the back and top surfaces are equal. What is more, all contributions from the layers at the bulk coincide.

The spin injection in zincblende semiconductors was studied by Bhat *et al.* [24]. They studied the spin injection due to one- and two-photon excitations in GaAs bulk. The degree of spin polarization (DSP) was calculated both theoretically and experimentally giving congruent results, 50% and 49 % respectively. These results were also confirmed experimentally by Stevens *et al.* [33]. The experimental DSP obtained by Bhat *et al.* for GaAs bulk is shown in Fig. 6.2. In this graphic the dynamics of the DSP in GaAs bulk are shown; circularly polarized pump pulses were measured using probe pulses. The first pulse leads to a DSP close to 50% which is congruent with our results, see Fig. 6.14.

6.2 Electric and spin current injection

Now we are going to show the explicit equations for the injection of electric and spin currents by an incident circularly polarized field. Following the same example

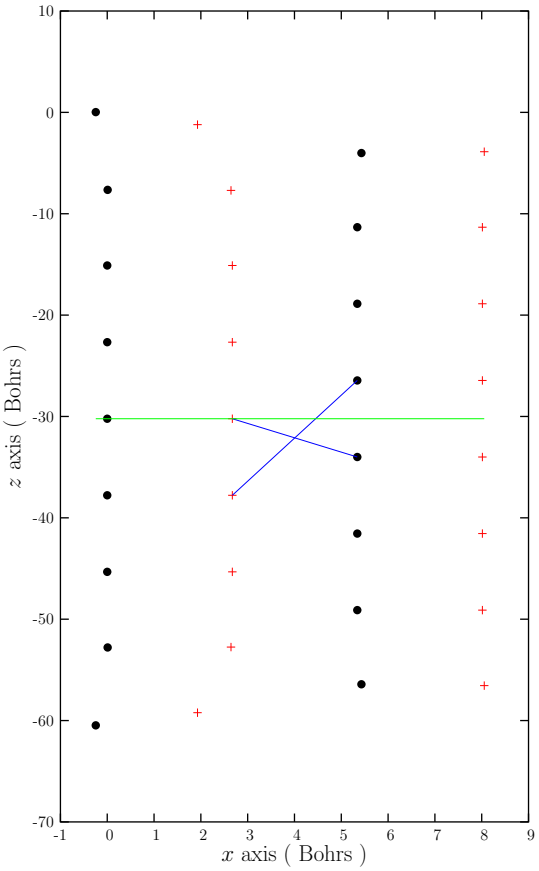

Figure 6.3 : A lateral view of the GaAs(110) surface along the z and x axis is shown. The arsenide atoms are drawn as black points while the gallium atoms are represented by red crosses. The blue solid lines at the center show that the system is not centro-symmetric. However, it is symmetric with respect to a plane parallel to the x and y axes that passes at the middle of the slab (green line).

we used in the last section, the incident field is given by:

$$\mathbf{E}(\omega) = E(\omega)e^{i\phi_\omega}\frac{\hat{\mathbf{x}} + \alpha_\omega i\hat{\mathbf{y}}}{\sqrt{2}} \tag{6.6}$$

where $e^{i\phi_\omega}$ is the phase and α_ω can be either 1 or -1 for left or right circular polarizations, respectively.

From Eq. (3.34) it follows that the electric current injection for this field polarization is:

$$\begin{aligned}\frac{\mathrm{d}\langle\hat{\mathbf{J}}^a\rangle}{\mathrm{d}t} &= \eta^{axy}(\omega)E^{x*}(\omega)E^{y}(\omega) + \eta^{axx}(\omega)E^{x*}(\omega)E^{x}(\omega) \\ &+ \eta^{ayx}(\omega)E^{y*}(\omega)E^{x}(\omega) + \eta^{ayy}(\omega)E^{y*}(\omega)E^{y}(\omega),\end{aligned} \tag{6.7a}$$

where,

$$\eta^{acd}(\omega) = \frac{1}{V}\sum_{\mathbf{k}} \eta^{acd}(\omega;\mathbf{k}), \tag{6.7b}$$

and,

$$\eta^{acd}(\omega;\mathbf{k}) = \frac{2\pi e^3}{\hbar^2}\sum_{c,v} \frac{\mathbf{v}^a_{c'c}(\mathbf{k})\mathbf{v}^{c*}_{c'v}(\mathbf{k})\mathbf{v}^d_{cv}(\mathbf{k})}{(2\omega)^2}\delta(\omega-\omega_{cv}(\mathbf{k})), \tag{6.7c}$$

here the super-index a indicates a cartesian component. In a similar way, the spin current injection along the z direction for this particular polarization is:

$$\begin{aligned}\frac{\mathrm{d}\langle\hat{K}^{zb}\rangle}{\mathrm{d}t} &= \mu^{zbxx}(\omega)E^{x*}(\omega)E^{x}(\omega) + \mu^{zbxy}(\omega)E^{x*}(\omega)E^{y}(\omega) \\ &+ \mu^{zbyy}(\omega)E^{y*}(\omega)E^{y}(\omega) + \mu^{zbyx}(\omega)E^{y*}(\omega)E^{x}(\omega),\end{aligned} \tag{6.8a}$$

where,

$$\mu^{abcd}(\omega) = \frac{1}{V}\sum_{\mathbf{k}} \eta^{abcd}(\omega;\mathbf{k}), \tag{6.8b}$$

and,

$$\mu^{abcd}(\omega;\mathbf{k}) = \frac{2\pi e^2}{\hbar^2}\sum_{c,v} \frac{K^{ab}_{c'c}(\mathbf{k})\mathbf{v}^{c*}_{c'v}(\mathbf{k})\mathbf{v}^d_{cv}(\mathbf{k})}{(2\omega)^2}\delta(\omega-\omega_{cv}(\mathbf{k})). \tag{6.8c}$$

Here the super-index b indicates a cartesian component.

6.2.1 Consequences of symmetry

We know look at the nonzero spin and current tensors that will contribute to the injection of currents in the surface. It is important to know the symmetries to reduce the number of tensors of all the possible tensors shown above.

When calculating the $\eta^{acd}(\omega)$ and $\mu^{abcd}(\omega)$ for the GaAs(110) surface we found that the following components are zero:

$$\eta^{xxx},\ \eta^{xyy},\ \eta^{yxy},\ \eta^{yyx},\ \eta^{zxx}\ ,\ \eta^{zyy}\ ,$$
$$\mu^{zxxx},\ \mu^{zxyy},\ \mu^{zyxy},\ \mu^{zyyx},\ \mu^{zzxx} \text{ and } \mu^{zzyy}.$$

Thus, the only components that contribute for spin and electrical current injection for this particular incident field polarization are:

$$\eta^{xxy},\ \eta^{xyx},\ \eta^{yxx},\ \eta^{yyy},\ \eta^{zxy}\ ,\ \eta^{zyx}\ ,$$
$$\mu^{zxxy},\ \mu^{zxyx},\ \mu^{zyxx},\ \mu^{zyyy},\ \mu^{zzxy} \text{ and } \mu^{zzyx}.$$

This surface at the **x** direction is different from the **y** direction. This fact has repercussions on the optical responses, e.g., $\eta^{zyy} \not\!\!/ \eta^{zxx}$. We found that because of symmetry reasons:

$$\eta^{xxy} = \eta^{xyx},\ \eta^{zxy} = \eta^{zyx},$$
$$\mu^{zxxy} = \mu^{zxyx} \text{ and } \mu^{zzxy} = \mu^{zzyx}.$$

Since η^{zxy} and η^{zyx} are four orders of magnitude smaller than η^{xxy}, η^{yxx} or η^{yyy}, they can be ignored for practical reasons.

6.2.2 Spin and current pseudo-tensors

We calculated the pseudo-tensors for spin and electric current by using Eqs. (3.35c) and (3.35d) respectively. The electric current pseudo-tensors (Figs. 6.8, 6.9 and 6.10) have a minimum at an energy close to 4.2 eV. Moreover, this energy is a maximum for the spin current pseudo-tensors shown in Figs. 6.11, 6.12 and 6.13. This behavior was expected because this energy is also a maximum of absorption (see Fig. 6.4). The reason why it is a minimum for η is the fact that the electron's charge is negative.

It is important to note that the η and μ pseudo-tensors are relationed to the absorption spectra. They all start at an energy close to 1 eV which is the energy at which the material starts to absorb. That is, they are congruent with the Fermi Golden's rule because a photon with less energy that the band gap size is not absorbed. At an energy close to 3.4 eV there is a minimum of absorption which is reflected as a maximum in η and a minimum in μ. What is more, all responses are almost zero after an energy of 8 eV according to the absorption spectra.

The slab is formed of 17 layers but we decided to show just the first 9 layered responses since the back and front surfaces are equal. All layered responses at the bulk layers ($\ell = 7 \text{ to } 9$) are similar. The responses from layers 1 to 6 have slightly differences as it was expected. At the end, the sum of all layered responses give us the total response of the material.

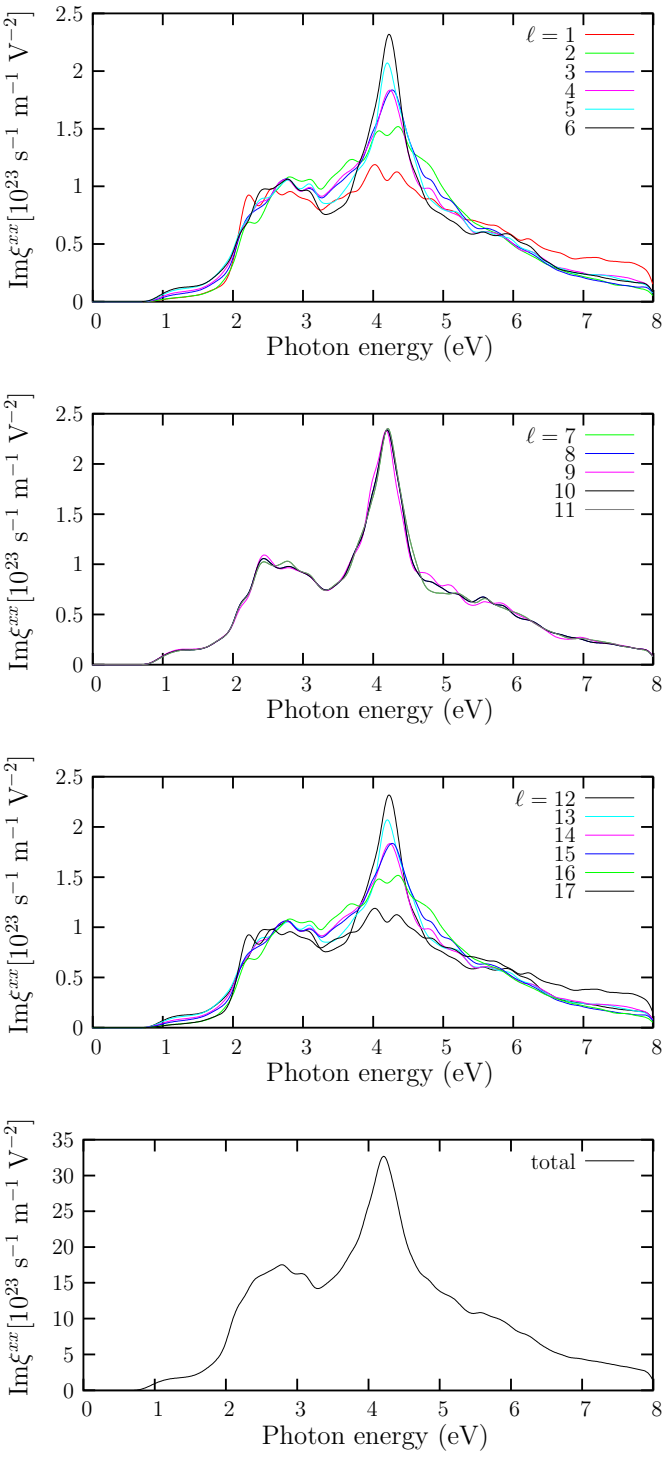

Figure 6.4 : Carrier population pseudo-tensor (ξ^{xx}) due to an incident polarized light of energy ω. We show all layered responses and at the bottom we show the total response for that surface.

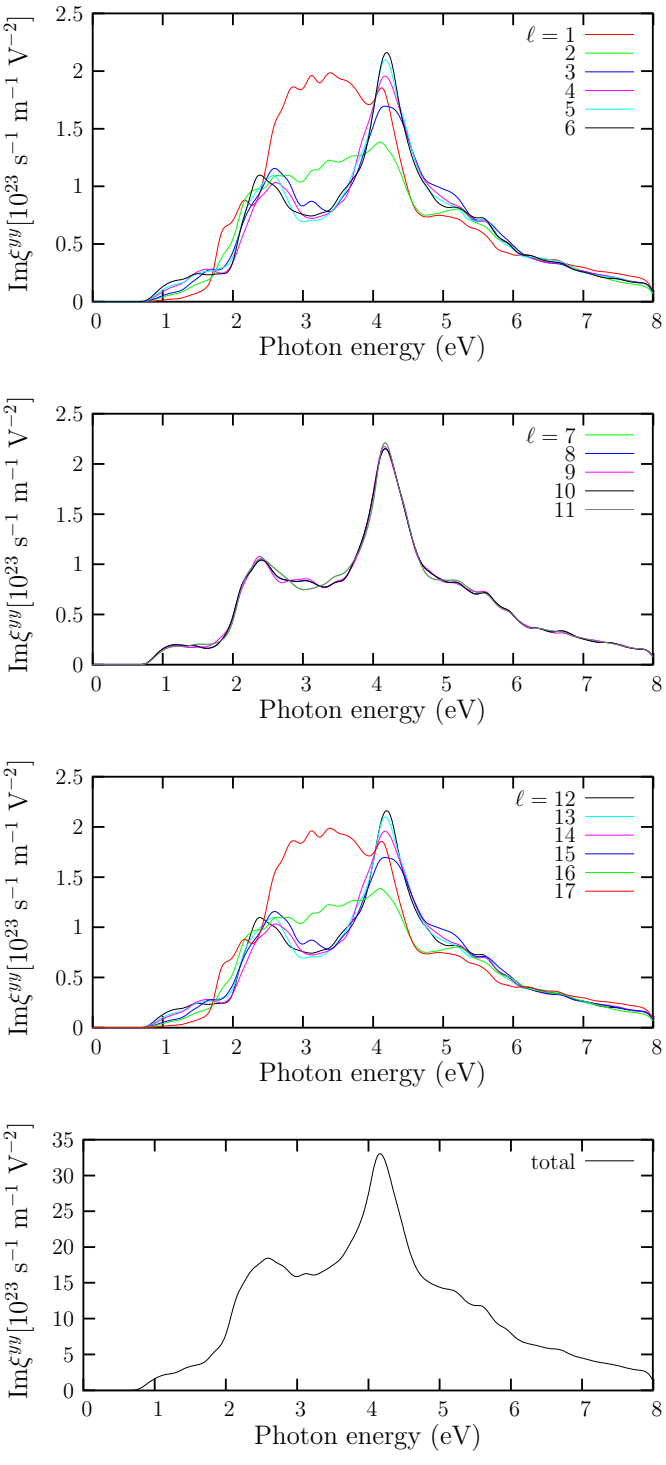

Figure 6.5 : Carrier population pseudotensor ξ^{yy} for one-photon excitations in a GaAs(110) surface. First, we present all layered responses. At the bottom we show the total response for the slab.

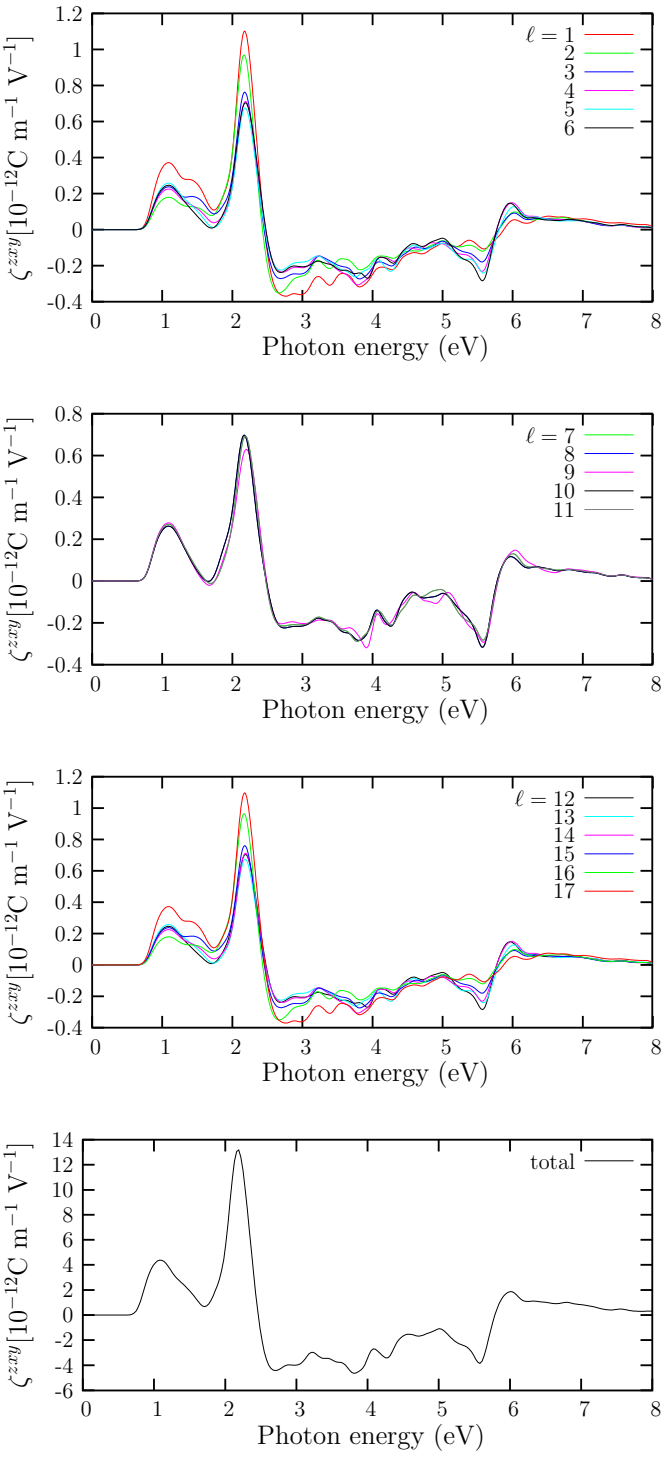

Figure 6.6 : *ab initio* calculation of the spin population pseudo-tensor (ζ^{zxy}) for one-photon excitations into a GaAs(110) surface. We show the responses of all the 17 layers conforming the slab, and at the end, the total response is shown.

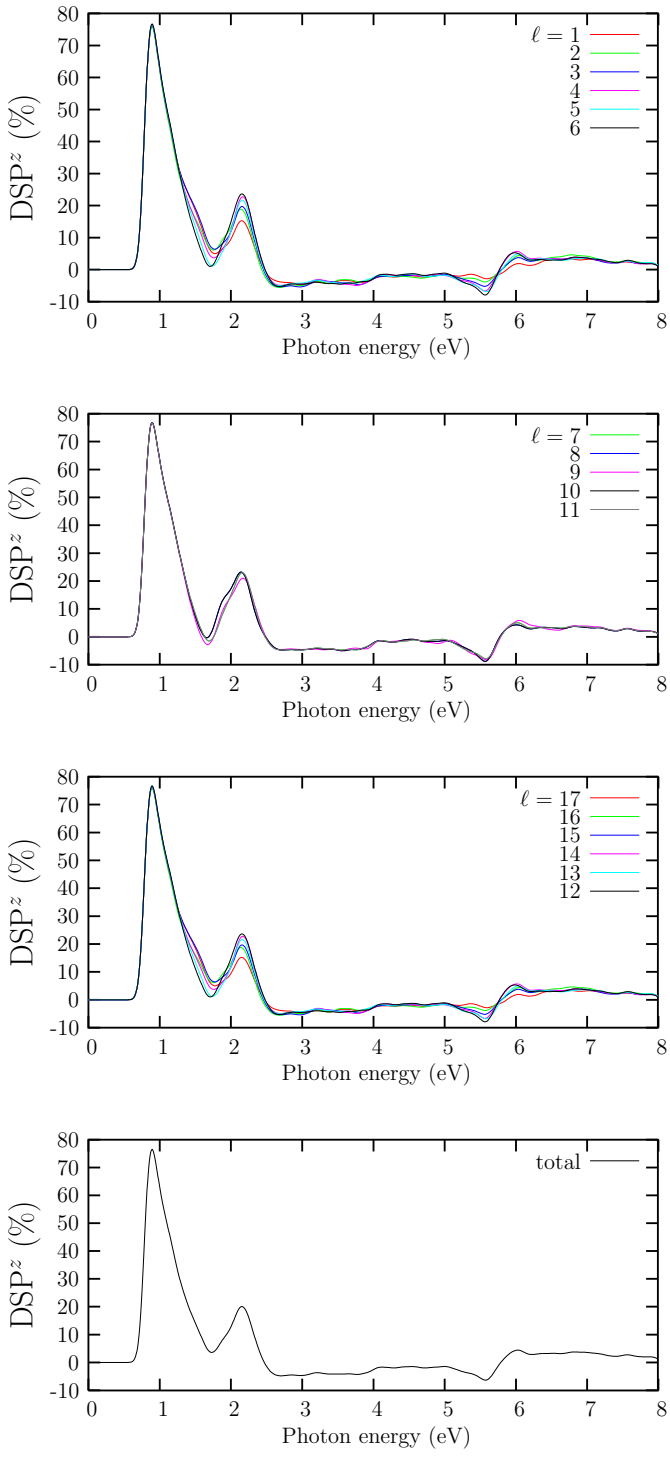

Figure 6.7 : DSP^z along z caused by one incident photon in a GaAs(110) surface. In the first two graphics a layer-by-layer calculation is shown. At the bottom, we present the total spin polarization.

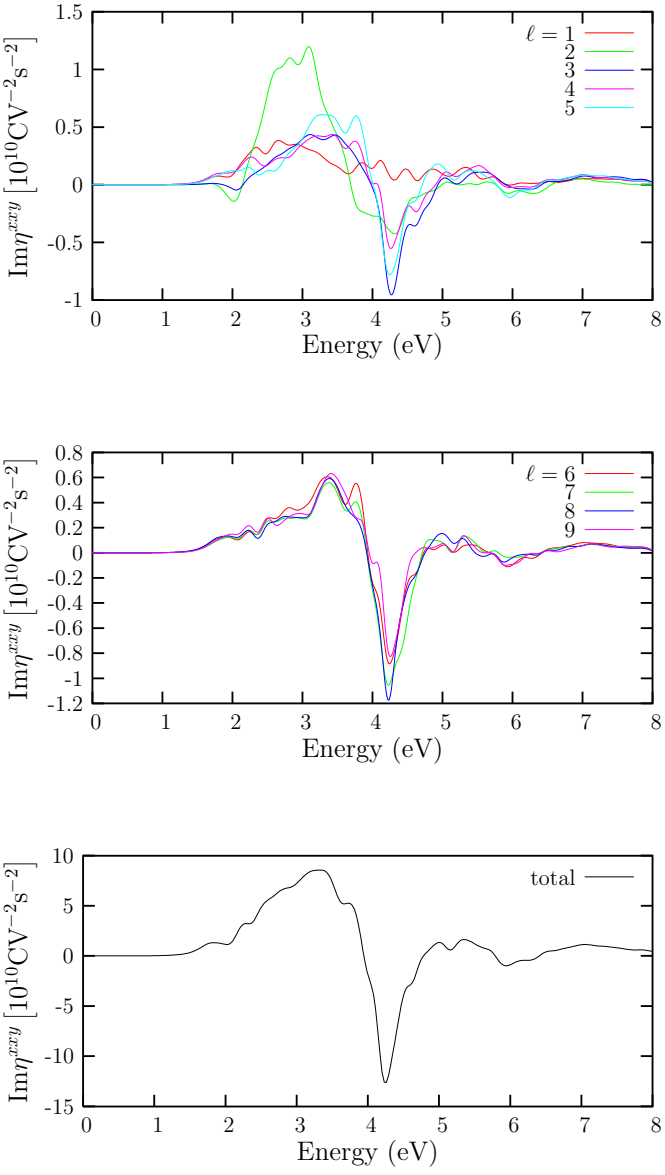

Figure 6.8 : Electric current injection pseudo-tensor η^{xxy} caused by one incident photon in a GaAs(110) surface. At the top: Layered responses. At the bottom: Total response.

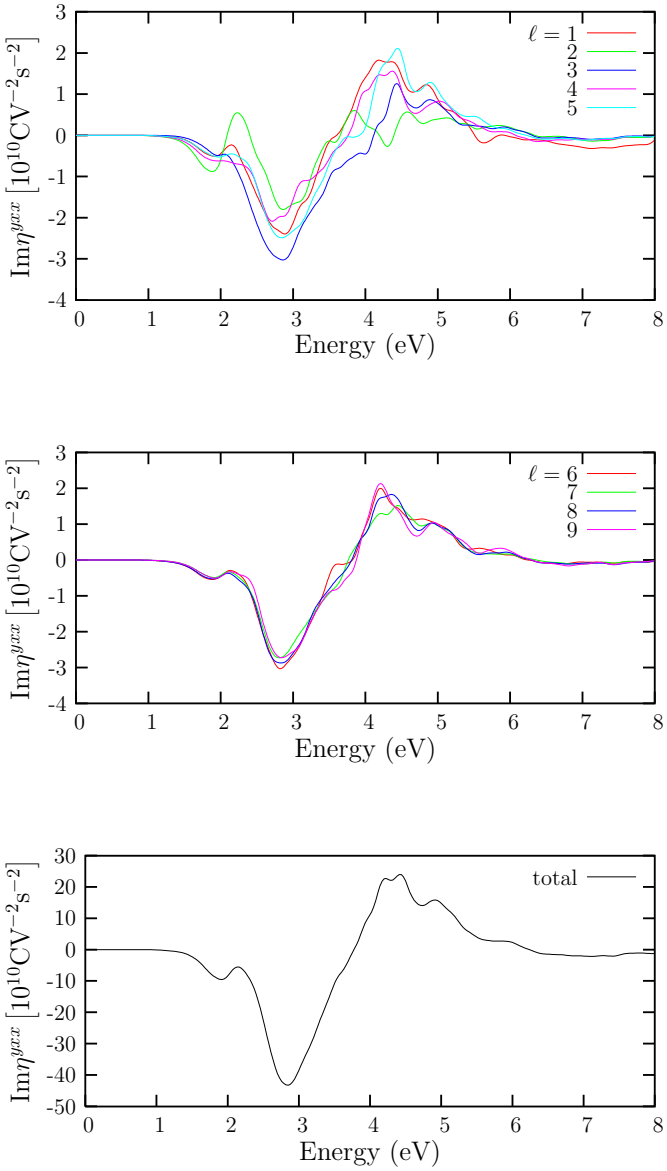

Figure 6.9 : Electric current injection pseudo-tensor η^{yxx} caused by one incident photon in a GaAs(110) surface. At the top: Layered responses. At the bottom: Total response.

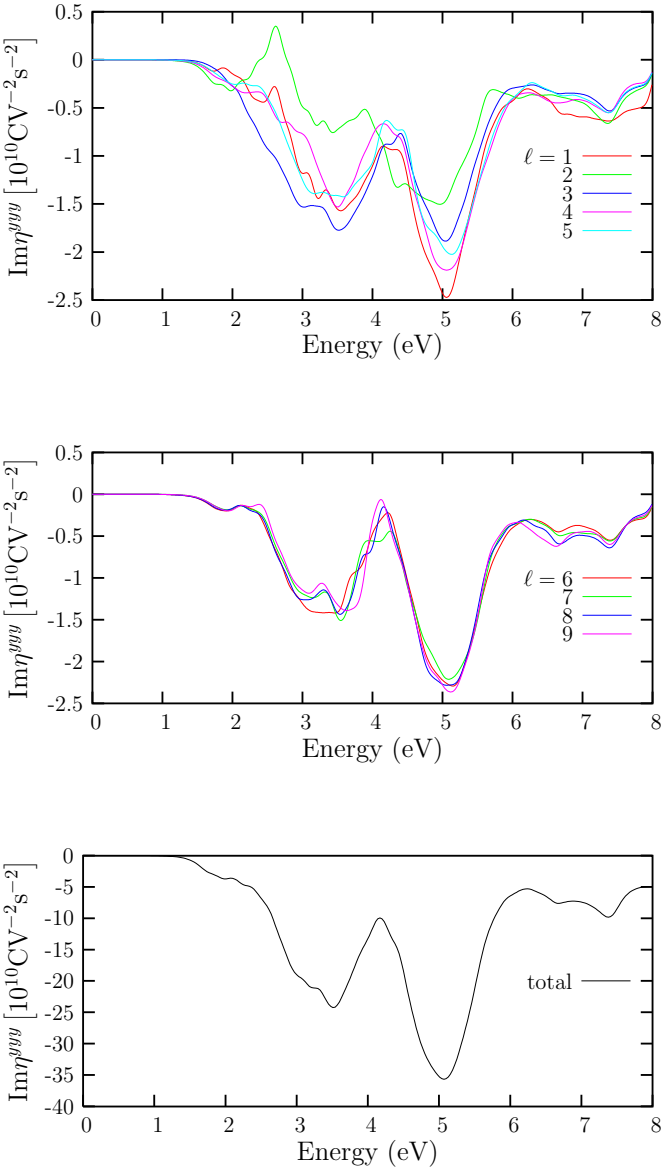

Figure 6.10 : Electric current injection pseudo-tensor η^{yyy} caused by one incident photon in a GaAs(110) surface. At the top: Layered responses. At the bottom: Total response.

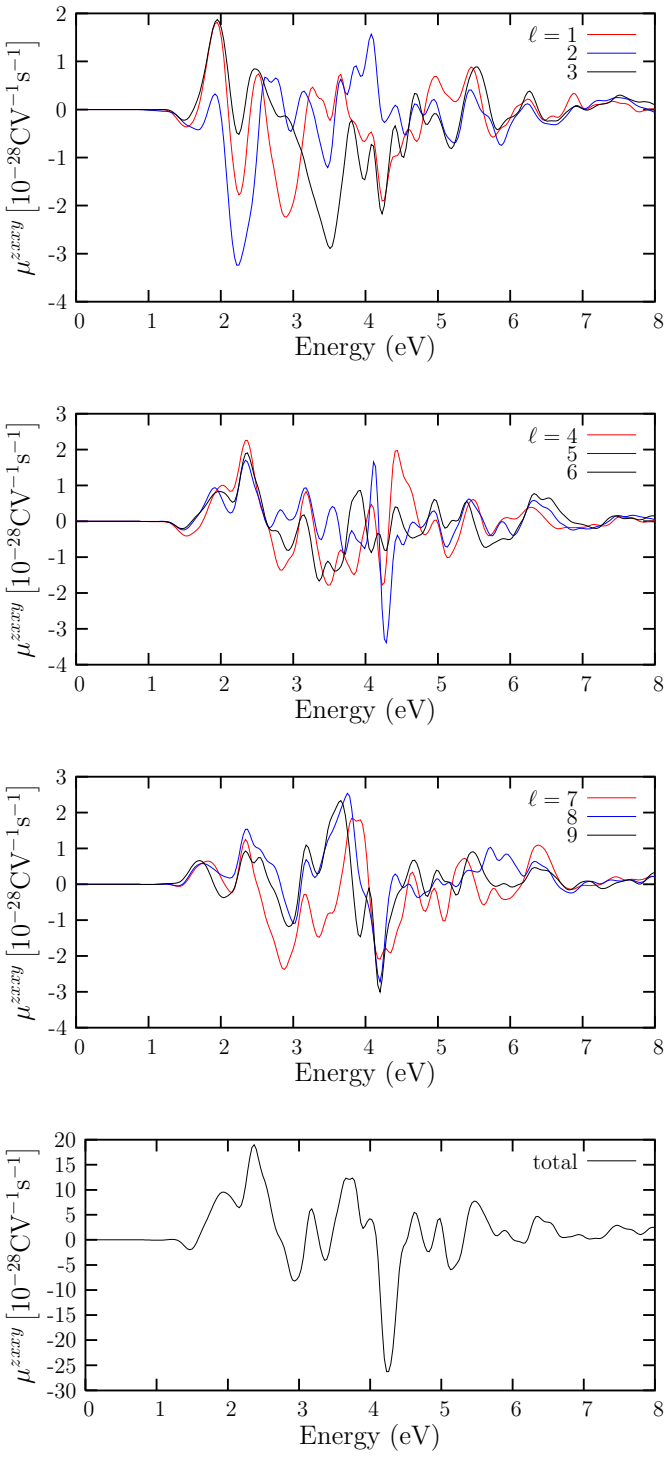

Figure 6.11 : Spin current injection pseudo-tensor μ^{zxxy} caused by one incident photon in a GaAs(110) surface. At the top: Layered responses. At the bottom: Total response.

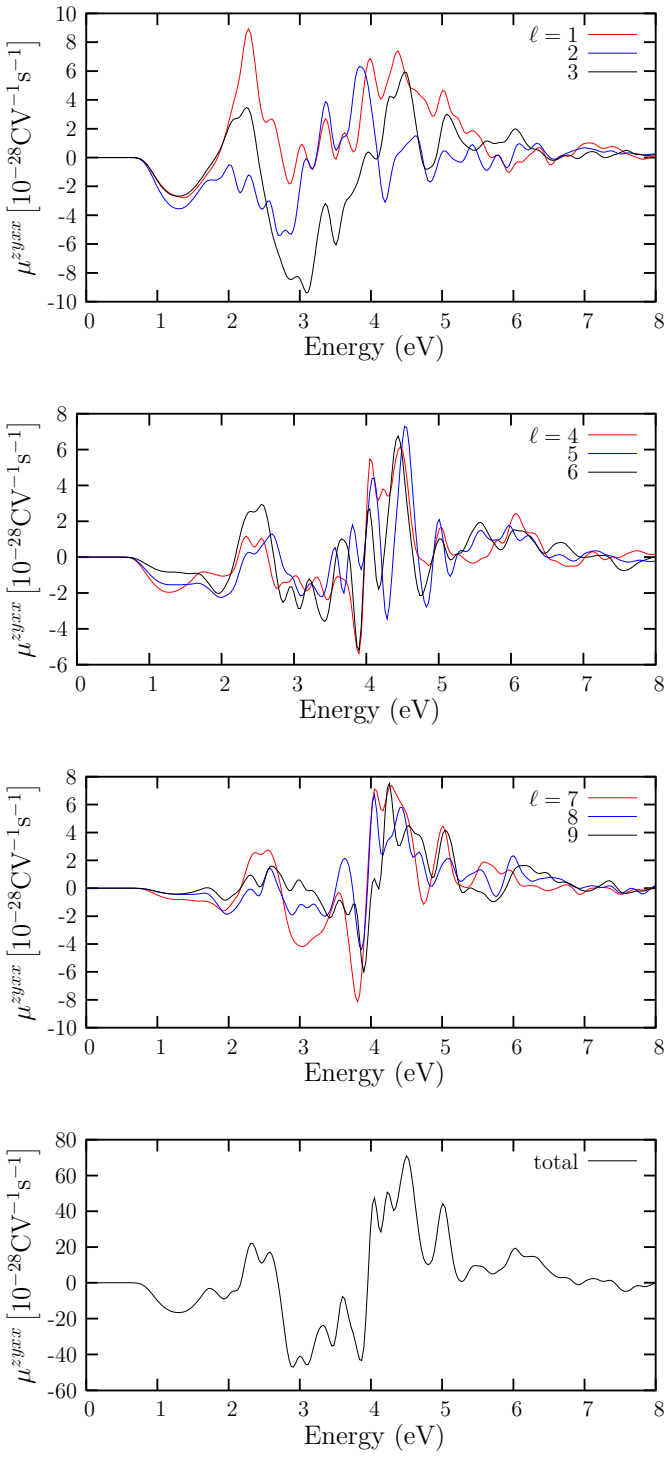

Figure 6.12 : Spin current injection pseudo-tensor μ^{zyxx} caused by one incident photon in a GaAs(110) surface. At the top: Layered responses. At the bottom: Total response.

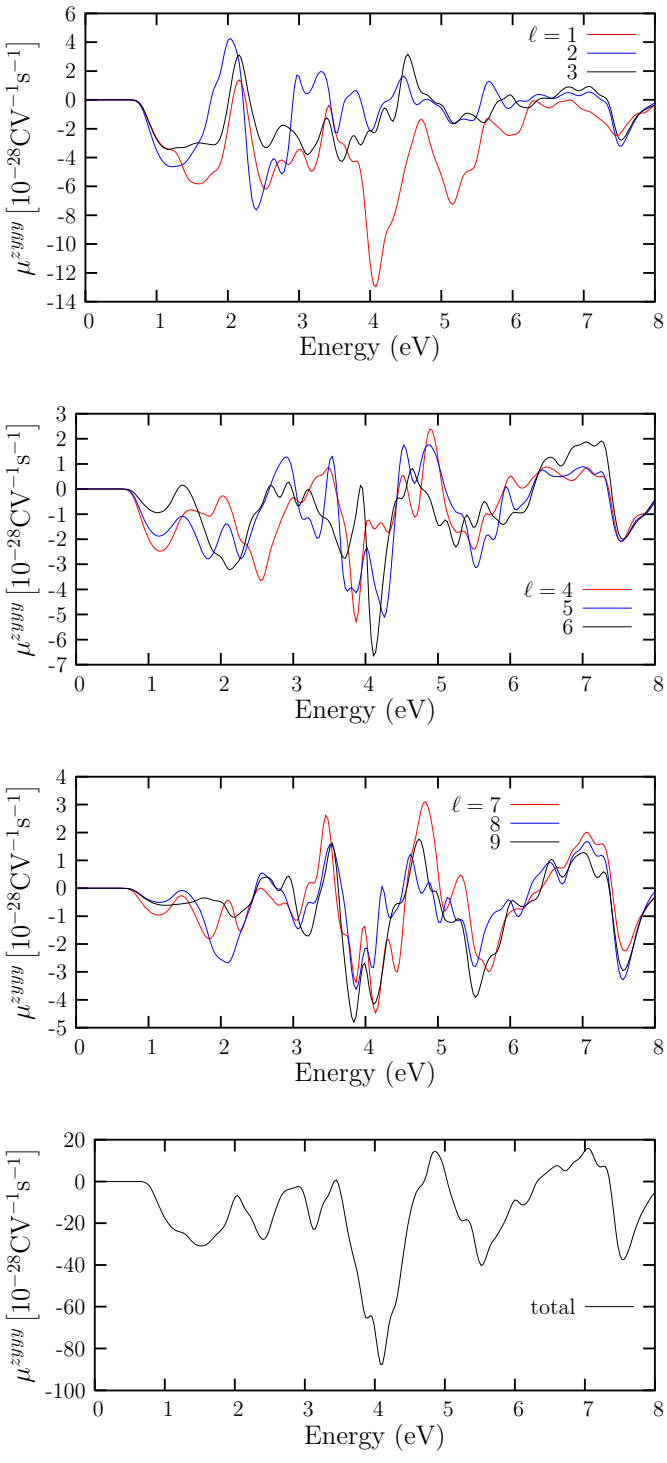

Figure 6.13 : Spin current injection pseudo-tensor μ^{zyyy} caused by one incident photon in a GaAs(110) surface. At the top: Layered responses. At the bottom: Total response.

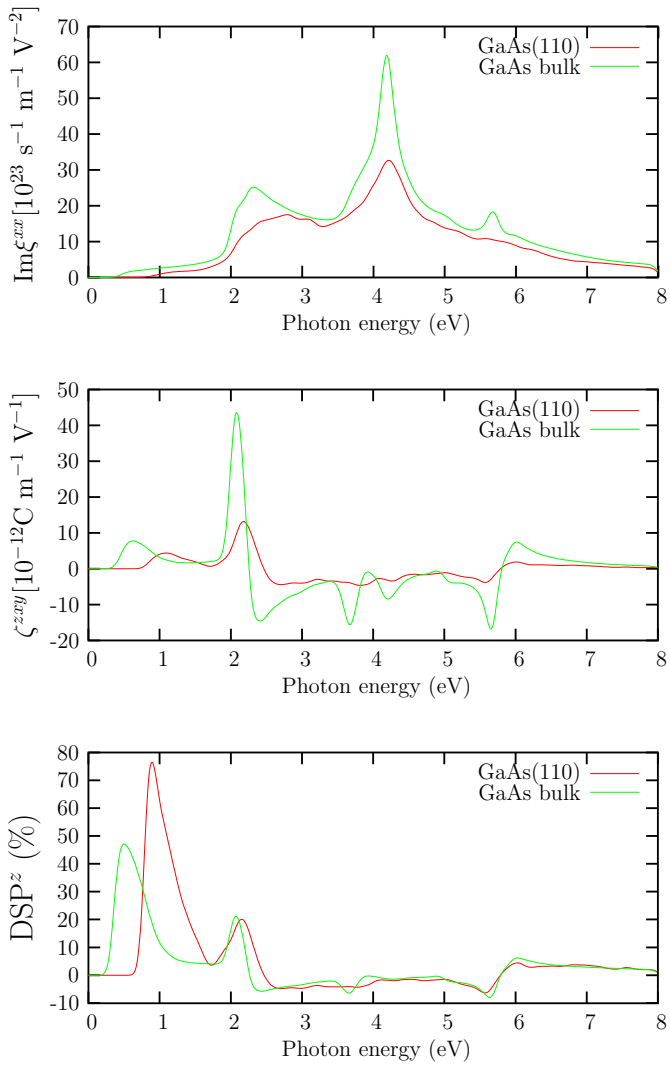

Figure 6.14 : Comparison between responses calculated for GaAs bulk and the GaAs(110) surface. We show ξ^{xx} at the top, ζ^{zyx} and DSP at the bottom. To calculate the responses for GaAs bulk we used an energy cutoff of 20 Ha and 5525 **k**-points distributed homogenuoslly on the first Brillouin zone.

Chapter 7

Conclusions

It was proved in 2003 that it was possible to inject carrier and spin currents into quantum dot due to the absorption of one or two photons [18]. In this work it was determined that the currents due to linear absorption of one photon were zero in bulk GaAs due to its symmetry. In several posterior works [24, 25] it was proved experimentally and theoretically that it was possible to inject currents into a non-centrosymmetric semiconductor.

In this case we made a theoretical study of a semiconductor surface. As it is shown in Fig. 6.3 the surface is non-centrosymmetric and as it was expected the injected currents due to one photon excitations were different from zero. We have exploded the non-centrosymmetry of the surface to show that an electric current together with a spin current can be injected into GaAs(110).

In our work we found that the DSP injected into GaAs(110) is close to 95%. This result shows that the optical properties of a semiconductor surface need not to be equal to the bulk case. This can be explained because the symmetry was broken in our theoretical model by relaxing the surface and imposing an artificial buckling. Moreover, the potential energy due to the ions at the surface is also different from that of the bulk case. In order to validate our results we also calculated the DSP for the GaAs bulk (Fig. 6.14) finding out that it was 50 % in accordance to the experiments made by Bhat *et al.* [24] in which they found it was close to 50 %.

We have shown that the method proposed by Mendoza *et al.* [29] for calculating the layer-by-layer contributions to the linear optical response gives congruent results. All of the responses calculated show a similar behavior; the contributions

of the top and bottom layers were slightly different from the contributions of the layers at the middle of the slab. As it was expected, the layers at the inner part of the slab gave similar results because of the fact that they are bulk layers, then the responses start to change as we approach to the surface. What is more, the sum of all layers contributions gives the total response of the slab.

The layered responses corresponding to the top and back surfaces were found to be equal although the slab was found to be non centro-symmetric. In Fig. 6.1 we can see that the system is not centro-symmetric. To make it clear lets choose the intersection of the two blue lines to be the center of symmetry. Then if it were centro-symmetric each of the two blue lines should connect identical atoms, but, what we see is that gallium atoms are connected to an arsenide atoms. Now that it is obvious that the system is not centro-symmetric how can we explained that both surfaces show the same responses?

As you can see on the same illustration there is a green line that marks a plane parallel to the x and y axes. It is easy to see that the system is symmetric with respect to this plane Thus, because of the fact that the top and back surfaces are equal their corresponding layered responses are also equal.

In order to give a physical meaning to the pseudo-tensors found for electrical injection current we can think of an experiment in which we radiate the sample with a laser light with an intensity $I = 1\,\mathrm{mWcm}^{-2}$ with a repetition rate of 130 fs. According to the pseudo-tensors for the electric current and carriers injection ($\eta^{abc} \sim 10^{11}\,\mathrm{AV}^{-2}\mathrm{s}^{-1}$ and $\xi^{ab} \sim 10^{24}\,\mathrm{V}^{-2}\mathrm{m}^{-1}\mathrm{s}^{-1}$) we obtain a density of carriers of $\sim 10^{9}\mathrm{cm}^{-3}$ and a current of $90\,\mu\mathrm{Acm}^{-3}$.

All in all, we made a full characterization of the spin and carrier population as well as spin and electric currents injected into the GaAs(110) surface. We studied the case of a circularly polarized optical field incident to the surface along the z direction. The injected currents and populations can be controlled by the incident field. It is shown in Eq. (6.5) that if we change the polarization of the incident field (from right-circular to left-circular or vice versa) the DSP injected will also change its spin polarization.

Appendix A

Second quantization

In order to understand the quantum many body theory we have to broaden the concept of a classical quantum field. In classical theories there are collective fields such as sound vibrations and electromagnetic fields. But there are also systems of identical particles like an electron gas that are not comprised in classical theories. Hence the importance of the concept of a *quantum field* . Loosely speaking, it has the function of adding or subtracting particles to the system and it is closely related to the second quantization (SQ) approach.

In quantum mechanics (QM) we use the Schrödinger's wave function to represent a system of just one body. Now, we have to take the next step, that is, we have to extend QM to a macroscopic number of particles. This can be achieved by quantizing the wave function ψ as it was proposed by Jordan and Wigner in 1928 [34]. Then particle field ψ becomes

$$\hat{\psi}(\mathbf{x}, t). \tag{A.1}$$

In order to comprehend the meaning of this particle field operator we will start by remembering the Born's expression for the probability density ρ. He concluded that $\rho(\mathbf{x}) = |\psi(\mathbf{x})|^2$ represents the probability of an electron being at $\mathbf{x}$. Using the new operator form of the wave function, it follows that

$$\hat{\rho}(\mathbf{x}, t) = |\hat{\psi}(\mathbf{x}, t)|^2 = \hat{\psi}^\dagger(\mathbf{x}, t)\hat{\psi}(\mathbf{x}, t). \tag{A.2}$$

From this definition the intensity of the quantum wave represents the fluctuating density of particles.

A.1 Operators in its second quantized form

When the quantized wave function is transformed into an operator $\hat{\psi}(\mathbf{x},t)$, it has to satisfy the Schrödinger's equation [21]

$$i\frac{\partial\hat{\psi}(\mathbf{x},t)}{\partial t} = -\frac{1}{2m}\nabla^2\hat{\psi}(\mathbf{x},t) + \mathcal{V}(\mathbf{x})\hat{\psi}(\mathbf{x},t) \equiv \hat{H}\hat{\psi}(\mathbf{x},t) \tag{A.3}$$

where $\hat{H}$ is not the Hamiltonian of the system but a *Hamiltonian density* .

Defining $u_{\mathbf{k}}(\mathbf{x})$ as eigenstates of $\hat{H}$ so that

$$\hat{H}u_{\mathbf{k}}(\mathbf{x}) = E_{\mathbf{k}}u_{\mathbf{k}}(\mathbf{x}) \tag{A.4}$$

we can construct the state $\hat{\psi}(\mathbf{x},t)$ and its adjoint $\hat{\psi}^\dagger(\mathbf{x},t)$ as follows,

$$\hat{\psi}(\mathbf{x},t) = \sum_{\mathbf{k}}\hat{a}_{\mathbf{k}}u_{\mathbf{k}}(\mathbf{x})e^{-iE_{\mathbf{k}}t}, \tag{A.5a}$$

$$\hat{\psi}^\dagger(\mathbf{x},t) = \sum_{\mathbf{k}}\hat{a}^\dagger_{\mathbf{k}}u^*_{\mathbf{k}}(\mathbf{x})e^{iE_{\mathbf{k}}t}, \tag{A.5b}$$

where $\mathbf{k}$ denotes vectors that exists on reciprocal space. Here $\hat{a}^\dagger_{\mathbf{k}}$ are the coefficients used to construct $\hat{\psi}(\mathbf{x},t)$. They are operators because of the fact that the wavefunction $\hat{\psi}(\mathbf{x},t)$ was defined as an operator. They are known as the *creation (annihilation)* $\hat{a}^\dagger(\hat{a})$ *operators* because they have the role of creating or destroying electrons at a particular $\mathbf{k}$-point.

This definition implies that a quantized wave function creates or destroys a wave-packet centered at $\mathbf{x}$. It sets the main difference between classical fields and quantum fields, the appearance of particles. In other words, a quantum field is no longer thought as a continuous field but as an entity that is composed of discrete particles.

Using these definitions we will proceed to construct the Hamitonian operator $\hat{\mathcal{H}}$. The system Hamitonian is defined as follows

$$\begin{aligned}\hat{\mathcal{H}} &= \int\hat{\psi}^\dagger(\mathbf{x},t)\hat{H}\hat{\psi}(\mathbf{x},t)d^3\mathbf{x} \\ &= \sum_{\mathbf{k},\mathbf{k}'}\int d^3\mathbf{x}\cdot e^{i(E_{\mathbf{k}}-E_{\mathbf{k}'})t}\hat{a}^\dagger_{\mathbf{k}}\hat{a}_{\mathbf{k}'}u^*_{\mathbf{k}}(\mathbf{x})\hat{H}u_{\mathbf{k}'}(\mathbf{x}).\end{aligned} \tag{A.6}$$

By using (A.4) we can obtain

$$\begin{aligned}\hat{\mathcal{H}} &= \sum_{\mathbf{k},\mathbf{k}'} e^{i(E_{\mathbf{k}}-E_{\mathbf{k}'})t} E_{\mathbf{k}'} \hat{a}^{\dagger}_{\mathbf{k}} \hat{a}_{\mathbf{k}'} \int d^3\mathbf{x} \cdot u^{*}_{\mathbf{k}}(\mathbf{x}) u_{\mathbf{k}'}(\mathbf{x}) \\ &= \sum_{\mathbf{k}} E_{\mathbf{k}} \hat{a}^{\dagger}_{\mathbf{k}} \hat{a}_{\mathbf{k}}. \end{aligned} \tag{A.7}$$

To interpret the meaning of the last expression we will define the number operation $\hat{N}_{\mathbf{k}}$ as $\hat{N}_{\mathbf{k}} = \hat{a}^{\dagger}_{\mathbf{k}} \hat{a}_{\mathbf{k}}$. It obeys an eigenvalue equation because when acting on a state $u_{\mathbf{k}}$ it gives us the number of particles $N_{\mathbf{k}}$ that conform the system represented by the ket. That is,

$$\hat{N}_{\mathbf{k}} u_{\mathbf{k}} = N_{\mathbf{k}} u_{\mathbf{k}}. \tag{A.8}$$

Now we can observe from the Eq. (A.7) that at every **k**-point **k** there is a number $N_{\mathbf{k}}$ of particles that have an energy $E_{\mathbf{k}}$. Moreover, in order to get the total energy we have to sum all the **k**-point contributions.

Similarly approach we can represent any operator as*,

$$\hat{\mathcal{O}} = \sum_{\mathbf{k}} \mathcal{O}_{\mathbf{k}} \hat{a}^{\dagger}_{\mathbf{k}} \hat{a}_{\mathbf{k}}. \tag{A.9}$$

A.2 Creation and annihilation operators

When solving the Shrödinger's equation for a periodic array of atoms we find that there are regions where energy is prohibited (gaps) and there are other regions where energy is permitted (bands). As shown in the Fig. A.1 there are valence bands v and conduction bands c. The valence bands are the bands that are occupied by electrons when the crystal is at its *ground state* or state of minimum energy. When there is a perturbation or when the system has more energy it experiments a transition to an *excited state*. That is, an electron from one of the valence bands was given enough energy to pass to a conduction band.

In the SQ approach a transition is performed by a combination of creation-annihilation processes. To illustrate, when an electron experiments a transition from a band v to a band c it is said that the electron was destroyed at the band v and it was created at the band c. These transitions are represented by the *creation*

*A more detailed description of the second quantization techniques can be found in [35].

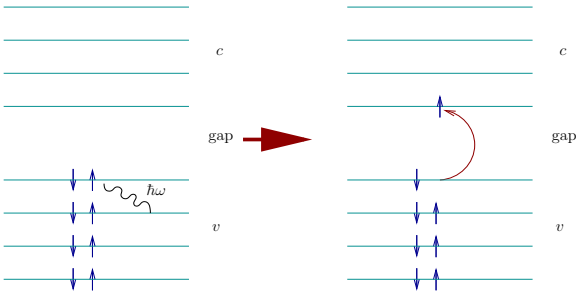

Figure A.1 : We show how a system evolves from its lower state energy to its first excited state. The letters c and v denote conduction and valence bands respectively. We are using the Pauli principle so that at most two electrons can occupy the same band, one with spin up and one with spin down. *Left:* The system is at its ground state, all of the valence bands are filled while the conduction bands are empty. *Right:* A photon of energy $\hbar\omega$ raises an electron to a conduction band leaving a hole in the valence band which was occupied by it.

and *annihilation operators*, namely, $\hat{a}^{\dagger}_{n,\mathbf{k}}$ is the creation operator and $\hat{a}_{n,\mathbf{k}}$ is the annihilation operator . When the creation (annihilation) operator $\hat{a}^{\dagger}_{n,\mathbf{k}}(\hat{a}_{n,\mathbf{k}})$ acts on a state at a given $\mathbf{k}$-point an electron is created (annihilated) in such a state.

We define an electronic state by a ket of the following form $|n,\mathbf{k}>$ in order to denote that we are referring to the band n and $\mathbf{k}$-point $\mathbf{k}$. By using this ket representation we can define

$$\hat{a}_{n,\mathbf{k}}|n,\mathbf{k}\rangle = \begin{cases} |c,\mathbf{k}\rangle & n=v \\ 0 & n=c \end{cases}, \tag{A.10a}$$

and

$$\hat{a}^{\dagger}_{n,\mathbf{k}}|n,\mathbf{k}\rangle = \begin{cases} 0 & n=v \\ |v,\mathbf{k}\rangle & n=c \end{cases}, \tag{A.10b}$$

Notice that when an electron is annihilated a hole is also created. In a similar way, when creating an electron we are destroying a hole. Therefore, it is necessary to define the creation-annihilation operators for holes.

We define the creation operator for holes as $\hat{b}^\dagger$ and the annihilation operator for holes as $\hat{b}$. It is important to note that both hole operators and electron operators act at the same time. Then, we can observe a direct relation between both sets of operators:

$$\begin{aligned} \hat{a}^\dagger \text{ acting on } c &\Rightarrow \hat{b} \text{ acting on } c \\ \hat{a} \text{ acting on } v &\Rightarrow \hat{b}^\dagger \text{ acting on } v. \end{aligned} \tag{A.11}$$

All in all, we define the creation-annihilation operators for holes as follows:

$$\hat{b}_{n,\mathbf{k}}|n,\mathbf{k}\rangle = \begin{cases} |c,\mathbf{k}\rangle & n=c \\ 0 & n=v \end{cases}, \tag{A.12a}$$

$$\hat{b}^\dagger_{n,\mathbf{k}}|n,\mathbf{k}\rangle = \begin{cases} 0 & n=c \\ |v,\mathbf{k}\rangle & n=v \end{cases}, \tag{A.12b}$$

These operators have the following properties:

$$\{\hat{a}_{n,\mathbf{k}}, \hat{a}^\dagger_{n',\mathbf{k}'}\} = \{\hat{b}_{n,\mathbf{k}}, \hat{b}^\dagger_{n',\mathbf{k}'}\} = \delta_{n,n'}\delta_{\mathbf{k},\mathbf{k}'} \tag{A.13a}$$

$$\{\hat{a}_{n,\mathbf{k}}, \hat{a}_{n',\mathbf{k}'}\} = \{\hat{a}^\dagger_{n,\mathbf{k}}, \hat{a}^\dagger_{n',\mathbf{k}'}\} = \{\hat{b}_{n,\mathbf{k}}, \hat{b}_{n',\mathbf{k}'}\} = \{\hat{b}^\dagger_{n,\mathbf{k}}, \hat{b}^\dagger_{n',\mathbf{k}'}\} = 0 \tag{A.13b}$$

where the anti-commutation of two operators $\hat{a}$ and $\hat{b}$ is defined as follows,

$$\{\hat{a}, \hat{b}\} = \hat{a}\hat{b} + \hat{b}\hat{a} \tag{A.14}$$

A.3 Ground state Hamitonian in the SQ approach

We can redefine the Hamitonian shown in Eq. (A.7). By using Planck's quantization of the energy $E = \hbar\omega$ and introducing band and $\mathbf{k}$-point degeneracies we get

$$\hat{\mathcal{H}}_o = \sum_{n,\mathbf{k}} \hbar\omega_{n,\mathbf{k}} \hat{a}^\dagger_{n,\mathbf{k}} \hat{a}_{n,\mathbf{k}}. \tag{A.15}$$

Our next step is to separate the terms that contain the contribution of the conduction bands from the ones for valence bands, to obtain

$$\hat{\mathcal{H}}_o = \sum_{c,\mathbf{k}} \hbar\omega_{c,\mathbf{k}} \hat{a}^\dagger_{c,\mathbf{k}} \hat{a}_{c,\mathbf{k}} + \sum_{v,\mathbf{k}} \hbar\omega_{v,\mathbf{k}} \hat{a}^\dagger_{v,\mathbf{k}} \hat{a}_{v,\mathbf{k}}. \tag{A.16}$$

In our formalism we will be using the creation-annihilation operators for electrons when treating conduction bands, but, we will be use the operators for holes when dealing with valence bands. Then the equation (A.16) becomes

$$\hat{\mathcal{H}_o} = \sum_{c,\mathbf{k}} \hbar\omega_{c,\mathbf{k}} \hat{a}^\dagger_{c,\mathbf{k}} \hat{a}_{c,\mathbf{k}} + \sum_{v,\mathbf{k}} \hbar\omega_{v,\mathbf{k}} \hat{b}_{v,\mathbf{k}} \hat{b}^\dagger_{v,\mathbf{k}}. \tag{A.17}$$

By using the anti-commutation relation (A.13a),

$$\hat{\mathcal{H}_o} = \sum_{c,\mathbf{k}} \hbar\omega_{c,\mathbf{k}} \hat{a}^\dagger_{c,\mathbf{k}} \hat{a}_{c,\mathbf{k}} + \sum_{v,\mathbf{k}} \hbar\omega_{v,\mathbf{k}} - \sum_{v,\mathbf{k}} \hbar\omega_{v,\mathbf{k}} \hat{b}^\dagger_{v,\mathbf{k}} \hat{b}_{v,\mathbf{k}}. \tag{A.18}$$

Since the second term is a constant energy E of the ground state, we will define the ground state Hamiltonian $\hat{\mathcal{H}_o}'$ as,

$$\hat{\mathcal{H}_o}' \equiv \hat{\mathcal{H}_o} - \sum_{v,\mathbf{k}} \hbar\omega_{v,\mathbf{k}} \tag{A.19}$$

Renaming the ground state Hamitonian $\hat{\mathcal{H}_o}'$ as $\hat{\mathcal{H}_o}$ we find that,

$$\hat{\mathcal{H}_o} = \sum_{c,\mathbf{k}} \hbar\omega_{c,\mathbf{k}} \hat{a}^\dagger_{c,\mathbf{k}} \hat{a}_{c,\mathbf{k}} - \sum_{v,\mathbf{k}} \hbar\omega_{v,\mathbf{k}} \hat{b}^\dagger_{v,\mathbf{k}} \hat{b}_{v,\mathbf{k}} \tag{A.20}$$

In a similar way, we can decompose Eq. (A.9) in conduction and valence bands to finally get the general form of an operator $\hat{\mathcal{O}}$ in SQ:

$$\begin{aligned} \hat{\mathcal{O}} = &\sum_{c,c'\mathbf{k}} \mathcal{O}_{cc'}(\mathbf{k}) \hat{a}^\dagger_{c,\mathbf{k}} \hat{a}_{c',\mathbf{k}} + \sum_{c,v\mathbf{k}} \mathcal{O}_{cv}(\mathbf{k}) \hat{a}^\dagger_{c,\mathbf{k}} \hat{b}^\dagger_{v,\mathbf{k}} \\ &+ \sum_{v,c\mathbf{k}} \mathcal{O}_{vc}(\mathbf{k}) \hat{b}_{v,\mathbf{k}} \hat{a}_{c,\mathbf{k}} - \sum_{v,v'\mathbf{k}} \mathcal{O}_{vv'}(\mathbf{k}) \hat{b}^\dagger_{v',\mathbf{k}} \hat{b}_{v,\mathbf{k}} \end{aligned} \tag{A.21}$$

Appendix B

The interaction Hamiltonian

In quantum mechanics (QM) there are two basic representations to work with. They are the *Schrödinger's picture* and the *Heisenberg's picture*. Moreover, there is another useful formalism named as the *interaction picture*. It is important to note that we can use any of these forms and the results have to be equal. They are consistent with each other because when we change of representation the eigenvalues of an operator do not change.

In this section our main goal is to find the interaction Hamiltonian $\hat{\mathcal{H}}_i$ in its second quantized (SQ) form. In order to do it, we will use the concepts developed in the last appendix, and we will use *the interaction picture*.

B.1 The interaction representation

In this section we will use the interaction representation to perform our calculations in order to work with matrices instead of functions as it is done in the Schrödinger's approach. At the end it will let us define the interaction Hamiltonian.

An operator in its interaction representation $O_I(t)$ is defined as

$$\hat{\mathcal{O}}_I(t) = \hat{U}_o^\dagger(t)\hat{\mathcal{O}}\hat{U}_o(t) \tag{B.1}$$

where $U_o^\dagger(t)$ and $\hat{U}_o(t)$ are unitary operators. As it will be shown in Eq. (C.4), they have the following form:

$$\hat{U}_o^\dagger(t) = e^{i\frac{\hat{\mathcal{H}}_o t}{\hbar}} \tag{B.2a}$$

and

$$\hat{U}_o(t) = e^{-i\frac{\hat{\mathcal{H}}_o t}{\hbar}}. \tag{B.2b}$$

Differentiating Eq. (B.1)

$$\begin{aligned}
\frac{\mathrm{d}\hat{\mathcal{O}}_I(t)}{\mathrm{d}t} &= i\frac{\hat{\mathcal{H}}_o}{\hbar}e^{i\frac{\hat{\mathcal{H}}_o t}{\hbar}}\hat{\mathcal{O}}e^{-i\frac{\hat{\mathcal{H}}_o t}{\hbar}} - i\frac{\hat{\mathcal{H}}_o}{\hbar}e^{i\frac{\hat{\mathcal{H}}_o t}{\hbar}}\hat{\mathcal{O}}e^{-i\frac{\hat{\mathcal{H}}_o t}{\hbar}} \\
&= \frac{i}{\hbar}e^{i\frac{\hat{\mathcal{H}}_o t}{\hbar}}\left(\hat{\mathcal{H}}_o\hat{\mathcal{O}} - \hat{\mathcal{O}}\hat{\mathcal{H}}_o\right)e^{-i\frac{\hat{\mathcal{H}}_o t}{\hbar}} \\
&= \frac{i}{\hbar}e^{i\frac{\hat{\mathcal{H}}_o t}{\hbar}}\left[\hat{\mathcal{H}}_o, \hat{\mathcal{O}}\right]e^{-i\frac{\hat{\mathcal{H}}_o t}{\hbar}} \\
&= \frac{i}{\hbar}\left(\hat{\mathcal{H}}_o e^{i\frac{\hat{\mathcal{H}}_o t}{\hbar}}\hat{\mathcal{O}}e^{-i\frac{\hat{\mathcal{H}}_o t}{\hbar}} - e^{i\frac{\hat{\mathcal{H}}_o t}{\hbar}}\hat{\mathcal{O}}e^{-i\frac{\hat{\mathcal{H}}_o t}{\hbar}}\hat{\mathcal{H}}_o\right) \\
&= \frac{i}{\hbar}\left(\hat{\mathcal{H}}_o\hat{\mathcal{O}}_I - \hat{\mathcal{O}}_I\hat{\mathcal{H}}_o\right) \\
&= \frac{i}{\hbar}\left[\hat{\mathcal{H}}_o, \hat{\mathcal{O}}_I\right]
\end{aligned} \tag{B.3}$$

where we used the fact that $\left[\hat{\mathcal{H}}_o, \hat{\mathcal{H}}_o\right] = 0$.Here, we used the commutator of two operators defined by $\left[\hat{a}, \hat{b}\right] = \hat{a}\hat{b} - \hat{b}\hat{a}$. For more information on this topic read [23].

Eq. (B.3) is the so called *equation of motion* because it defines the time evolution of an operator $\hat{\mathcal{O}}$ in terms of its commutator with the ground state Hamiltonian.

B.2 Some useful commutators

Now we are going to show some equations that will be helpful in the future. From the commutator of $\hat{\mathcal{H}}_o$ and $\hat{a}_c$ and Eq. (A.7),

$$\left[\hat{\mathcal{H}}_o, \hat{a}_c\right] = \sum_n \hbar\omega_n \left[\hat{a}_n^\dagger \hat{a}_n, \hat{a}_c\right], \tag{B.4}$$

by using the relations (A.13a) and (A.13b) we can find the following relations:

$$\begin{aligned}
\left[\hat{a}_n^\dagger \hat{a}_n, \hat{a}_c\right] &= \hat{a}_c\hat{a}_n^\dagger\hat{a}_n \\
&= \hat{a}_n^\dagger\hat{a}_n\hat{a}_c - \delta_{c,n}\hat{a}_n + \hat{a}_n^\dagger\hat{a}_c\hat{a}_n \\
&= \hat{a}_n^\dagger\hat{a}_n\hat{a}_c - \delta_{c,n}\hat{a}_n - \hat{a}_n^\dagger\hat{a}_n\hat{a}_c \\
&= -\delta_{c,n}\hat{a}_n
\end{aligned} \tag{B.5}$$

Then, Eq. (B.4) becomes

$$\begin{aligned}\left[\hat{\mathcal{H}}_o, \hat{a}_c\right] &= \sum_n -\hbar\omega_n \delta_{c,n}\hat{a}_n \\ &= -\hbar\omega_c \hat{a}_c \end{aligned} \tag{B.6}$$

B.3 The equation of motion

Now we have the elements to build the equation of motion for the annihilation operator $\hat{a}_c$. Using eq (B.3)

$$\begin{aligned}\frac{\mathrm{d}\hat{a}_{cI}(t)}{\mathrm{d}t} &= -i\omega_c e^{i\frac{\hat{\mathcal{H}}_o t}{\hbar}}\hat{a}_c e^{-i\frac{\hat{\mathcal{H}}_o t}{\hbar}} \\ &= -i\omega_c \hat{a}_{cI} \end{aligned} \tag{B.7}$$

From the commutator (B.6),

$$\begin{aligned}\hat{a}_c\hat{\mathcal{H}}_o &= \hat{\mathcal{H}}_o\hat{a}_c + \hbar\omega_c\hat{a}_c = \left(\hat{\mathcal{H}}_o + \hbar\omega_c\right)\hat{a}_c \\ \hat{a}_c\hat{\mathcal{H}}_o{}^2 &= \hat{a}_c\hat{\mathcal{H}}_o\hat{\mathcal{H}}_o = \left(\hat{\mathcal{H}}_o + \hbar\omega_c\right)\hat{a}_c\hat{\mathcal{H}}_o = \left(\hat{\mathcal{H}}_o + \hbar\omega_c\right)^2\hat{a}_c. \end{aligned} \tag{B.8}$$

This result will be used to express the equation of motion in another way. By making a Taylor's expansion

$$\begin{aligned}\hat{a}_c e^{-i\frac{\hat{\mathcal{H}}_o t}{\hbar}} &= \hat{a}_c\left(1 - \frac{i}{\hbar}\left(\hat{\mathcal{H}}_o + \hbar\omega_c\right) + \frac{1}{2}\left(-\frac{i}{\hbar}\right)^2\left(\hat{\mathcal{H}}_o + \hbar\omega_c\right)^2 + ...\right) \\ &= e^{-\frac{i}{\hbar}(\hat{\mathcal{H}}_o + \hbar\omega_c)t}\hat{a}_c \end{aligned} \tag{B.9}$$

By substituting Eq. (B.9) into Eq. (B.7) the equation of motion for the operator $\hat{a}_c$ can be written as

$$\begin{aligned}\frac{\mathrm{d}\hat{a}_{cI}(t)}{\mathrm{d}t} &= -i\omega_c e^{-i\frac{\hat{\mathcal{H}}_o t}{\hbar}} e^{-\frac{i}{\hbar}(\hat{\mathcal{H}}_o + \hbar\omega_c)t}\hat{a}_c \\ &= -i\omega_c e^{-i\omega_c t}\hat{a}_c \end{aligned} \tag{B.10}$$

Solving this last equation we find out that

$$\hat{a}_{cI}(t) = e^{-i\omega_c t}\hat{a}_c \tag{B.11}$$

In a similar way, it is easy to prove that

$$\begin{aligned}\frac{\mathrm{d}\hat{a}^{\dagger}_{cI}(t)}{\mathrm{d}t} &= i\omega_c e^{i\frac{\hat{\mathcal{H}}_o t}{\hbar}} e^{-\frac{i}{\hbar}(\hat{\mathcal{H}}_o-\hbar\omega_c)t}\hat{a}_c \\ &= i\omega_c e^{i\omega_c t}\hat{a}^{\dagger}_c \qquad \text{(B.12a)}\end{aligned}$$

$$\hat{a}^{\dagger}_{cI}(t) = e^{i\omega_c t}\hat{a}^{\dagger}_c \qquad \text{(B.12b)}$$

To summarize:

$$\hat{a}_{cI}(t) = e^{-i\omega_c t}\hat{a}_c \qquad \text{(B.13a)}$$

$$\hat{a}^{\dagger}_{cI}(t) = e^{i\omega_c t}\hat{a}^{\dagger}_c \qquad \text{(B.13b)}$$

$$\hat{b}_{vI}(t) = e^{i\omega_v t}\hat{b}_v \qquad \text{(B.13c)}$$

$$\hat{b}^{\dagger}_{vI}(t) = e^{-i\omega_v t}\hat{b}^{\dagger}_v \qquad \text{(B.13d)}$$

B.4 The momentum operator

Now, we are going to use these expressions to find the momentum operator $\hat{\mathbf{p}}$ in its second-quantized form. By using (A.21) the momentum operator can be written as follows:

$$\hat{\mathbf{p}}_I = e^{i\frac{\hat{\mathcal{H}}_o t}{\hbar}}\hat{\mathbf{p}}e^{-i\frac{\hat{\mathcal{H}}_o t}{\hbar}} \qquad \text{(B.14a)}$$

$$\begin{aligned}\hat{\mathbf{p}}_I = &\sum_{c,c',\mathbf{k}} \mathbf{p}_{cc'}(\mathbf{k}) e^{i\frac{\hat{\mathcal{H}}_o t}{\hbar}}\hat{a}^{\dagger}_{c,\mathbf{k}}\hat{a}_{c',\mathbf{k}}e^{-i\frac{\hat{\mathcal{H}}_o t}{\hbar}} + \sum_{c,v,\mathbf{k}} \mathbf{p}_{cv}(\mathbf{k}) e^{i\frac{\hat{\mathcal{H}}_o t}{\hbar}}\hat{a}^{\dagger}_{c,\mathbf{k}}\hat{b}^{\dagger}_{v,\mathbf{k}}e^{-i\frac{\hat{\mathcal{H}}_o t}{\hbar}} \\ &+ \sum_{v,c,\mathbf{k}} \mathbf{p}_{vc}(\mathbf{k}) e^{i\frac{\hat{\mathcal{H}}_o t}{\hbar}}\hat{b}_{v,\mathbf{k}}\hat{a}_{c,\mathbf{k}}e^{-i\frac{\hat{\mathcal{H}}_o t}{\hbar}} - \sum_{v,v',\mathbf{k}} \mathbf{p}_{vv'}(\mathbf{k}) e^{i\frac{\hat{\mathcal{H}}_o t}{\hbar}}\hat{b}^{\dagger}_{v',\mathbf{k}}\hat{b}_{v,\mathbf{k}}e^{-i\frac{\hat{\mathcal{H}}_o t}{\hbar}}\end{aligned} \qquad \text{(B.14b)}$$

Working on the first term of (B.14b) and using Eqs. (B.10), (B.12) , (B.13) and (B.14b) we find out that:

$$\begin{aligned}\hat{\mathbf{p}}^{(1)}_I(t) &= \sum_{c,c',\mathbf{k}} \mathbf{p}_{cc'}(\mathbf{k}) e^{i\frac{\hat{\mathcal{H}}_o t}{\hbar}}\hat{a}^{\dagger}_{c,\mathbf{k}}e^{-\frac{i}{\hbar}(\hat{\mathcal{H}}_o+\hbar\omega_c)t}\hat{a}_{c',\mathbf{k}} \\ &= \sum_{c,c',\mathbf{k}} \mathbf{p}_{cc'}(\mathbf{k}) e^{i\frac{\hat{\mathcal{H}}_o t}{\hbar}} e^{-\frac{i}{\hbar}(\hat{\mathcal{H}}_o-\hbar\omega_c)t}\hat{a}^{\dagger}_{c,\mathbf{k}}e^{-i\omega_{c'}t}\hat{a}_{c',\mathbf{k}} \\ &= \sum_{c,c',\mathbf{k}} \mathbf{p}_{cc'}(\mathbf{k})\hat{a}^{\dagger}_{c,\mathbf{k}}\hat{a}_{c',\mathbf{k}}e^{i(\omega_c-\omega_{c'})t} \qquad \text{(B.15)}\end{aligned}$$

The remaining terms can be calculated similarly:

$$\sum_{c,v,\mathbf{k}} \mathbf{p}_{cv}(\mathbf{k}) e^{i\frac{\hat{\mathcal{H}}_o t}{\hbar}} \hat{a}^\dagger_{c,\mathbf{k}} \hat{b}^\dagger_{v,\mathbf{k}} e^{-i\frac{\hat{\mathcal{H}}_o t}{\hbar}} = \sum_{c,v,\mathbf{k}} \mathbf{p}_{cv}(\mathbf{k}) \hat{a}^\dagger_{c,\mathbf{k}} \hat{b}^\dagger_{v,\mathbf{k}} e^{i(\omega_c - \omega_v)}, \tag{B.16a}$$

$$\sum_{c,v,\mathbf{k}} \mathbf{p}_{vc}(\mathbf{k}) e^{i\frac{\hat{\mathcal{H}}_o t}{\hbar}} \hat{b}_{v,\mathbf{k}} \hat{a}_{c,\mathbf{k}} e^{-i\frac{\hat{\mathcal{H}}_o t}{\hbar}} = \sum_{c,v,\mathbf{k}} \mathbf{p}_{vc}(\mathbf{k}) \hat{b}_{v,\mathbf{k}} \hat{a}_{c,\mathbf{k}} e^{i(\omega_v - \omega_c)t}, \tag{B.16b}$$

$$\sum_{v,v',\mathbf{k}} \mathbf{p}_{vv'}(\mathbf{k}) e^{i\frac{\hat{\mathcal{H}}_o t}{\hbar}} \hat{b}^\dagger_{v',\mathbf{k}} \hat{b}_{v,\mathbf{k}} e^{-i\frac{\hat{\mathcal{H}}_o t}{\hbar}} = \sum_{v,v',\mathbf{k}} \mathbf{p}_{vv'}(\mathbf{k}) \hat{b}^\dagger_{v',\mathbf{k}} \hat{b}_{v,\mathbf{k}} e^{i(\omega_v - \omega_{v'})t} \tag{B.16c}$$

With the last four terms we can construct the momentum operator in its SQ form. It will be helpful to rewrite the interaction Hamiltonian $\hat{\mathcal{H}}_i$ defined in Eq. (3.8c). By substituting the second-quantized form of the momentum into the definition of $\hat{\mathcal{H}}_i$ we can find out that the interaction Hamiltonian can be expressed by a combination of creation-annihilation operators as follows:

$$\hat{\mathcal{H}}_i = -\frac{e}{mc}\mathbf{A}(t) \cdot \left\{ \begin{array}{c} \sum_{c,c',\mathbf{k}} \mathbf{p}_{cc'}(\mathbf{k}) \hat{a}^\dagger_{c,\mathbf{k}} \hat{a}_{c',\mathbf{k}} e^{i\omega_{cc'}t} \\ + \sum_{c,v,\mathbf{k}} \mathbf{p}_{cv}(\mathbf{k}) \hat{a}^\dagger_{c,\mathbf{k}} \hat{b}^\dagger_{v,\mathbf{k}} e^{i\omega_{cv}t} \\ + \sum_{c,v,\mathbf{k}} \mathbf{p}_{vc}(\mathbf{k}) \hat{b}_{v,\mathbf{k}} \hat{a}_{c,\mathbf{k}} e^{i\omega_{vc}t} \\ - \sum_{v,v',\mathbf{k}} \mathbf{p}_{vv'}(\mathbf{k}) \hat{b}^\dagger_{v',\mathbf{k}} \hat{b}_{v,\mathbf{k}} e^{i\omega_{vv'}t} \end{array} \right\} \tag{B.17}$$

where $\omega_{ij} = \omega_i - \omega_j$.

Appendix C

Perturbation Theory

Frequently, for a given system it is not possible to solve the Schrödinger's equation exactly. In these kind of situations we need to use approximations to simplify the problem. In quantum mechanics (QM) there are many approximations that can be used. In this Chapter we will introduce the perturbations theory (PT) as a method that will simplify the problem of a system radiated by an external field.

The idea behind the PT is that of making a small modification to a solved problem. As we saw in Eq. (3.8b) the Hamiltonian that describes an atom inside a radiative field is $\hat{\mathcal{H}} = \hat{\mathcal{H}}_o + \hat{\mathcal{H}}_i$. Where $\hat{\mathcal{H}}_o$ is the Hamiltonian of the system without the external field and $\hat{\mathcal{H}}_i$ is the interaction Hamiltonian between a particle's orbit and the electromagnetic (EM) field. In this case, if the external field is not excessively high, the Hamiltonian's effect will be reduced to the extent of making small modifications on $\hat{\mathcal{H}}_o$. Therefore, the problem can be thought of a Hamiltonian $\hat{\mathcal{H}}_o$ plus a sequence of small perturbations.

Now we are going to construct mathematical expressions to obtain the expected value of an observable due to a perturbation. We will introduce unitary operators $\hat{U}_o(t)$ and $\hat{U}(t)$ to represent the perturbations that will interact with the the system. We start with the time dependent Schrödinger's equation:

$$i\hbar\frac{\partial}{\partial t}\psi = \hat{\mathcal{H}}_o\psi \tag{C.1}$$

We can say that the wave function $\psi(t)$ at an initial time t_o evolves by small perturbations given by $\hat{U}()$, *i.e.*,

$$\psi(t) = \hat{U}(t)\psi(t_o). \tag{C.2}$$

Then we can construct the following two relations:

$$i\hbar\frac{\mathrm{d}}{\mathrm{d}t}\hat{U}_o(t) = \hat{\mathcal{H}}_o\hat{U}_o(t), \tag{C.3a}$$

$$i\hbar\frac{\mathrm{d}}{\mathrm{d}t}\hat{U}(t) = \hat{\mathcal{H}}\hat{U}(t). \tag{C.3b}$$

Solving Eq. (C.3a) we find that

$$\hat{U}_o(t) = Ae^{-i\frac{\hat{\mathcal{H}}_o t}{\hbar}}. \tag{C.4}$$

Where A is an arbitrary constant. In order to find A we make the perturbation to start at time t equal to zero. So that,

$$\hat{U}_o(t=0) = 1 \Rightarrow A = 1. \tag{C.5}$$

It is important to note that $\hat{\mathcal{H}}_o$ is the ground state Hamiltonian, and after $\hat{\mathcal{H}}_o$ has been perturbed it becomes the perturbed Hamiltonian $\hat{\mathcal{H}}$. Therefore at time t equal to minus infinity $\hat{\mathcal{H}}$ and $\hat{\mathcal{H}}_o$ have to be equivalent.

$$\hat{\mathcal{H}}(t \to -\infty) = \hat{\mathcal{H}}_o. \tag{C.6}$$

Similarly, the unitary operators:

$$\hat{U}(t \to -\infty) = \hat{U}_o(t \to -\infty). \tag{C.7}$$

Now, we are going to represent $\hat{U}$ as an operator originally equivalent to $\hat{U}_o$ but modified over the time by numerous small perturbations. In order to do so, we start with the following equation:

$$\begin{aligned}
i\hbar\frac{\mathrm{d}}{\mathrm{d}t}\left(\hat{U}_o^\dagger(t)\hat{U}(t)\right) &= i\hbar\frac{\mathrm{d}\hat{U}_o^\dagger(t)}{\mathrm{d}t}\hat{U}(t) + i\hbar\hat{U}_o^\dagger(t)\frac{\mathrm{d}\hat{U}(t)}{\mathrm{d}t} \\
&= -\hat{U}_o^\dagger(t)\hat{\mathcal{H}}_o{}^\dagger\hat{U}(t) + \hat{U}_o^\dagger(t)\hat{\mathcal{H}}\hat{U}(t) \\
&= -\hat{U}_o^\dagger(t)\hat{\mathcal{H}}_o\hat{U}(t) + \hat{U}_o^\dagger(t)\hat{\mathcal{H}}\hat{U}(t) \\
&= -\hat{U}_o^\dagger(t)\hat{\mathcal{H}}_o\hat{U}(t) + \hat{U}_o^\dagger(t)\left(\hat{\mathcal{H}}_o + \hat{\mathcal{H}}_i\right)\hat{U}(t) \\
&= \hat{U}_o^\dagger(t)\hat{\mathcal{H}}_i\hat{U}(t)
\end{aligned} \tag{C.8}$$

where we have used the set of equations (C.3) and the fact that $\hat{\mathcal{H}}_o$ is a Hermitian operator. This equation is important because it is an explicit way to explain that

the time evolution is given by $\hat{\mathcal{H}}_i$. In other words, the system evolutions by small perturbations over the time.

Integrating both sides of (C.8):

$$\int_{-\infty}^{t} \mathrm{d}t' \cdot i\hbar \frac{\mathrm{d}}{\mathrm{d}t}\left(\hat{U}_o^\dagger(t')\hat{U}(t')\right) = \int_{-\infty}^{t} \hat{U}_o^\dagger(t')\hat{\mathcal{H}}_i\hat{U}(t')\ \mathrm{d}t',$$

$$i\hbar\left(\hat{U}_o^\dagger(t')\hat{U}(t') - \hat{U}_o^\dagger(-\infty)\hat{U}(-\infty)\right)\int_{-\infty}^{t} \hat{U}_o^\dagger(t')\hat{\mathcal{H}}_i\hat{U}(t')\ \mathrm{d}t'. \tag{C.9}$$

The second term inside the parenthesis is equal to one. This can be achieved by applying the relation (C.7) and the fact that unitary operators obey $\hat{U}\hat{U}^\dagger = \hat{U}^\dagger\hat{U} = 1$.* Rearranging and premultiplying by $\hat{U}_o(t)$ we get

$$\hat{U}_o(t)\left[\hat{U}_o^\dagger(t)\hat{U}(t) = 1 + \frac{1}{i\hbar}\int_{-\infty}^{t} \hat{U}_o^\dagger(t')\hat{\mathcal{H}}_i\hat{U}(t')\ \mathrm{d}t'\right],$$

$$\hat{U}(t) = \hat{U}_o(t) + \frac{1}{i\hbar}\int_{-\infty}^{t} \hat{U}_o(t)\hat{U}_o^\dagger(t')\hat{\mathcal{H}}_i\hat{U}(t')\ \mathrm{d}t'. \tag{C.10}$$

To a first order approximation we choose $\hat{U}$ to be equal to the unperturbed operator $\hat{U}_o$ at time t'. We proceed to insert $\hat{U}(t') = \hat{U}_o(t')$ into (C.10) to get:

$$\hat{U}(t) - \hat{U}_o(t) = \hat{U}_o(t)\frac{1}{i\hbar}\int_{-\infty}^{t} \hat{\mathcal{H}}_{iI}(t')\ \mathrm{d}t' \tag{C.11}$$

where $\hat{\mathcal{H}}_{iI}(t) = \hat{U}_o^\dagger(t)\hat{\mathcal{H}}_{iI}(t)\hat{U}_o(t)$. In this equation we see that $\hat{U}(t)$ has a linear dependence on the perturbation.

To find the second order approximation we introduce the first order solution into (C.10). So that we obtain a unitary operator $\hat{U}(t)$ with squared dependence on the perturbation $\hat{\mathcal{H}}_i$:

*Any operator $\hat{U}$ that behaves as $\hat{U}\hat{U}^\dagger = \hat{U}^\dagger\hat{U} = 1$ is a unitary operator. To know more about unitary operators and their properties please refer to reference [21].

$$\begin{aligned}
\hat{U}(t) &= \hat{U}_o(t) + \frac{1}{i\hbar}\int_{-\infty}^{t} \hat{U}_o(t)\hat{U}_o^\dagger(t')\hat{\mathcal{H}}_i\hat{U}(t')\ \mathrm{d}t' \\
&= \hat{U}_o(t) + \frac{1}{i\hbar}\int_{-\infty}^{t} \hat{U}_o(t)\hat{U}_o^\dagger(t')\hat{\mathcal{H}}_i\left(\hat{U}_o(t') + \hat{U}_o(t')\frac{1}{i\hbar}\int_{-\infty}^{t'} \hat{\mathcal{H}}_{iI}(t'')\ \mathrm{d}t''\right)\ \mathrm{d}t' \\
&= \hat{U}_o(t) + \frac{1}{i\hbar}\hat{U}_o(t)\int_{-\infty}^{t} \hat{U}_o^\dagger(t')\hat{\mathcal{H}}_i\hat{U}_o(t') \\
&\quad + \frac{1}{(i\hbar)^2}\hat{U}_o(t)\int_{-\infty}^{t} \hat{U}_o^\dagger(t')\hat{\mathcal{H}}_i\hat{U}_o(t')\int_{-\infty}^{t'} \hat{\mathcal{H}}_{iI}(t'')\ \mathrm{d}t''\ \mathrm{d}t' \qquad \text{(C.12)}
\end{aligned}$$

Now repeating this procedure we get a general expression for $U(t)$. Each of its terms will have different dependence on the perturbation, *i.e.*, the first one $\hat{U}_o$ does not depends on the perturbation, the second term has a linear dependence on it, and so on. In general:

$$\hat{U}(t) = \hat{U}_o(t)\hat{U}_{int}(t) \qquad \text{(C.13)}$$

where,

$$\hat{U}_{int}(t) = 1 + \frac{1}{i\hbar}\int_{-\infty}^{t} \hat{\mathcal{H}}_{iI}(t')\ \mathrm{d}t' + \frac{1}{(i\hbar)^2}\int_{-\infty}^{t} \mathrm{d}t' \int_{-\infty}^{t'} \mathrm{d}t''\ \hat{\mathcal{H}}_{iI}(t')\hat{\mathcal{H}}_{iI}(t'') + ... \qquad \text{(C.14)}$$

This means that the wave function originally defined as $\psi(t) = \hat{U}(t)\psi(t_o)$ evolves from its original state at time t_o by a series of small perturbations given explicitly by Eq. (C.14).

Appendix D

Carrier and spin population

This appendix has the purpose of deriving explicitly Eqs. (3.28), (3.29) and (3.30) parting from the results obtained in the last chapter.

In Eq. (3.18a) we obtained that the probability of experimenting a transition to an excited state $\mathcal{C}_{c,v,\mathbf{k}}(t)$ is given by

$$\mathcal{C}_{c,v,\mathbf{k}}(t) \quad = \quad \langle c,v,\mathbf{k}|e^{-i\frac{\hat{\mathcal{H}}_o t}{\hbar}}\hat{U}_{int}(t)|0\rangle, \tag{D.1}$$

where $\hat{U}_{int}$, originally found in Eq. (C.14), is given by

$$\hat{U}_{int}(t) = 1 + \frac{1}{i\hbar}\int_{-\infty}^{t}\hat{\mathcal{H}}_{iI}(t')\ \mathrm{d}t' + \frac{1}{(i\hbar)^2}\int_{-\infty}^{t}\mathrm{d}t'\int_{-\infty}^{t'}\mathrm{d}t''\ \hat{\mathcal{H}}_{iI}(t')\hat{\mathcal{H}}_{iI}(t'') + ... \tag{D.2}$$

Taking the terms for first and second order in the perturbation we obtained in Eq. (3.19) that

$$\mathcal{C}^{(1)}_{c,v,\mathbf{k}}(t) = \frac{1}{i\hbar}\langle c,v,\mathbf{k}|e^{-i\frac{\hat{\mathcal{H}}_o t}{\hbar}}\int_{-\infty}^{t}\mathrm{d}t'\hat{\mathcal{H}}_i(t')|0\rangle, \tag{D.3a}$$

$$\mathcal{C}^{(2)}_{c,v,\mathbf{k}}(t) = \frac{1}{(i\hbar)^2}\langle c,v,\mathbf{k}|e^{-i\frac{\hat{\mathcal{H}}_o t}{\hbar}}\int_{-\infty}^{t}\mathrm{d}t'\int_{-\infty}^{t'}\mathrm{d}t''\ \hat{\mathcal{H}}_i(t')\hat{\mathcal{H}}_i(t'')|0\rangle. \tag{D.3b}$$

We can observe that $\mathcal{C}_{c,v}(t)$ is composed of two terms: a term that is linear in the perturbation $\mathcal{C}^{(1)}_{c,v}(t)$ and a second order term $\mathcal{C}^{(2)}_{c,v}(t)$ that is quadratic in the perturbation. We will start by deriving the first one.*

*In this chapter we will ignore the k-point dependence in order to simplify the notation.

D.1 First order approximation

As it was stated in Eq. (3.19) that the coefficient $\mathcal{C}^{(1)}_{c,v}(t)$ has the following form:

$$\mathcal{C}^{(1)}_{c,v}(t) = \frac{1}{i\hbar}\langle c,v|e^{-i\frac{\hat{\mathcal{H}}_o t}{\hbar}} \int_{-\infty}^{t} \mathrm{d}t' \;\; \hat{\mathcal{H}}_i(t')|0\rangle, \tag{D.4}$$

by using the closure relation $\sum_{c',v'} |c',v'\rangle\langle c',v'| = 1$:

$$\mathcal{C}^{(1)}_{c,v}(t) = \frac{1}{i\hbar}\int_{-\infty}^{t} \mathrm{d}t' \;\; \sum_{c',v'} \langle c,v|e^{-i\frac{\hat{\mathcal{H}}_o t}{\hbar}}|c',v'\rangle\langle c',v'|\hat{\mathcal{H}}_i(t')|0\rangle. \tag{D.5}$$

The first term $\langle c,v|e^{-i\frac{\hat{\mathcal{H}}_o t}{\hbar}}|c',v'\rangle$ can be expanded in Taylor series as $\langle c,v|\{1 + (-i\frac{t}{\hbar})\,\hat{\mathcal{H}}_o + (-i\frac{t}{\hbar})^2\,\hat{\mathcal{H}_o}^2 + ...\ \}|c',v'\rangle$. In this expansion the operator $\hat{\mathcal{H}}_o$ acts several times. Therefore, we have to study how it acts on the ket $|c',v'\rangle$. If we replacing $\hat{\mathcal{H}}_o$ by its second quantized form (A.20) we get to:

$$\begin{aligned}
\hat{\mathcal{H}}_o|c',v'\rangle &= \left(\sum_{c''}\hbar\omega_{c''}\hat{a}^{\dagger}_{c''}\hat{a}_{c''} - \sum_{v''}\hbar\omega_{v''}\hat{b}^{\dagger}_{v''}\hat{a}_{v''}\right)|c',v'\rangle \\
&= \left(\sum_{c''}\hbar\omega_{c''}\delta_{c',c''}\sum_{v''}\hbar\omega_{v''}\delta_{v',v''}\right)|c',v'\rangle \\
&= \hbar\omega_{c',v'}|c',v'\rangle
\end{aligned} \tag{D.6}$$

Premultiplying by $\langle c,v|$ we can find that,

$$\langle c,v|\hat{\mathcal{H}}_o|c',v'\rangle = \hbar\omega_{c',v'}\delta_{c',c}\delta_{v',v}. \tag{D.7}$$

It follows that the first term in Eq. (D.5) becomes:

$$\begin{aligned}
\langle c,v|e^{-i\hat{\mathcal{H}}_o t/\hbar}|c',v'\rangle &= \delta_{c',c}\delta_{v',v}\left(1 + \left(-i\frac{t}{\hbar}\right)\hbar\omega_{cv} + \frac{1}{2!}\left(-i\frac{t}{\hbar}\right)^2\hbar^2\omega^2_{cv} + ...\right) \\
&= \delta_{c',c}\delta_{v',v}e^{-i\omega_{cv}t}.
\end{aligned} \tag{D.8}$$

By inserting (D.8) into (D.5) we can easily find that

$$\mathcal{C}^{(1)}_{c,v}(t) = \frac{1}{i\hbar}\int_{-\infty}^{t} \mathrm{d}t' \;\; e^{-i\omega_{cv}t'}\langle c,v|\hat{\mathcal{H}}_i(t')|0\rangle \tag{D.9}$$

It is obvious that the next step is to simplify the second term of Eq. (D.9). To this end, we start by substituting the operator $\hat{\mathcal{H}}_i$ in its second-quantized form Eq. (B.17):

$$\begin{aligned}\langle c,v|\hat{\mathcal{H}}_i(t)|0\rangle &= \langle c,v| - \frac{e}{mc}\mathbf{A}(t)\sum_{c,c'}\mathbf{p}_{cc'}\hat{a}_c^\dagger\hat{a}_{c'}e^{i\omega_{cc'}t}|0\rangle \\ &+ \langle c,v| - \frac{e}{mc}\mathbf{A}(t)\sum_{c,v,\mathbf{k}}\mathbf{p}_{cv}\hat{a}_c^\dagger\hat{b}_v^\dagger e^{i\omega_{cv}t}|0\rangle \\ &+ \langle c,v| - \frac{e}{mc}\mathbf{A}(t)\sum_{c,v,\mathbf{k}}\mathbf{p}_{vc}\hat{b}_v\hat{a}_c e^{i\omega_{v,c}t}|0\rangle \\ &+ \langle c,v| - \frac{e}{mc}\mathbf{A}(t)\sum_{v,v'}\mathbf{p}_{vv'}\hat{b}_{v'}^\dagger\hat{b}_v e^{i\omega_{v,v'}t}|0\rangle \qquad \text{(D.10)}\end{aligned}$$

Using the definitions of the creation-annihilation operators in Eqs. (A.10) and (A.12). We can easily find that three of the four terms composing the last equation are zero. That is, $\hat{a}_c|0\rangle = \hat{a}_{c'}|0\rangle = \hat{b}_v|0\rangle = 0$. The reason is simple: there are no electrons to anihilate at conduction bands or holes to annihilate at valence bands at the ground state of the system. Then it follows that,

$$\langle c,v|\hat{\mathcal{H}}_i(t)|0\rangle = \langle c,v| - \frac{e}{mc}\mathbf{A}(t)\sum_{c,v,\mathbf{k}}\mathbf{p}_{cv}\hat{a}_c^\dagger\hat{b}_v^\dagger e^{i\omega_{cv}t}|0\rangle \qquad \text{(D.11)}$$

Substituting (D.11) into (D.9) we get,

$$\mathcal{C}_{c,v}^{(1)}(t) = -\frac{e}{i\hbar mc}\mathbf{p}_{cv}e^{-i\omega_{cv}t}\int_{-\infty}^{t}\mathrm{d}t'\ \mathbf{A}(t')e^{i\omega_{cv}t'}. \qquad \text{(D.12)}$$

The next step is to substitute the vector potential $\mathbf{A}(t)$ defined by Eq. (3.1). We set $\mathbf{A}(t) = \mathbf{A}(\omega)e^{-i(\omega+i\epsilon)t}$ because it is sufficient for our purposes. Then making a simple integration on (D.12) and substituting the vector potential $\mathbf{A}(t)$ we get that:

$$\begin{aligned}\mathcal{C}_{c,v}^{(1)}(t;\omega) &= -\frac{e}{i\hbar mc}\mathbf{p}_{cv}e^{-i\omega_{cv}t}\int_{-\infty}^{t}\mathrm{d}t'\ \mathbf{A}(\omega)e^{-i(\omega+i\epsilon)t}e^{i\omega_{cv}t'}. \\ &= -\frac{e}{\hbar mc}\mathbf{p}_{cv}\cdot\mathbf{A}(\omega)\frac{e^{-i(\omega+i\epsilon)t}}{\omega-\omega_{cv}+i\epsilon} \qquad \text{(D.13)}\end{aligned}$$

D.2 Second order approximation

As it was done in the last section we will find $\mathcal{C}_{c,v}$ at a second order. Eq. (3.19) has a term that is twice perturbed by the Hamiltonian $\hat{\mathcal{H}}_i$. This will be the term that give us the second order approximation. Namely, the second order coefficient $\mathcal{C}^{(2)}_{c,v}$ is given by:

$$\mathcal{C}^{(2)}_{c,v}(t) = \frac{1}{(i\hbar)^2}\langle c,v|e^{-i\frac{\hat{\mathcal{H}}_o t}{\hbar}} \int_{-\infty}^{t} \mathrm{d}t' \int_{-\infty}^{t'} \mathrm{d}t'' \ \hat{\mathcal{H}}_i(t')\hat{\mathcal{H}}_i(t'')|0\rangle. \tag{D.14}$$

Following the same procedure that we used to find Eq. (D.9) it is easy to demonstrate the following:

$$\begin{aligned}
\mathcal{C}^{(2)}_{c,v}(t) &= \frac{1}{(i\hbar)^2}\langle c,v| \int_{-\infty}^{t} \mathrm{d}t' \int_{-\infty}^{t'} \mathrm{d}t'' \ \sum_{c',v'} e^{-i\frac{\hat{\mathcal{H}}_o t}{\hbar}}|c',v'\rangle\langle c,v'|\hat{\mathcal{H}}_i(t')\hat{\mathcal{H}}_i(t'')|0\rangle, \\
&= \frac{1}{(i\hbar)^2} \int_{-\infty}^{t} \mathrm{d}t' \int_{-\infty}^{t'} \mathrm{d}t'' \ \sum_{c',v'} \delta_{c,c'}\delta_{v,v'} e^{-i\omega_{cv}t}\langle c',v'|\hat{\mathcal{H}}_i(t')\hat{\mathcal{H}}_i(t'')|0\rangle, \\
&= \frac{1}{(i\hbar)^2} \int_{-\infty}^{t} \mathrm{d}t' \int_{-\infty}^{t'} \mathrm{d}t'' \ e^{-i\omega_{cv}t}\langle c',v'|\hat{\mathcal{H}}_i(t')\hat{\mathcal{H}}_i(t'')|0\rangle
\end{aligned} \tag{D.15}$$

Up to this point, we have to reduce the following expression $\langle c',v'|\hat{\mathcal{H}}_i(t')\hat{\mathcal{H}}_i(t'')|0\rangle$. introducing the closure relation to make each operator act separately,

$$\langle c,v|\hat{\mathcal{H}}_i(t')\hat{\mathcal{H}}_i(t'')|0\rangle = \sum_{c'',v''}\langle c,v|\hat{\mathcal{H}}_i(t')|c'',v''\rangle\langle c'',v''|\hat{\mathcal{H}}_i(t'')|0\rangle, \tag{D.16}$$

so that we can analyze each term separately.

First, we are going to study the second term of the last equation $\langle c'',v''|\hat{\mathcal{H}}_i(t'')|0\rangle$. By using Eq. (B.17) it is easy to prove that:

$$\begin{aligned}
\langle c'',v''|\hat{\mathcal{H}}_i(t'')|0\rangle &= -\frac{e}{mc}\mathbf{A}(t'')\cdot \sum_{c''',v'''} \mathbf{p}_{c'''v'''}\langle c'',v''\hat{a}^{\dagger}_{c'''}\hat{b}^{\dagger}_{v'''}|0\rangle e^{i\omega_{c''',v'''}t''} \\
&= -\frac{e}{mc}\mathbf{A}(t'')\cdot \sum_{c''',v'''} \mathbf{p}_{c'''v'''}\delta_{c'',c'''}\delta_{v'',v'''}e^{i\omega_{c''',v'''}t''} \\
&= -\frac{e}{mc}\mathbf{A}(t'')\cdot \mathbf{p}_{c''v''}e^{i\omega_{c'',v''}t''}.
\end{aligned} \tag{D.17}$$

There will be two terms different from zero when substituting Eq. (B.17) into (D.16). Namely, they are:

$$\begin{aligned}\langle c,v|\hat{\mathcal{H}}_i(t')|c'',v''\rangle &= \frac{e}{mc}\mathbf{A}(t')\left(\sum_{c''',c'}\mathbf{p}_{c'''c'}\langle c,v|\hat{a}^\dagger_{c'''}\hat{a}_{c'}|c'',v''\rangle e^{i\omega_{c''',c'}t'}\right.\\ &\left.-\sum_{c''',c'}\mathbf{p}_{c'''c'}\langle c,v|\hat{a}^\dagger_{c'''}\hat{a}_{c'}|c'',v''\rangle e^{i\omega_{c'''_,c'}t'}\right)\end{aligned} \tag{D.18}$$

Knowing that $\langle c,v|\hat{a}^\dagger_{c'''}\hat{a}_{c'}|c'',v''\rangle = \delta_{c',c''}\delta_{c,c'''}\delta_{v,v''}$, and that $\langle c,v|\hat{b}^\dagger v'\hat{b}v'''|c'',v''\rangle = \delta_{v''',v''}\delta_{v,v'}\delta_{c,c''}$. By using Eq. (D.17) we can rewrite (D.16) as

$$\begin{aligned}\langle c,v|\hat{\mathcal{H}}_i(t')\hat{\mathcal{H}}_i(t'')|0\rangle &= \left(-\frac{e}{mc}\right)^2\left\{\sum_{c'}\mathbf{A}(t')\cdot\mathbf{p}_{cc'}\mathbf{A}(t'')\mathbf{p}_{c'v}e^{i\omega_{cc'}t'}e^{i\omega_{c'v}t''}\right.\\ &\left.-\sum_{v'}\mathbf{A}(t')\cdot\mathbf{p}_{v'v}\mathbf{A}(t'')\mathbf{p}_{cv'}e^{i\omega_{cv'}t''}e^{i\omega_{v'v}t'}\right\}\end{aligned} \tag{D.19}$$

by substituting this result into equation(D.15) the coefficient $\mathcal{C}^{(2)}_{c,v}(t)$ becomes:

$$\begin{aligned}\mathcal{C}^{(2)}_{c,v}(t) &= \frac{1}{(im\hbar)^2}\left(-\frac{e}{mc}\right)^2 e^{-i\omega_{cv}t}\\ &\left\{\sum_{c'}\mathbf{p}_{cc'}\cdot\int_{-\infty}^{t}\mathrm{d}t'\ \mathbf{A}(t')e^{i\omega_{cc'}t'}\mathbf{p}_{c'v}\cdot\int_{-\infty}^{t'}\mathrm{d}t''\ \mathbf{A}(t'')e^{i\omega_{c'v}t''}\right.\\ &\left.-\sum_{v'}\mathbf{p}_{v'v}\cdot\int_{-\infty}^{t}\mathrm{d}t'\ \mathbf{A}(t')e^{i\omega_{v'v}t'}\mathbf{p}_{cv'}\cdot\int_{-\infty}^{t'}\mathrm{d}t''\ \mathbf{A}(t'')e^{i\omega_{cv'}t''}\right\}\end{aligned} \tag{D.20}$$

Now, it is time to substitute the vector potential $A(t)$ by the expression shown in Eq. (3.1). But, it is important to know that the only term that will be considered is $A(t) = A(\omega)e^{-i(\omega+i\epsilon)t}$. This is because of the fact that in this approximation two photons have to sum a frequency of 2ω, therefore, each one must have a frequency of ω. Having this in mind and solving the integrals shown

in the last expression we get:

$$
\begin{aligned}
\mathcal{C}^{(2)}_{c,v}(t) &= \frac{1}{(im\hbar)^2}\left(-\frac{e}{mc}\right)^2 e^{-i\omega_{cv}t} \\
&\quad \left\{ \sum_{c'} \mathbf{p}_{cc'}\cdot\mathbf{A}(\omega)\mathbf{p}_{c'v}\cdot\mathbf{A}(\omega) \int_{-\infty}^{t} \mathrm{d}t' \; e^{i(\omega_{cc'}-\omega-i\epsilon)t'} \int_{-\infty}^{t'} \mathrm{d}t'' \; e^{i(\omega_{c'v}-\omega-i\epsilon)t''} \right. \\
&\quad \left. - \sum_{v'} \mathbf{p}_{v'v}\cdot\mathbf{A}(\omega)\mathbf{p}_{cv'}\cdot\mathbf{A}(\omega) \int_{-\infty}^{t} \mathrm{d}t' \; e^{i(\omega_{v'v}-\omega-i\epsilon)t'} \int_{-\infty}^{t'} \mathrm{d}t'' \; e^{i(\omega_{cv'}-\omega-i\epsilon)t''} \right\} \\
&= \frac{1}{(im\hbar)^2}\left(-\frac{e}{mc}\right)^2 e^{-i\omega_{cv}t} \\
&\quad \left\{ \sum_{c'} \mathbf{p}_{cc'}\cdot\mathbf{A}(\omega)\mathbf{p}_{c'v}\cdot\mathbf{A}(\omega) \int_{-\infty}^{t} \mathrm{d}t' \; e^{i(\omega_{cc'}+\omega+i\epsilon)t'} \left(\frac{e^{i(\omega_{c'v}+\omega+i\epsilon)t'}}{i(\omega_{c'v}-\omega-i\epsilon)} \right) \right. \\
&\quad \left. - \sum_{v'} \mathbf{p}_{v'v}\cdot\mathbf{A}(\omega)\mathbf{p}_{cv'}\cdot\mathbf{A}(\omega) \int_{-\infty}^{t} \mathrm{d}t' \; e^{i(\omega_{v'v}-\omega-i\epsilon)t'} \left(\frac{e^{i(\omega_{cv'}+\omega+i\epsilon)t'}}{i(\omega_{cv'}-\omega-i\epsilon)t'} \right) \right\}
\end{aligned}
\tag{D.21}
$$

Using the definition of $\omega_{ab} = \omega_a - \omega_b$, the last equation becomes:

$$
\begin{aligned}
\mathcal{C}^{(2)}_{c,v}(t) &= \frac{1}{(im\hbar)^2}\left(-\frac{e}{mc}\right)^2 e^{-i\omega_{cv}t} \\
&\quad \left\{ \sum_{c'} \mathbf{p}_{cc'}\cdot\mathbf{A}(\omega)\mathbf{p}_{c'v}\cdot\mathbf{A}(\omega) \int_{-\infty}^{t} \mathrm{d}t' \; \frac{e^{i(\omega_{cv}-2\omega-i2\epsilon)t'}}{i(\omega_{c'v}-\omega-i\epsilon)} \right. \\
&\quad \left. - \sum_{v'} \mathbf{p}_{v'v}\cdot\mathbf{A}(\omega)\mathbf{p}_{cv'}\cdot\mathbf{A}(\omega) \int_{-\infty}^{t} \mathrm{d}t' \; \frac{e^{i(\omega_{cv}-2\omega-i2\epsilon)t'}}{i(\omega_{cv'}-\omega-i\epsilon)} \right\} \\
&= \frac{1}{(m\hbar)^2}\left(-\frac{e}{mc}\right)^2 e^{-i\omega_{cv}t} \\
&\quad \left\{ \sum_{c'} \mathbf{p}_{cc'}\cdot\mathbf{A}(\omega)\mathbf{p}_{c'v}\cdot\mathbf{A}(\omega) \frac{e^{i(\omega_{cv}-2\omega-i2\epsilon)t}}{(\omega_{c'v}-\omega-i\epsilon)(\omega_{cv}-2\omega-i2\epsilon)} \right.
\end{aligned}
$$

$$
\begin{aligned}
&- \sum_{v'} \mathbf{p}_{v'v} \cdot \mathbf{A}(\omega) \mathbf{p}_{cv'} \cdot \mathbf{A}(\omega) \frac{e^{i(\omega_{cv} - 2\omega - i2\epsilon)t}}{(\omega_{cv'} - \omega - i\epsilon)(\omega_{cv} - 2\omega - i2\epsilon)} \Bigg\} \\
= \quad & \left(\frac{e}{\hbar mc}\right)^2 \left\{ \sum_{c'} \frac{\mathbf{p}_{cc'} \cdot \mathbf{A}(\omega) \mathbf{p}_{c'v} \cdot \mathbf{A}(\omega)}{\omega - \omega_{c'v}} \right. \\
& \left. - \sum_{v'} \frac{\mathbf{p}_{vv'} \cdot \mathbf{A}(\omega) \mathbf{p}_{cv'} \cdot \mathbf{A}(\omega)}{\omega - \omega_{cv'}} \right\} \frac{e^{-i(2\omega + 2i\epsilon)t}}{2\omega - \omega_{cv} + i2\epsilon}
\end{aligned} \tag{D.22}
$$

D.3 Fermi's golden rule

In section (3.1) ϵ was defined as a number that tends to zero to make the vector potential $\mathbf{A}(t)$ be zero at a time equal to minus infinity ($\mathbf{A}(-\infty) = 0$). Because of the fact that it is a small number, we can make the following approximation $2\epsilon \approx \epsilon$. Therefore, the coefficients $\mathcal{C}^{(1)}_{c,v}$ and $\mathcal{C}^{(2)}_{c,v}$ have as a common term $\frac{e^{-i(2\omega + i\epsilon)t}}{2\omega - \omega_{cv} + i\epsilon}$. Thus,

$$
\mathcal{C}_{c,v}(t) = \mathcal{K}_{c,v}(t) \frac{e^{-i(2\omega + i\epsilon)t}}{2\omega - \omega_{cv} + i\epsilon} \tag{D.23}
$$

where,

$$
\begin{aligned}
\mathcal{K}_{c,v}(t) \quad = \quad & -\frac{e}{\hbar mc} \mathbf{A}(2\omega) \cdot \mathbf{p}_{cv} \\
& + \left(\frac{e}{\hbar mc}\right)^2 \left\{ \sum_{c'} \frac{\mathbf{p}_{cc'} \cdot \mathbf{A}(\omega) \mathbf{p}_{c'v} \cdot \mathbf{A}(\omega)}{\omega - \omega_{c',v}} - \sum_{v'} \frac{\mathbf{p}_{vv'} \cdot \mathbf{A}(\omega) \mathbf{p}_{cv'} \cdot \mathbf{A}(\omega)}{\omega - \omega_{cv'}} \right\}.
\end{aligned} \tag{D.24}
$$

The probability of being at a state $|c, v\rangle$ is given by $|\mathcal{C}_{c,v}(t)|^2$, using the last result we find out that

$$
|\mathcal{C}_{c,v}(t)|^2 = |\mathcal{K}_{c,v}(t)|^2 \frac{e^{2\epsilon t}}{(2\omega - \omega_{cv})^2 + \epsilon^2} \tag{D.25}
$$

As it can be seen in Eq. (3.21) we are interested in the time evolution of an operator. When finding $\mathrm{d}\mathcal{C}_{c,v}(t)/\mathrm{d}t$ we find out that the last equation acquires a particular form. This is because the constant ϵ was defined to be a number close to zero, and, at the limit of ϵ tending to zero this function has a well-known form.

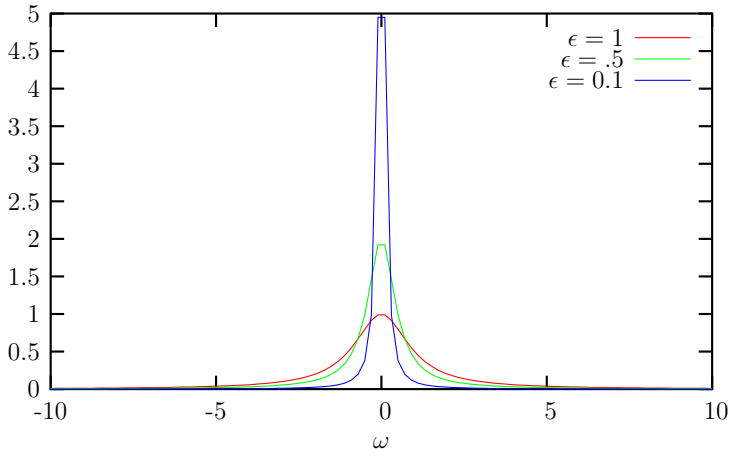

Figure D.1 : It is shown that the equation $\lim_{\epsilon\to 0}\epsilon/(\omega^2+\epsilon^2)$ behaves as a Dirac's delta function. As the value of ϵ decreases the function acquires the form of a Dirac's delta function.

Namely, it becomes a Dirac's delta function as you can see on Fig. D.1.[†]

$$\lim_{\epsilon\to 0}\frac{\mathrm{d}}{\mathrm{d}t}|\mathcal{C}_{c,v}(t)|^2 = |\mathcal{K}_{c,v}(t)|^2 \lim \epsilon \to 0 \frac{e^{2\epsilon t}}{(2\omega-\omega_{cv})^2+\epsilon^2} = 2\pi|\mathcal{K}_{c,v}(t)|^2\delta(2\omega-\omega_{cv}) \tag{D.26}$$

This equation is also known as the Fermi's Golden Rule. It shows that a transition from v to c is only allowed when the frequency of the incident photon 2ω is equal to the energy difference between both bands. Moreover, there should be a coupling between the bands given explicitly by $\mathcal{K}_{c,v}(t)$.

Using this delta function we are able to find $\mathcal{C}_{c,v}$ at its final form. From $\delta(2\omega-\omega_{cv})$ we have that $\omega_{cv}=2\omega$, additionally, we define $\overline{\omega}$ as an average of ω_c and ω_v. Explicitly, $\overline{\omega}=(\omega_c+\omega_v)/2$. By substituting Eq. (3.3) and $\overline{\omega}$ into Eq. (D.23) we finally get:

$$\mathcal{K}_{c,v}(t) = \frac{ie}{\hbar m\omega_{cv}}\mathbf{E}(2\omega)\cdot\mathbf{p}_{cv} - \left(\frac{2e}{\hbar m\omega_{cv}}\right)^2\sum_n \frac{\mathbf{p}_{cn}\cdot\mathbf{E}(\omega)\mathbf{p}_{nv}\cdot\mathbf{E}(\omega)}{\overline{\omega}-\omega_n} \tag{D.27}$$

where $n\in\{c,v\}$.

D.4 Responses

Now that we have found the coefficient $\mathcal{C}_{c,v}$ shown in Eq. (D.23). We will show the algebra needed to find the set of equations shown in Sections 3.4 and 3.5.

[†]For more information about the Dirac Delta function read [36].

In those sections our goal was to find an expression for the time evolution of some operators. In particular, we were interested in the areal electrical current density operator $\hat{\mathbf{J}}$, spin areal density operator $\hat{S}^a$, spin current density operator $\hat{K}$ and areal carrier density $\hat{n}$, *i.e.*, we wanted to find the following quantities:

$$\frac{\mathrm{d}\langle\hat{n}\rangle}{\mathrm{d}t},\ \frac{\mathrm{d}\langle\hat{S}^a\rangle}{\mathrm{d}t},\ \frac{\mathrm{d}\langle\hat{K}\rangle}{\mathrm{d}t},\ \text{and}\ \frac{\mathrm{d}\langle\hat{\mathbf{J}}\rangle}{\mathrm{d}t}.$$

Thus, we can use Eq. (3.21) which give us the time evolution for an operator $\hat{\mathcal{O}}$ in its SQ form:

$$\frac{\mathrm{d}\langle\hat{\mathcal{O}}\rangle}{\mathrm{d}t} = \frac{\mathrm{d}\langle\psi'|\hat{\mathcal{O}}|\psi\rangle}{\mathrm{d}t} = \frac{\mathrm{d}}{\mathrm{d}t}\sum_{c,v,\mathbf{k}}\sum_{c',v',\mathbf{k}'}\mathcal{C}^*_{c',v',\mathbf{k}'}\mathcal{C}_{c,v,\mathbf{k}}\langle c',v',\mathbf{k}'|\hat{\mathcal{O}}|c,v,\mathbf{k}\rangle, \tag{D.28}$$

where the coefficients $\mathcal{C}_{c,v}(t)$ given by Eq. (D.23) are:

$$\mathcal{C}_{c,v}(t) = \mathcal{K}_{c,v}(t)\frac{e^{-i(2\omega+i\epsilon)t}}{2\omega-\omega_{cv}+i\epsilon}, \tag{D.29a}$$

and from Eq. (D.26):

$$|\mathcal{C}_{c,v}(t)|^2 = |\mathcal{K}_{c,v}(t)|^2\delta(2\omega-\omega_{cv}). \tag{D.29b}$$

Moreover, using Eq. (D.27) we have,

$$\mathcal{K}_{c,v}(t) = \frac{ie}{\hbar m\omega_{cv}}\mathbf{E}(2\omega)\cdot\mathbf{p}_{cv} - \left(\frac{2e}{\hbar m\omega_{cv}}\right)^2\sum_n\frac{\mathbf{p}_{cn}\cdot\mathbf{E}(\omega)\mathbf{p}_{nv}\cdot\mathbf{E}(\omega)}{\overline{\omega}-\omega_n} \tag{D.29c}$$

By just substituting the observable $\hat{\mathcal{O}}$ in Eq. (D.29a) by the operators $\hat{n}$, $\hat{S}^a$, $\hat{\mathbf{J}}$ or $\hat{K}$ we can find the time evolution of those operators. Thus, we directly get the set of equations (3.27) and (3.34) shown in Chapter 3.

Appendix E

Matrix elements

This chapter has the purpose of explaining how the matrix elements can be obtained. In particular, we are interested in the momentum matrix elements $\mathbf{p}_{m,n}$ and the spin areal matrix elements S^a_{mn}.

We part from the wave function ψ expanded in plane waves,

$$\psi_m(\mathbf{k};\mathbf{r}) = \sum_{\mathbf{G}} C_{m\mathbf{k}}(\mathbf{G})\, e^{i(\mathbf{k}+\mathbf{G})\cdot\mathbf{r}}, \tag{E.1}$$

where the sub-indices m indicates bands, $\mathbf{G}$ is a reciprocal lattice vector and $\mathbf{k}$ is the plane wave vector (or Block wave vector) introduced in section (3.2).

The matrix elements of a particular operator $\hat{A}$ are defined as

$$\hat{A}_{mn} = \langle\psi_m|\hat{A}|\psi_n\rangle = \int \mathrm{d}^3\mathbf{r}\, \psi^*_m \hat{A}\psi_n. \tag{E.2}$$

It follows that once we have obtained the wave function ψ it is easy to obtain the matrix elements for any operator. We just have to substitute the wave function (E.1) into the definition of a matrix element (E.2). Thus, all the information of the system is represented by the wave function.

E.1 Momentum Matrix Elements

For example, if we want to obtain the momentum matrix elements we just have to introduce the momentum operator $\hat{\mathbf{p}} = -i\hbar\nabla$ into Eq. (E.2) . That is,

$$\mathbf{p}_{mn}(\mathbf{k}) \quad = \quad \langle\psi_m|\hat{\mathbf{p}}|\psi_n\rangle$$

$$= \int \mathrm{d}^3\mathbf{r}\, \psi^* \left(-i\hbar\nabla\right) \psi$$

The last expression can be reduced by using Eq. (E.1) in the following way,

$$\begin{aligned} \mathbf{p}_{mn}(\mathbf{k}) &= \sum_{\mathbf{G},\mathbf{G}'} C^*_{m\mathbf{k}}\left(\mathbf{G}\right) C_{n\mathbf{k}}\left(\mathbf{G}'\right) \hbar\left(\mathbf{k}+\mathbf{G}\right) \int \mathrm{d}^3\mathbf{r}\, e^{-i\mathbf{r}\cdot(\mathbf{G}-\mathbf{G}')} \\ &= \hbar \sum_{\mathbf{G}} C^*_{m\mathbf{k}}\left(\mathbf{G}\right) C_{n\mathbf{k}}\left(\mathbf{G}\right)\left(\mathbf{k}+\mathbf{G}\right) \end{aligned} \tag{E.3}$$

In this deduction we used the Kronecker Delta function $\int \mathrm{d}^3\mathbf{r}\, e^{-i\mathbf{r}\cdot(\mathbf{G}-\mathbf{G}')} = \delta_{\mathbf{G},\mathbf{G}'}$.

E.1.1 Spin degeneracy

If we take into account the spin degeneracy, the wave function becomes an spinor Ψ, defined as: [21]

$$\Psi = \begin{pmatrix} \psi^+ \\ \psi^- \end{pmatrix} \tag{E.4}$$

where $+$ and $-$ are the two possible spin orientations.

In this case the matrix elements have the following form:

$$\begin{aligned} \langle\Psi|\hat{\mathbf{p}}|\Psi\rangle &= \int \mathrm{d}^3\mathbf{r}\, \begin{pmatrix} \psi^{+*}_m & \psi^{-*}_m \end{pmatrix} \begin{pmatrix} \hat{\mathbf{p}}\psi^+_n \\ \hat{\mathbf{p}}\psi^-_n \end{pmatrix} \\ &= \langle\psi^+_m|\hat{\mathbf{p}}|\psi^+_n\rangle + \langle\psi^-_m|\hat{\mathbf{p}}|\psi^-_n\rangle. \end{aligned} \tag{E.5}$$

Now taking into account spin degeneracy, we can expand the wave functions for spin down (ψ^-) and spin up(ψ^+), as follows:

$$\psi^-_m(\mathbf{k};\mathbf{r}) = \sum_{\mathbf{G}} C^-_{m\mathbf{k}}\left(\mathbf{G}\right) e^{i(\mathbf{k}+\mathbf{G})\cdot\mathbf{r}} \tag{E.6a}$$

and

$$\psi^+_m(\mathbf{k};\mathbf{r}) = \sum_{\mathbf{G}} C^+_{m\mathbf{k}}\left(\mathbf{G}\right) e^{i(\mathbf{k}+\mathbf{G})\cdot\mathbf{r}} \tag{E.6b}$$

where we used the superscripts $+$ and $-$ to indicate the two possible spin degeneracies.

Using Eqs. (E.3) , (E.3) we get:

$$\begin{aligned} \mathbf{p}_{mn}(\mathbf{k}) &= \hbar \sum_{\mathbf{G}} C^{+}_{m\mathbf{k}}(\mathbf{G})\, C^{+}_{n\mathbf{k}}(\mathbf{G})^{*}(\mathbf{k}+\mathbf{G}) \\ &+ \hbar \sum_{\mathbf{G}} C^{-}_{m\mathbf{k}}(\mathbf{G})\, C^{-}_{n\mathbf{k}}(\mathbf{G})^{*}(\mathbf{k}+\mathbf{G}) \end{aligned} \tag{E.7}$$

As you may notice Eqs. (E.3) and (E.7) are similar, but, when our wave function is a spinor we have a sum for each of the two possible spin polarizations.

E.2 Spin Matrix Elements

The operators for angular momentum 1/2 are known as the Pauli matrices,

$$\hat{S}^{a} = \frac{\hbar}{2}\sigma^{a} \tag{E.8a}$$

$$\sigma^{x} = \begin{pmatrix} 0 & 1 \\ 1 & 0 \end{pmatrix} \ , \ \sigma^{y} = \begin{pmatrix} 0 & -i \\ i & 0 \end{pmatrix} \ , \ \sigma^{z} = \begin{pmatrix} 1 & 0 \\ 0 & -1 \end{pmatrix} \tag{E.8b}$$

We are going to use them to find the spin matrix elements. For example, to find the spin polarization in the x coordinate we just substitute S^{x} into the definition of a matrix element (E.2):

$$\begin{aligned} \langle \Psi_m | S^{x} | \Psi_n \rangle &= \int \mathrm{d}^{3}\mathbf{r}\, \frac{\hbar}{2} \begin{pmatrix} \psi^{+*}_{m} & \psi^{-*}_{m} \end{pmatrix} \begin{pmatrix} 0 & 1 \\ 1 & 0 \end{pmatrix} \begin{pmatrix} \psi^{+}_{n} \\ \psi^{-}_{n} \end{pmatrix} \\ &= \frac{\hbar}{2} \left(\langle \psi^{-}_{m} | \psi^{+}_{n} \rangle + \langle \psi^{+}_{m} | \psi^{-}_{n} \rangle \right) \end{aligned} \tag{E.9a}$$

In a similar way we find the spin matrix elements in the y and z coordinates:

$$\langle \Psi_m | S^{y} | \Psi_n \rangle = \frac{i\hbar}{2} \left(\langle \psi^{-}_{m} | \psi^{+}_{n} \rangle - \langle \psi^{+}_{m} | \psi^{-}_{n} \rangle \right) \tag{E.9b}$$

$$\langle \Psi_m | S^{z} | \Psi_n \rangle = \frac{\hbar}{2} \left(\langle \psi^{+}_{m} | \psi^{+}_{n} \rangle - \langle \psi^{-}_{m} | \psi^{-}_{n} \rangle \right) \tag{E.9c}$$

Finally, using Eqs. (E.6) we find:

$$\begin{aligned}\langle\psi_m^+|\psi_n^-\rangle &= \sum_{\mathbf{G},\mathbf{G}'} C_{m\mathbf{k}}^+(\mathbf{G})^* C_{n\mathbf{k}}^-(\mathbf{G}') \int \mathrm{d}^3\mathbf{r}\, e^{-i\mathbf{r}\cdot(\mathbf{G}-\mathbf{G}')} \\ &= \sum_{\mathbf{G},\mathbf{G}'} C_{m\mathbf{k}}^+(\mathbf{G})^* C_{n\mathbf{k}}^-(\mathbf{G}')\,\delta_{\mathbf{G},\mathbf{G}'} \\ &= \sum_{\mathbf{G}} C_{m\mathbf{k}}^+(\mathbf{G})^* C_{n\mathbf{k}}^-(\mathbf{G}) \qquad \text{(E.10a)}\end{aligned}$$

In a similar way the following terms are:

$$\langle\psi_m^-|\psi_n^+\rangle = \sum_{\mathbf{G}} C_{m\mathbf{k}}^-(\mathbf{G})^* C_{n\mathbf{k}}^+(\mathbf{G}) \qquad \text{(E.10b)}$$

$$\langle\psi_m^+|\psi_n^+\rangle = \sum_{\mathbf{G}} C_{m\mathbf{k}}^+(\mathbf{G})^* C_{n\mathbf{k}}^+(\mathbf{G}) \qquad \text{(E.10c)}$$

$$\langle\psi_m^-|\psi_n^-\rangle = \sum_{\mathbf{G}} C_{m\mathbf{k}}^-(\mathbf{G})^* C_{n\mathbf{k}}^-(\mathbf{G}) \qquad \text{(E.10d)}$$

Now using Eqs. (E.9) and (E.10) we can construct the spin matrix elements as:

$$S_{mn}^x = \frac{\hbar}{2}\sum_{\mathbf{G}}\left(C_{m\mathbf{k}}^-(\mathbf{G})^* C_{n\mathbf{k}}^+(\mathbf{G}) + C_{m\mathbf{k}}^+(\mathbf{G})^* C_{n\mathbf{k}}^-(\mathbf{G})\right) \qquad \text{(E.11)}$$

$$S_{mn}^y = \frac{i\hbar}{2}\sum_{\mathbf{G}}\left(C_{m\mathbf{k}}^-(\mathbf{G})^* C_{n\mathbf{k}}^+(\mathbf{G}) - C_{m\mathbf{k}}^+(\mathbf{G})^* C_{n\mathbf{k}}^-(\mathbf{G})\right) \qquad \text{(E.12)}$$

$$S_{mn}^z = \frac{\hbar}{2}\sum_{\mathbf{G}}\left(C_{m\mathbf{k}}^+(\mathbf{G})^* C_{n\mathbf{k}}^+(\mathbf{G}) - C_{m\mathbf{k}}^-(\mathbf{G})^* C_{n\mathbf{k}}^-(\mathbf{G})\right) \qquad \text{(E.13)}$$

$$\qquad \text{(E.14)}$$

With these sets of equations we have found that the spin and momentum matrix elements are summations over reciprocal lattice vectors that can be constructed easily from the wave function Ψ.

Appendix F

List of abbreviations

BFGS	Broyden-Fletcher-Goldfarb-Shanno minimization
DFT	Density Functional Theory
DSP	Degree of Spin Polarization
ecut	Energy cutoff
EM	Electro Magnetic
GMR	Giant Magneto Resistance
HFM	Hartree-Fock Method
KS	Kohn-Sham
LDA	Local Density Approximation
nkpt	Number of **k**-points
nlayer	Number of layers
QM	Quantum Mechanics
RTD	Resonant Tunneling Devices
SCF	Self Consistent Field
SQ	Second Quantized or Second Quantization

PST	Pseudopotential Theory
PT	Perturbation Theory
toldfe	Tolerance on the difference of total energy

Appendix G

List of symbols

$\mathbf{A}(t)$	Magnetic vector potential
$\hat{a}^\dagger$	Electrons creation operator
$\hat{a}$	Electrons anihilation operator
$\hat{b}^\dagger$	Holes creation operator
$\hat{b}$	Holes anihilation operator
$\mathbf{B}$	Magnetic field vector
c	Speed of light
$\lvert\mathcal{C}_{c,v,\mathbf{k}}\rvert^2$	Electronic transition probability coeficient
e	Electron charge
E	Energy
$\mathbf{E}$	Electric field vector
$E_{xc}[\rho]$	Exchange-correlation energy functional
$\mathbf{F}$	Force
$G[\rho]$	Universal functional of the density
$\mathbf{G}$	Reciprocal lattice vector

$\hat{\mathcal{H}}_o$	Ground-state Hamiltonian operator
$\hat{\mathcal{H}}$	Hamiltonian operator
$\hat{\mathbf{J}}^a$	Areal electric current density operator
$\mathbf{k}$	k-point vector
$\hat{K}^{ab}$	Areal spin current density operator
$\hat{n}$	Areal carrier density operator
$\hat{\mathcal{O}}$	Arbitrary operator used to represent an observable
$\hat{\mathbf{p}}$	Momentum operator
$\mathbf{r}$,$\mathbf{R}$	Position vector
$\hat{S}^a$	Spin areal density operator
t	Time
$T_s[\rho]$	Kinetic energy functional
$\hat{U}$	Unitary operator
$\mathcal{V}$	Electro-magnetic potential
V_H	Hartree potential
V_{ec}	Electron-core interaction potential
V_{xc}	Exchange-correlation potential
V^{eff}	Effective potential
$V(\mathbf{R})$	Potential energy
ω	Angular frequency
Z	Atomic number
$\|0\rangle$	Ket representing the system at its ground state
$\|c, v, \mathbf{k}\rangle$	Ket representing the system at an excited state
$\delta(x)$	Dirac's delta

δ_{ab}	Kronecker's delta
$\epsilon_{xc}(\rho)$	Exchange and correlation energy per electron
ρ	Probability density
ρ_o	Ground state density
$\hat{\rho}(\mathbf{r};\mathbf{k})$	Charge density operator
ψ,Ψ	Wave function
Φ	Scalar potential
Ω	Volume
ξ^{ab}	Carrier population pseudo-tensor
ζ^{abc}	Spin population pseudo-tensor
η^{abc}	electric current pseudo-tensor
μ^{abcd}	spin current pseudo-tensor

References

[1] D. D. Awchalom, R. A. Buhrman, J. M. Daughton, S. von Molnar, and M. L. Roukes, *Spin Electronics* (Kluwer Academic Publishers, 2004).

[2] J. M. Kikkawa and D. D. Awschalom, *Resonant spin amplification in n-type GaAs*, Phys. Rev. Lett. **80**(19), 4313 (1998).

[3] I. Malajovich, J. M. Kikkawa, and D. D. Awschalom, *Coherent transfer of spin through a semiconductor heterointerface*, Phys. Rev. Lett. **84**(5), 1015 (2000).

[4] E. Kaxiras, *Atomic and Electronic Structure of Solids* (Cambridge University Press, 2003).

[5] M. C. Payne, M. P. Teter, D. C. Allan, T. A. Arias, and J. D. Joannopoulos, *Iterative minimization techniques for ab initio total-energy calculations: molecular dynamics and conjugate gradients*, Rev. Mod. Phys. **64**(4), 1045 (1992).

[6] P.-O. Lowdin, *Studies of atomic self-consistent fields. i. calculation of slater functions*, Phys. Rev. **90**(1), 120 (1953).

[7] P.-O. Lowdin, *Correlation problem in many-electron quantum mechanics. i. review of different approaches and discussion of some current ideas*, Adv. Chem. Phys. **2**, 207 (1959).

[8] S. Fahy, X. W. Wang, and S. G. Louie, *Variational quantum monte carlo nonlocal pseudopotential approach to solids: Cohesive and structural properties of diamond*, Phys. Rev. Lett. **61**(14), 1631 (1988).

[9] P. Hohenberg and W. Kohn, *Inhomogeneous electron gas*, Phys. Rev. **136**(3B), B864 (1964).

[10] W. Kohn and L. J. Sham, *Self-consistent equations including exchange and correlation effects*, Phys. Rev. **140**(4A), A1133 (1965).

[11] N. W. Aschroft and N. D. Mermin, *Solid State Physics* (Thomson Learning Inc., 1976).

[12] D. R. Hamann, M. Schluter, and C. Chiang, *Norm-conserving pseudopotentials*, Phys. Rev. Lett. **43**(20), 1494 (1979).

[13] M. T. Yin and M. L. Cohen, *Theory of ab initio pseudopotential calculations*, Phys. Rev. B **25**(12), 7403 (1982).

[14] M. T. Yin and M. L. Cohen, *Theory of static structural properties, crystal stability, and phase transformations*, Phys. Rev. B **26**(10), 5668 (1982).

[15] R. M. Martin, *Electronic Structure. Basic Theory and Practical Methods* (Cambridge University Press, 2004).

[16] M. Johnson and R. H. Silsbee, *Thermodynamic analysis of interfacial transport and of the termomagnetoelectric system*, Phys. Rev. B **35**(35), 4959 (1987).

[17] S. Datta and B. Das, *Electronic analog of the electro-optic modulator*, Appl. Phys. Lett. **56**(7), 665 (1990).

[18] A. Najmaie, R. D. R. Bhat, and J. E. Sipe, *All-optical injection and control of spin and electrical currents in quantum wells*, Phys. Rev. B **68**, 165348 (2003).

[19] J. E. Sipe and A. I. Shkrebtii, *Second-order optical response in semiconductors*, Phys. Rev. B **61**(8), 5338 (1999).

[20] J. D. Jackson, *Classical electrodynamics* (John Wiley & Sons. Inc., 1962).

[21] L. de la Peña, *Introducción a la mecánica cuántica* (Fondo de cultura económica, 2006), 3rd ed.

[22] C. Cohen-Tannoudji, B. Diu, and F. Laloe, *Quantum mechanics* (Wiley-Interscience, 1997).

[23] J. J. Sakurai, *Quantum mechanics* (Addison-Wesley, 1976).

[24] R. D. R. Bhat, P. Nemec, Y. Kerachian, H. M. van Driel, and J. E. Sipe, *Two-photon spin injection in semiconductors*, Phys. Rev. B **71**, 035309 (2005).

[25] N. Laman, A. I. Shkrebtii, J. E. Sipe, and H. M. van Driel, *Quantum interference control of currents in cdse with a single optical beam*, Appl. Phys. Lett. **75**(17), 2581 (1999).

[26] S. J. Clarck, *Complex structures in tetrahedrally bonded semiconductors*, Ph.D. thesis, University of Edinburgh (1994).

[27] R. P. Feynman, *Forces in molecules*, Phys. Rev. **56**, 340 (1939).

[28] H. B. Schlegel, *Optimization of equilibrium geometries and transition structures*, The Journal of Computational Chemistry **3**, 214 (1982).

[29] B. S. Mendoza, F. Nastos, N. Arzate, and J. Sipe, *Band structure calculations of the surface linear optical response of clean and hydrogenated Si(100) surface*, Phys. Rev. B **74**, 075318 (2006).

[30] L. Reining, R. D. Sole, M. Cini, and J. G. Ping, *Microscopic calculation of second-harmonic generation at semiconductor surfaces: As/si(111) as a test case*, Phys. Rev. B **50**, 8411 (1994).

[31] B. S. Mendoza, M. Palummo, G. Onida, and R. D. Sole, *Ab initio calculation of second-harmonic-generation at the si(100) surface*, Phys. Rev. B **63**(205406), 8411 (2001).

[32] J. E. Mejia, C. Salazar, and B. S. Mendoza, *Layer-by-layer analysis of surface second harmonic generation at a simple surface*, Rev. Mex. Fis. **50**, 134 (2004).

[33] M. J. Stevens, R. D. R. Bhat, J. E. Sipe, H. M. van Driel, and A. L. Smirl, Phys. Status Solidi B **238**, 568 (2003).

[34] P. Jordan and E. P. Wigner, *Zusammenfassung die arbeit enthält eine fortsetzung der kürzlich von einem der verfasser vorgelegten note zur quantenmechanik der gasentartung*, Z. Phys. **47**, 631 (1928).

[35] Sagoskin, *Quantum theory of many-body systems* (Springer-Verlag, 1998).

[36] G. Arfken, *Mathematical Methods for Physicists* (Academic Press, Inc., 1985), 3rd ed.